TARGETING NICOTINAMIDE ADENINE DINUCLEOTIDE METABOLISM FOR THE TREATMENT OF CHRONIC LYMPHOCYTIC LEUKEMIA

BY

ERIC DAVID JOSEPH BOUCHARD

A Thesis Submitted to the Faculty of Graduate Studies of

The University of Manitoba

in Partial Fulfillment of the Requirements for the Degree of

MASTER OF SCIENCE

Department of Biochemistry and Medical Genetics

University of Manitoba

Winnipeg, Manitoba

Canada

ABSTRACT

The nicotinamide adenine dinucleotide (NAD) biosynthetic enzyme nicotinamide phosphoribosyltransferase (NAMPT) has emerged as a promising new target for the treatment of multiple malignancies, including chronic lymphocytic leukemia (CLL). However, results of early phase clinical trials suggest that effective use of NAMPT inhibitors will require the dose reduction and improved treatment efficacy afforded by combination therapy. In this study, we assessed the downstream effects of NAMPT inhibition on NAD-dependent pathways in primary CLL cells *in vitro* in order to identify promising targets for novel combinations therapies. We then investigated drug-drug interactions between the NAMPT inhibitors FK866 and GMX-1778, and chemotherapeutics and targeted agents in current clinical use, as well as agents targeting mitochondrial metabolism, glycolysis and oxidative stress. We identified several promising novel drug combinations for further investigation and development for CLL treatment.

ACKNOWLEDGEMENTS

I would first like to thank my supervisor Dr. Versha Banerji whose unique perspective as a clinician and scientist has inspired me, challenged me, and ultimately shaped this research and my approach to scientific enquiry. I would also like to express my gratitude to my committee members, Drs. Spencer Gibson, Aaron Marshall and Christine Doucette, who have provided invaluable guidance throughout my program.

Additionally, I would like to thank past and present members of the Banerji lab; Armando Poeppl and Cheryl Peltier for the long hours of training and advice on assay design and troubleshooting, and especially Dr. Iris Gehrke, who performed the preliminary work leading to this study, and Ryan Saleh, whom it was a pleasure to mentor and who contributed many hours of data collection.

Many others have contributed and supported me throughout this project. While I cannot list them all, I would like to acknowledge a few without whom this thesis would not have been possible.

Christine Zhang, at the Faculty of Medicine Flow Cytometry Core Facility, for training and support. Michelle Queau, Kristin Hunt, Laurie Lange and the rest of the Manitoba Tumour Bank staff. Mandy Squires for navigating the sea of patient databases on my behalf. Donna Hewitt for her work recruiting and consenting donors, and collecting research samples. Darlene Zwarych for ensuring regulatory approval. And, of course, the many patients and healthy donors who gave blood to make this research possible.

Finally, I'd like to thank the Thorlakson Foundation, the CancerCare Manitoba Foundation, Research Manitoba and the Manitoba Medical Services Foundation for the funding which supported this study.

TABLE OF CONTENTS

LIST OF TABLES

LIST OF FIGURES

LIST OF ABREVIATIONS

2-DG	2-deoxy-D-glucose
7-AAD	7-amino-actinomycin D
ADP	Adenosine diphosphate
ADPR	ADP-ribose
AGAT	O6-alkylguanine-DNA alkyltransferase
alloHCT	allogeneic hematopoietic cell transplantation
AML	acute myeloid leukemia
AMP	adenosine monophosphate
ART	ADP-ribosyltransferase
ASCT	autologous hematopoietic stem cell transplantation
ATG	autophagy protein
ATP	adenosine triphosphate
BCL-2	B-cell CLL/lymphoma 2
BCR	B-cell antigen receptor
BMSC	bone marrow stromal cell
BN-PAGE	Blue-Native Polyacrylamide Gel Electrophoresis
BTK	Bruton's tyrosine kinase
CCR	CC-chemokine receptor
CI	Combination Index
CLL	chronic lymphocytic leukemia
CR	complete remission
CXCL	CXC-chemokine ligand
CXCR	CXC-chemokine receptor
dATP	deoxyadenosine triphosphate
DCFH-DA	2',7'-dichlorodihydrofluorescein diacetate
DHE	dihydroethidium
DISC	death-inducing signaling complex
DLBCL	diffuse large B-cell lymphoma
DR	dose-response
ECAR	extracellular acidification rates
eNAMPT	nicotinamide phosphoribosyltransferase (extracellular isoform)
ETC	electron transport chain
exNAD	exogenous NAD
FC	fludarabine and cyclophosphamide treatment
FCCP	carbonyl cyanide-p-trifluoromethoxyphenylhydrazone
FCR	fludarabine, cyclophosphamide and rituximab treatment
FDC	follicular dendritic cell
FFA	free fatty acids

FISH	fluorescence in-situ hybridization
GAPDH	glyceraldehyde-3-phosphate dehydrogenase
GSH	glutathione (reduced form)
GSSG	glutathione disulfide
GVL	graft-versus-leukemia activity
HSC	hematopoietic stem cell
Ig	immunoglobulin
IgVH	immunoglobulin heavy chain
iNAMPT	nicotinamide phosphoribosyltransferase (intracellular isoform)
ITAM	immunoreceptor tyrosine-based activation motif
LD_{50}	median lethal dose
LDH	lactate dehydrogenase
LDT	lymphocyte doubling time
MAPK	mitogen-activated protein kinase
MMP	mitochondrial membrane potential
MRD	minimal residual disease
MSC	mesenchymal stromal cell
NAD	nicotinamide adenine dinucleotide
NAD+	nicotinamide adenine dinucleotide (oxidised form)
NADH	nicotinamide adenine dinucleotide (reduced form)
NADP	nicotinamide adenine dinucleotide phosphate
NADP+	nicotinamide adenine dinucleotide phosphate (oxidised form)
NADPH	nicotinamide adenine dinucleotide phosphate (reduced form)
Nam	nicotinamide
NAMPT	nicotinamide phosphoribosyltransferase
NF-κB	nuclear factor kappa-light-chain-enhancer of activated B cells
NK	natural killer cell
NMN	nicotinamide mononucleotide
NMNAT	NMN adenylyl transferase
NOX	nicotinamide adenine dinucleotide phosphate oxidase
OAADPR	O-acetyl-ADP-ribose
OCR	oxygen consumption rates
OR	overall response
OS	overall survival
PARP	poly-ADP-ribose polymerases
PBMC	peripheral blood mononuclear cells
PFS	progression-free survival

PI	propidium iodide
PI3K	phosphatidylinositide 3 kinase
PKC	protein kinase C
PMA	phorbol 12-myristate 13-acetate
PRPP	phosphoribosyl pyrophosphate
ROS	reactive oxygen species
SLL	small lymphocytic lymphoma
smIg	surface membrane immunoglobulin
SOD	superoxide dismutase
SYK	spleen tyrosine kinase
TCA	tricarboxylic acid
TCR	T-cell antigen receptor
TMRM	tetramethylrhodamine methyl ester
TNF	tumor necrosis factor
Zap-70	zeta-chain-associated protein of 70 kD
Z-VAD, Z-VAD-fmk	N-benzlyoxycarbonyl-valyl-alanylaspartyl-fluoromethylketone

1. INTRODUCTION

1.1. Chronic Lymphocytic Leukemia

1.1.1. Epidemiology and Diagnosis

Chronic lymphocytic leukemia (CLL) is the most common blood cancer among adults in Western countries.[1,2] It is characterised by the abnormal accumulation, in the peripheral blood, bone marrow and secondary lymphatic tissues (lymph nodes, spleen), of clonal, morphologically mature B-lymphocytes (B-cells), co-expressing antigens CD19, CD20 and CD23, and the T-lymphocyte antigen CD5.[1,3] Available treatments often induce remission; however, as almost all patients eventually relapse, CLL remains incurable.[1,2,4] CLL and the related small lymphocytic lymphoma (SLL), where CLL cells are present primarily in the lymph nodes and spleen, are most frequently seen in North America where they represent one quarter of all adult leukemias.[3] Their reported age-adjusted, combined incidence is 5.13/100,000 with a median age at diagnosis between 67 and 72 years, and a slight predominance in males (1.3:1 to 1.7:1).[1,2,5] However, as many patients are now diagnosed by flow cytometry and these may not be included in cancer registries, their true incidence has been placed as high as 7.99/100,000 and continues to rise.[1,2] While this may be attributable, in part, to improved diagnostics, incidence also increases with age and is therefore expected to continue to rise as the populations of western countries age.[1,2,6]

As most patients are asymptomatic in the early stages of CLL, the first evidence of the disease is often lymphocytosis detected as part of routine blood tests.[3,7] When patients do present with symptoms, these may include anemia or thrombocytopenia due to bone marrow failure or autoimmunity, splenomegaly and/or hepatomegaly, unintended weight loss, fatigue, fever, night sweats, or frequent or severe infections due to immune disfunction.[1,3,7] In either case,

confirmation of CLL diagnosis requires a monoclonal B-lymphocyte count greater than 5000 per µL in the peripheral blood, which persists for a minimum of 3 months, along with flow cytometric confirmation of the restricted expression of either the immunoglobulin kappa or lambda light chain and co-expression of CD19, CD20, CD23 and CD5.[1]

1.1.2. CLL Biology

1.1.2.1. Cell-Cell Interactions

CLL has historically been viewed as an accumulative disease where malignant cells proliferate slowly and accumulate in the body due to aberrantly long lifespans.[8–10] This was largely based on the study of CLL cells isolated from the peripheral blood and supported by a low number of proliferating CLL cells in this compartment and their appearance, which is indistinguishable from resting B-lymphocytes. In addition, some CLL patients exhibit stable disease and do not require treatment for a decade or more.[11–13] It was therefore believed that CLL resulted primarily from defects in these cells' apoptotic machinery.[8–10]

While many of the most common genetic aberrations seen in CLL do impart a relative resistance to apoptosis, recent studies have also demonstrated a high turnover of CLL cells *in vivo*, indicating that they both proliferate and die at appreciable rates.[11,12,14] These cells are now known to depend on complex interactions with non-malignant cells, matrix and soluble factors in the bone marrow and lymph nodes for their survival and proliferation.[15] *In vitro* and even in circulation, these cells become increasingly fragile and prone to apoptosis without these supporting factors.[15,16] The bone marrow and lymph node microenvironments and the signalling pathways they activate in CLL cells are therefore attractive targets for new treatment strategies and several novel agents aimed at them have shown promise in recent years.

1.1.2.1.1. Microenvironment in Lymphopoiesis

In normal biology, B-lymphocytes arise from hematopoietic stem cells (HSCs) in the bone marrow. There, their proliferation and differentiation into CD19-, CD20- and CD38-expressing immature B-cells is regulated and directed by interactions with bone marrow stromal cells (BMSCs).[17–19] Much of this early maturation process concerns somatic recombination of the immunoglobulin (Ig) genes, which encode both secreted antibodies and the surface membrane immunoglobulin (smIg) component of the B-cell antigen receptor (BCR). By nearly random rearrangement of variable (V), diversity (D), and joining (J) gene segments, each maturing B-lymphocyte acquires the ability to produce immunoglubulins with a unique complementarity determining region, allowing them to bind a wide variety of target epitopes and protect the organism from diverse pathogens; however, this introduces the risk of producing lymphocytes reactive to "autoantigens" produced by the organism's own cells.[15,19] BMSCs also play an important role in eliminating these potentially harmful B-cells by protecting clones destined to progress to maturity while allowing damaged and self-reactive precursor B-cells to undergo apoptosis or macrophage mediated cell death.[18,20] Surviving B-cells then enter a transitional stage, characterised by CD5 expression, leave the bone marrow and enter into circulation where most mature into IgM and IgD producing, CD5 negative, CD38 low, CD19, CD20, and CD23 positive follicular B-cells, which circulate through the lymph nodes and spleen.[19,21] There, binding of the BCR to soluble antigens or those presented by follicular dendritic cells (FDCs) and co-stimulation from activated T cells leads to the CXC-chemokine receptor 5 (CXCR5) and CC-chemokine receptor 7 (CCR7) dependent formation of "germinal center" structures where their antigen specificity is fine-tuned by class-switch recombination and somatic hypermutation of their Ig genes.[21,22] B-cells proliferate and differentiate into CD38 high, CD20 negative

plasmablasts (precursors to antibody producing plasma cells) or long lived, CD38 negative, CD20 positive memory cells which maintain the plasmablast pool, ensuring the persistence of acquired immunity.[19,21] A small subset of CXCR4 expressing plasmablasts home to CXC-chemokine ligand 12 (CXCL12) –rich survival niches in the bone marrow, where they become long lived plasma cells which do not proliferate but can survive and produce antibodies for the lifetime of the individual.[21] Others differentiate in the periphery and produce large quantities of antibodies but die shortly after removal of their target antigen.[19,21] In either case, the ongoing survival of mature B-cells is dependent on a combination of "tonic" antigen-independent, and antigen-dependent BCR signalling.[23–25]

1.1.2.1.2. The CLL Microenvironments

Similarly, CLL cells are arrested in the G0-G1 phase of the cell cycle and relatively fragile in the peripheral blood, but become highly resistant to chemotherapy and proliferate rapidly within the bone marrow and lymph nodes.[13] As much as 1% of the total CLL cell population dies each day *in vivo*, however this is offset and often exceeded by the number CLL cells newly generated, primarily within specialized structures resembling germinal centres in the lymph nodes and spleen.[12,26] These "proliferation centres" are populated by large, proliferating CLL cells, BMSC-like mesenchymal stromal cells (MSCs), FDCs, CD4 positive T-lymphocytes and monocyte derived nurse-like cells.[17,27–29] Through chemokine receptors such as CXCR4 and CXCR5, integrins such as very late antigen-4, and tumor necrosis factor (TNF) receptor family members, these neighboring cells attract CLL cells, act as attachment points to retain them in the microenvironment and initiate survival signals.[17,18] However, comparative gene expression analyses have identified BCR signalling as the most prominent pathway activated in the bone

marrow and lymph nodes, leading to prolonged cell survival, proliferation and the metabolic adaptation required to support them.[13]

1.1.2.1.3. BCR Signalling

The BCR is composed of four proteins; the immunoglobulin heavy and light chains, which compose the antigen-specific smIg, and the signal transducing CD79A and CD79B.[23] Binding of the smIg to its target epitope leads to the activation of cytoplasmic members of the SRC family of kinases, such as tyrosine-protein kinases LYN, FYN, or BLK.[23] These kinases then phosphorylate spleen tyrosine kinase (SYK), Bruton's tyrosine kinase (BTK), and phosphatidylinositide 3-kinases (PI3Ks), leading to the activation of the phospholipase Cγ, MAPK, protein kinase Cβ and NF-κB signaling pathways, culminating in cell survival and proliferation, and the expression of chemokines, such as CCL3 and CCL4 that attract T-lymphocytes and monocytes.[17,23,30]

Unlike some B-cell malignancies, CLL cells lack recurrent activating mutations in the BCR pathway.[23,31,32] Instead, antigen-dependant BCR signalling, selection and clonal expansion are thought to be the major driving forces behind CLL initiation and progression.[23,33,34] While there is no evidence that oncogenic transformation precedes the follicular B-cell stage, certain V(D)J combinations seem to be selected during CLL initiation. As many as 1/3 of CLL patients express "stereotyped" BCRs that correlate with poor prognosis, suggesting that a common antigen may be involved in the initial expansion of the CLL clone.[35–38] Additionally, in only 60% of CLL cases, termed mutated CLL (M-CLL), CLL cells' Ig genes have undergone somatic hypermutation while the remaining unmutated (U-CLL) cases retain 98% homology or more between the variable region of their immunoglobulin heavy chain gene (IgVH) and the germline sequence;[35] however, it is the U-CLL group that caries the worse prognosis, with a median

survival for early-stage patients of only 8 years, compared to 24 years for M-CLL patients.[39] This may be explained by evidence that M-CLL cells are selected based on their high affinity for relatively few antigens while U-CLL cells express polyreactive Ig, which bind weakly to multiple ubiquitous antigens including bacterial, fungal and a variety of autoantigens, potentially leading to more frequent BCR activation and increased expression of active B-lymphocyte markers.[23,40–48]

One such marker, the non-receptor tyrosine kinase Zeta-chain-associated protein of 70 kD (Zap-70), was long thought to be uniquely expressed in T-lymphocytes but is now known to also be expressed by activated B-lymphocytes.[49–51] While it plays a central role in T-cell antigen receptor (TCR) signalling, the role of Zap-70 in B-lymphocytes is not yet fully understood. It is structurally similar to SYK and its expression in a subset of CLL cases it associated with increased BCR signalling, enhanced cell survival and migration in response to chemokines present in the lymph nodes, and increased binding to stromal cells.[52–56] Due to similar findings involving unmutated IgVH and CD38 expression, and a strong correlation between the three, these prognostic markers are all thought to identify a subset of CLL clones, which are more responsive to their microenvironment, leading to increased cell survival and proliferation and a more aggressive disease course.[23,57]

Some evidence also suggests a role for tonic BCR signalling in CLL pathogenesis, such as persistent LYN, SYK, MAPK and NF-κB phosphorylation in CLL cells in the peripheral blood and *in vitro*;[58–61] however, this remains controversial as it may simply reflect recent antigen-dependent BCR activation, as CLL cells circulate between lymph nodes and the peripheral blood.[23] The question is further complicated by the discovery that CLL BCRs are capable of binding and being activated by epitopes located in framework regions of smIg and secreted

antibodies. This form of cell-autonomous signalling is thought to be unique to CLL but independent of IgVH stereotypy or mutational status, and may represent the common antigen driving CLL initiation.[62,63] While this mechanism is not sufficient to induce cell proliferation alone, it is thought to contribute indirectly to clonal selection and tumour initiation by prolonging the survival of CLL cells until stronger activating signals are received.[34]

In addition to proliferation and survival, BCR signalling also regulates the metabolic pathways required to meet the energy demands of proliferating cells.[64] For instance, the expression of nicotinamide phosphoribosyltransferase (NAMPT) is upregulated by the NF-κB pathway, and the gene encoding this enzyme is among those most upregulated in the lymph node microenvironment.[13] NAMPT catalyses the rate limiting step in generating nicotinamide adenine dinucleotide (NAD), a cofactor for reductive and oxidative (redox) reactions involved in energy metabolism by both glycolysis and mitochondrial respiration,[65–67] and a substrate for signalling events involved in regulating other metabolic enzymes, immune response, DNA damage repair, cell survival and proliferation.[68–75] High expression of the intracellular isoform of NAMPT (iNAMPT) is linked to increased cell survival, proliferation, and resistance to chemotherapy and oxidative stress. [76–81] In addition, its extracellular isoform, eNAMPT, acts as a cytokine to promote inflammation, and drives the differentiation of monocytes into supportive NLCs, completing a feed-forward loop where CLL cells promote the formation of microenvironments that, in turn, promote their own survival and proliferation.[82]

1.1.2.2. Reactive Oxygen Species

Cellular peroxides, superoxides and hydroxyl radicals, collectively termed reactive oxygen species (ROS), are a class of highly reactive oxidants capable of causing damage to lipids, proteins and nucleic acids; leading to impaired metabolism and cell death.[83–85] Their primary

source is the partial reduction of oxygen to superoxide anions by electron transport chain (ETC) complexes I and III, involved in mitochondrial respiration.[84,86] While this process is mitigated by the assembly of ETC complexes I, III and IV into larger, supramolecular structures called respirasomes or supercomplexes in response to increases in cellular energy demands, these supercomplexes continue to produce considerable quantities of superoxide anions.[87,88] The cellular defense against superoxides consists of their conversion to peroxides by enzymes of the superoxide dismutase (SOD) family. By reaction with cuprous (Cu^{+}) or ferrous (Fe^{2+}) ions, these peroxides also give rise to hydroxyl radicals. Alternately, peroxides can be further reduced by direct reaction with the tripeptide glutathione, or through the enzymatic activity of glutathione peroxidases, peroxiredoxins, thioredoxin and catalase.[83–85,89] While the interplay between ROS and apoptosis is complex and not fully understood, it is clear that apoptotic signalling pathways can both be activated by ROS and induce mitochondrial ROS production, and that ROS is necessary for apoptotic cell death in many contexts.[85,90,91] Additionally, ROS play important roles in cell signalling pathways, notably involved in regulating metabolism and cell survival in response to environmental stress. These include the activation of receptor tyrosine kinases,[92] the nuclear factor kappa-light-chain-enhancer of activated B cells (NF-κB) signalling pathway[93] and macroautophagy; a process by which long-lived proteins and organelles are degraded.[83,84,94] The latter serves both as a mechanism to dispose of damaged or unnecessary cellular components, and as a source of macromolecules for energy metabolism, but can lead to cell death if unchecked.[95–97]

In B-lymphocytes ROS are also produced by nicotinamide adenine dinucleotide phosphate (NADP) oxidase (NOX), notably allowing rapid activation of mitogen-activated protein kinase (MAPK) and cell proliferation upon B-cell antigen receptor (BCR) engagement.[98,99] Though

CLL cells exhibit low NOX expression and activity consistent with sustained BCR activation, high levels of cellular ROS are observed, likely due to increased mitochondrial respiration in these cells.[100–102] This may contribute to the accumulation of oncogenic mutations in cells resistant to DNA damage induced apoptosis; however, as excessive MAPK activation can also signal for the initiation of apoptosis, it is unsurprising that ROS levels are tightly regulated in CLL by high expression of the antioxidant peptide glutathione and the rate limiting enzyme for its synthesis, glutamate-cysteine ligase.[100,103,104] Finally, elevated ROS are also thought to contribute to the formation and maintenance of the CLL microenvironments by inducing natural killer (NK) cell and T-lymphocyte dysfunction.[98,105–107]

1.1.2.3. Metabolism in CLL

The prevalence of metabolic dysregulation in cancer and its importance for meeting the energy demands of tumour growth were recognized as early as the 1920s;[108] however, study of this metabolic adaptation has been focussed on a process known as the Warburg effect, where malignant cells show increased glucose uptake and propensity for anaerobic glycolysis and lactate production, even in normoxic conditions. This process has been identified in several lymphoproliferative disorders and is predictive of patient outcome in diffuse large B-cell lymphoma (DLBCL).[109,110] Conversely, despite having a functional glycolytic pathway, CLL cells absorb glucose at a reduced rate *in vitro* and *in vivo* and high glucose uptake in secondary lymphatic tissues is highly suggestive of CLL transformation to DLBCL or the development of an aggressive secondary lymphoma.[64,111–115] Instead, evidence suggests that CLL cells are reliant primarily on lipid metabolism to meet their energy demands. Constitutive and CXCR4-mediated activation of signal transducer and activator of transcription 3 (STAT3) leads these cells to aberrantly express lipoprotein lipase, the master regulator of cellular lipoprotein uptake and

triglyceride hydrolysis into free fatty acids (FFA), the levels of which correlate with disease agressivity.[107,116–120] Low-density lipoprotein drives the formation of cytoplasmic lipid vacuoles and preferential use of FFA as an energy source.[107] Accordingly, CLL cells exhibit increased mitochondrial biogenesis, mitochondrial number and overall ETC activity and capacity, supporting a reliance on mitochondrial lipid oxidation for ATP synthesis.[100]

1.1.3. Prognosis and Treatment

1.1.3.1. Prognosis

Two widely accepted staging systems are used to stratify patients at diagnosis and throughout the disease course. Binet Staging, which is based on the number of involved areas of the body, is primarily use in Europe (Table 1).[121] Rai Staging, based on signs of CLL cell infiltration into the bone marrow and lymphatic tissues, is the preferred system in North America and was used in this study (Table 2).[122] Both systems have seen some evolution since their inception and now define low (Rai stage 0, Binet A), intermediate (Rai I-II, Binet B), and highrisk categories (Rai III-IV, Binet C);[1,123] however, as the disease course varies greatly, with some patients exhibiting stable, asymptomatic disease for extended periods while others progress rapidly to aggressive disease requiring treatment, staging alone is not sufficient for prognosis and several other factors are used to predict disease progression (Table 3).[1,6,7]

After staging, lymphocyte doubling time (LDT) represents the most important prognostic factor. Both an early requirement for treatment and shortened survival are predicted for patients with LDT of less than 12 months.[3,7] Shorter relative survival times are also predicted for males and patients aged 70 years or more.[3,124–126] Furthermore, routine clinical blood test provide additional information as low vitamin D levels predict a more aggressive disease course including shorter time to treatment and survival, and elevated β2-microglobulin serves as a

Table 1: Rai Staging[1,7,122]		
Rai Stage	**Modified Stage**	**Description**
0	Low Risk	Lymphocytosis only
I	Intermediate Risk	Lymphocytosis + Lymphadenopathy
II	Intermediate Risk	Lymphocytosis + Splenomegaly
III	High Risk	Lymphocytosis + Hemoglobin < 110 g/L
IV	High Risk	Lymphocytosis + Platelets < 100 x 10^9/L

Table 2: Binet Staging[1,121]		
Binet Stage	**Modified Stage**	**Description**
A	Low Risk	Hb ≥ 10 g/dL + Platelets ≥ 100 x 10^9/L + ≤ 2 Areas of nodal or organ enlargement
B	Intermediate Risk	Hb ≥ 10 g/dL + Platelets ≥ 100 x 10^9/L + > 2 Areas of nodal or organ enlargement
C	High Risk	Hb ≤ 10 g/dL and/or Platelets < 100 x 10^9/L

Table 3: Routinely Measured Prognostic Markers[7]		
Prognostic Marker	**Better Prognosis**	**Worse Prognosis**
Sex	Female	Male
Age	< 70 years	≥ 70 years
Plasma vitamin D level	Sufficient	Insufficient
Lymphocyte count	< 12 x 10^9/L	≥ 12 x 10^9/L
Lymphocyte doubling time	> 12 months	< 12 months
Number of “Smudge cells”	≥ 30%	< 30%
β2-microglobulin level	Low	High
B cell count	< 11 x 10^9/L	≥ 11 x 10^9/L
CD38	< 20% cells positive	≥ 20% cells positive
ZAP-70	< 20% cells positive	≥ 20% cells positive
FISH	del13q	del11q or del17p
IgVH gene	Mutated	Unmutated

general marker for high tumour burden, low renal function and increased production of inflammatory cytokines, interleukin 6 and interleukin 8.[7,125,127–129] The latter is also predictive of shorter time to treatment, progression-free survival (PFS, Table 4), overall survival (OS, Table 4), and the development of second malignancies.[3,7,124]

Each patient's CLL cells are typically identical with respect to IgVH mutation and IgVH mutational status remains stable throughout the course of the disease.[39] Roughly 40% of CLL patients present with IgVH unmutated U-CLL and these have a more aggressive disease course than M-CLL patients. They respond more poorly to chemotherapy, and have shorter remissions and survival.[130] Though IgVH mutational status is not yet routinely tested in many centers, it is often determined in the context of research and clinical trials.[7] Two surrogate markers, Zap-70 and CD38 expression, are more commonly tested in the course of prognosis. Both have negative prognostic value and are correlated with U-CLL, but can vary during the disease course.[131–133] CLL cases where no less than 20% of circulating CLL cells express these proteins, as determined by flow cytometry, are considered Zap-70 or CD38 positive and typically have shorter time to treatment and survival.[132,133]

Finally, fluorescence in-situ hybridization (FISH) analysis of the CLL clone is used to identify the presence of recurrent large chromosomal aberrations including deletions involving the 14th cytogenetic band of the long arm of chromosome 13 (del13q14, del13q), del11q22-23 (del11q) and del17p13 (del17p).[1,3,6,7] Due to the duration and cost of this assay, FISH data is often unavailable at the time of first treatment and primarily informs second line therapy.[7] While isolated del13q indicates a good prognosis, del11q predicts an aggressive disease course, early requirement for treatment and early relapse from chemotherapy, and patients with del17p respond poorly to nucleoside analogs.[35]

Table 4: Measures of Clinical Response[7,134]		
Response	**Abbreviation**	**Description**
Complete Remission	CR	No symptoms, hepatosplenomegaly or lymphadenopathy. Normal complete blood cell count. < 30% lymphocytes and no lymphoid nodules in the bone marrow.
Partial Remission	PR	> 50% decrease in peripheral blood lymphocyte count and > 50% decrease in lymphadenopathy or hepatosplenomegaly, with normal or improved hemoglobin, neutrophil or platelet count.
Partial Remission with Lymphocytosis	PR-L	As above, with < 50% decrease in peripheral blood lymphocyte count.
Overall Response	OR	Combined rate of complete, and partial remission.
Progression-Free Survival	PFS	The length of time between the start of treatment, and disease progression or death.
Overall Survival	OS	The length of time between the start of treatment, and the patient's death from any cause.
Time to Next Treatment	TTNT	The length of time between the end of treatment and start of the next therapy.
Minimal Residual Disease	MRD	Measure of remaining CLL cells in the bone marrow or peripheral blood following treatment.

1.1.3.2. Indication to treat

Patients with early-stage, asymptomatic disease are typically monitored but not treated as evidence suggests that treatment at this stage is not beneficial and may even be harmful.[1,3,7] Asymptomatic patients in the intermediate risk category may also be monitored without treatment until the apparition of symptoms. Treatment is indicated for patients with high risk disease as well as those with signs of disease progression, as evidenced by doubling of lymphocyte count, lymph node or spleen size within six month, a 50% increase in any of these within two months, or progressive anemia, neutropenia or thrombocytopenia. Treatment is also indicated for patients with symptomatic disease regardless of stage or progression.[1,3,6,7]

1.1.3.3. Treatment Components

1.1.3.3.1. Alkylating Agents

Nitrogen mustards such as 4-[bis(2-chlorethyl)amino]benzenebutanoic acid (chlorambucil, Fig. 1A) and N,N-bis(2-chloroethyl)-1,3,2-oxazaphosphinan-2-amine 2-oxide (cyclophosphamide, Fig. 1B) have formed the backbone of CLL therapy for several decades and chlorambucil remains the treatment of choice for patients unable to tolerate more aggressive regimens.[1,3,6,7] As a single agent, the latter achieves overall response (OR, Table 4) rates around 50%, but very low complete remission (CR, Table 4) rates, as measured by the absence of symptoms, hepatosplenomegaly and lymphadenopathy, and normal complete blood cell count.[135–137] Cyclophosphamide produces similar results.[137] These agents also carry strong myelosupressive effects and increase the risk of secondary acute leukemia.[1,3] They exert their antitumour activity primarily through the transfer of alkyl groups to DNA at the N7 positions of guanine forming N^7-guaninyl and N^7-bis-guaninyl products, the latter of which is capable of crosslinking DNA strands.[138–140] While this DNA damage can be directly repaired by O6-

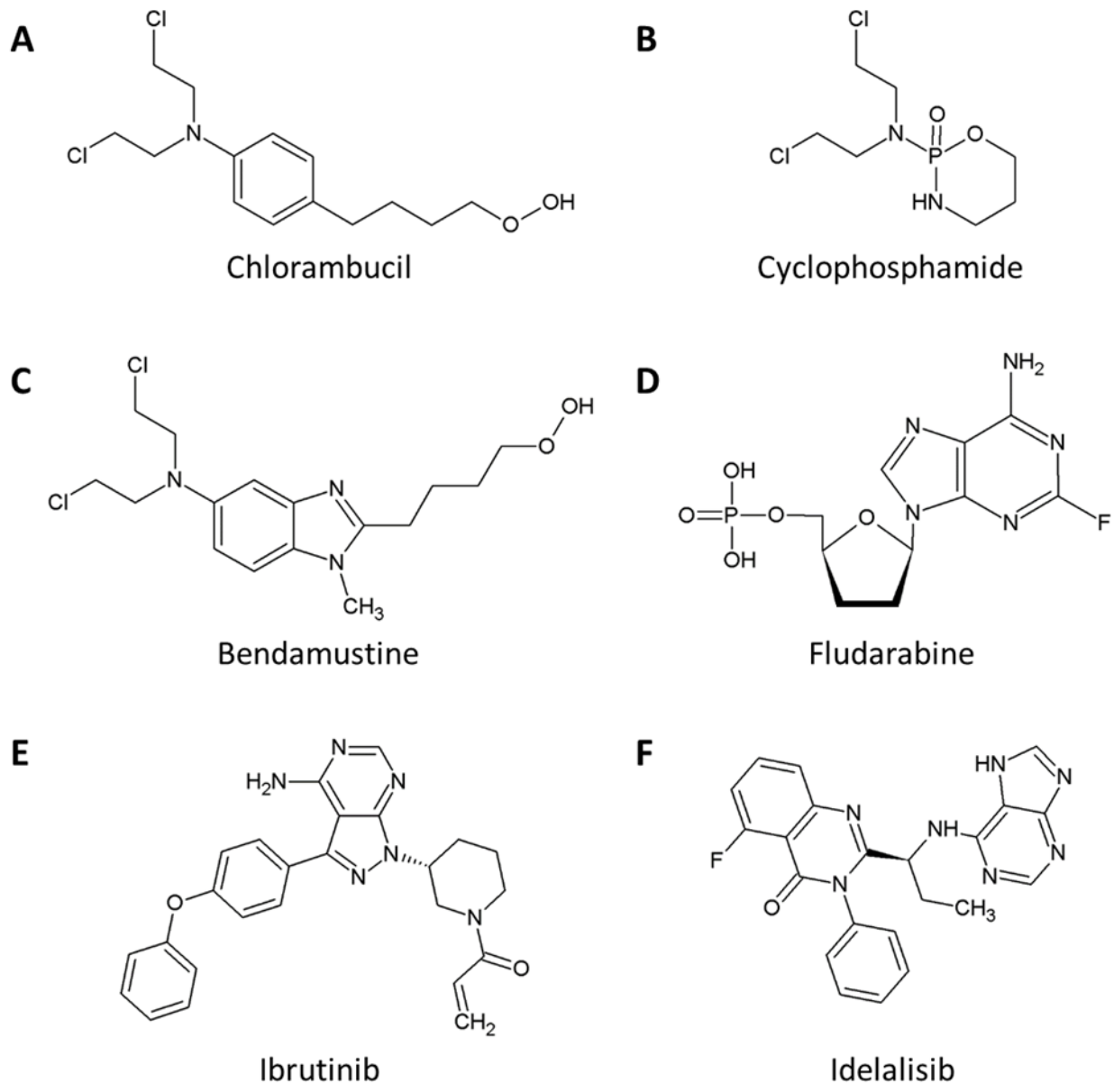

Figure 1: Agents commonly used in CLL treatment. Common chemotherapeutics used in CLL treatment include the alkylating agents chlorambucil (A), cyclophosphamide (B) and bendamustine (C), and the adenosine monophosphate analogue fludarabine (D). The novel tyrosine kinase inhibitors ibrutinib (E) and idelalisib (F) are also seeing increasing clinical use.

alkylguanine-DNA alkyltransferase (AGAT), or removed by either non-homologous end joining or homologous recombination repair, accumulation of DNA damage results in activation of P53 and apoptosis as described above.[138,141] Though the mechanism is unknown, alkylating agents also induce ROS production, which contributes to their cytotoxic activity.[92,95] Finally, these agents are able to alkylate thiol groups in peptides and proteins, most notably glutathione.[142] This may cooperate with ROS production in the induction of apoptosis. Nevertheless, CLL cases harboring del17p or TP53 mutations are resistant to these agents.[143]

4-[5-[Bis(2-chloroethyl)amino]-1-methylbenzimidazol-2-yl]butanoic acid (bendamustine, Fig. 1C) was designed to combine alkylating and antimetabolite activity. In addition to a 2-chloroethylamine alkylating group and a butyric acid side chain it shares with chlorambucil, it contains a unique a benzimidazole ring.[141] Unlike other alkylating agents, it does not activate AGAT and is active in P53 deficient cells.[141,144] It is thought to act through apoptosis and mitotic catastrophe, a caspase independent mechanism of cell death following errors in mitosis caused by persistent DNA damage.[141,144,145] As a single agent, bendamustine produces higher CR rates, progression-free survival (PFS) and time to next treatment (TTNT, Table 4) than chlorambucil, but with a higher incidence of serious side effects.[146]

1.1.3.3.2. Nucleoside Analogs

Multiple deoxynucleoside analogs, including 2'-deoxyadenosine, 2-chloro-2'-deoxyadenosine (cladribine), 9-β-D-arabinofuranosyl-2-fluoroadenine monophosphate (F-ara-AMP, fludarabine, Fig. 1D), and 2-chloro-2'-fluorodeoxyadenosine, have been investigated for CLL treatment.[147,148] Due to its more favorable toxicity profile and efficacy in CLL, fludarabine has been the backbone of standard care for many years.[1,139,148] After being taken up into lymphocytes, this agent is phosphorylated to F-ara-ATP which can be incorporated into

elongating nucleic acids, terminating DNA or RNA synthesis and leading to DNA single strand breaks and P53 dependent apoptosis. [90,139,149,150] Additionally, F-ara-ATP inhibits several enzymes involved in DNA synthesis and repair, including DNA polymerases and DNA ligase.[151,152] Accordingly, fludarabine is thought to act primarily on actively proliferating cells.[153] It was therefore proposed that, by combining fludarabine with a DNA damaging alkylating agent, DNA repair mechanisms involving DNA synthesis could be activated and increase fludarabine's efficacy in quiescent CLL cells.[153] This lead to the development of synergistic combination chemotherapy regimens.[139,148,149,153–155]

As a single agent, fludarabine produced varied results ranging from no benefit over previous regimens, to improved OR, PFS, response duration or overall survival (OS).[135,136,156–158] But, the introduction of combination chemotherapy with fludarabine and cyclophosphamide (FC) increased OR and CR rates to 74.3% and 23.4% respectively in previously untreated patients and significantly increased the duration of remission.[155] However, fludarabine is not effective in P53 mutated or deleted CLL cases and is poorly tolerated by many patients due significant toxicities including neurotoxicity, severe immunosuppression, and increased risk of developing acute myeloid leukemia (AML), especially in combination with alkylators.[143,150,159,160]

1.1.3.3.3. Immunotherapy

Rituximab is a chimeric monoclonal antibody composed of a human IgG1 constant region and a murine variable region.[3] Its target, the CD20 surface antigen, is expressed by B-cells from the pro-B-cell stage to maturity, including CLL cells.[161] While this antibody has been shown to activate complement mediated cell lysis and to directly induce apoptosis as a result of CD20 binding, the importance of these mechanisms *in vivo* remain controvercial.[162] Instead, the *in vivo* activity of rituximab is likely reliant on antibody-dependent cell-mediated cytotoxicity affected

by monocytes, macrophages, natural killer cells and neutrophils.[162] As a single agent rituximab is effective against CLL cells in the peripheral blood, but fails to effectively clear these cells from the lymph nodes.[163,164] This has been attributed to lower levels of CD20 expression on CLL cells in the tissue microenvironments,[165] but may also relate to rituximab-induced increases in interleukin-6 expression by CLL cell, leading to increased CLL cell adhesion and expression of proinflammatory interleukin-8 and TNFα in the tissue microenvironments.[15,125,166] Additionally, high dose rituximab treatment is characterised by sudden and severe side effects related to chemokine release, including fever, chills, nausea, vomiting, hypotension, and dyspnea.[164] This led to the exclusion of patients with high tumour burden from later trials.[163] The true impact of anti-CD20 antibodies came with the addition of rituximab to the existing FC regimen (FCR), which produced unprecedented OR and CR rates of 95% and 70% respectively, leading to its adoption as the preferred regimen for clinically fit patients.[1,6,7,167] Though this synergy is poorly understood, it may be due, in part, to rituximab induced alterations in cytokine expression, and subsequent downregulation of anti-apoptotic BCL-2 family proteins in CLL cells.[3,168]

Novel humanized anti-CD20 antibodies have also been developed, including ofatumumab and obinutuzumab, and are currently in clinical trials.[169] Notably, the combination of obinutuzumab and chlorambucil has demonstrated improved response rates, PFS and OS over rituximab and chlorambucil for unfit, previously untreated patients.[170] Other antibody targets have also been explored, including CD52, present on B- and T-lymphocytes, monocytes and natural killer cells. The humanized anti-CD52 antibody alemtuzumab is active on CLL cells in the bone marrow, spleen and peripheral blood, but less effective in CLL cells in lymph nodes, and induces cytokine related side effects as seen with rituximab.[171] It is typically used in the

treatment of patients resistant to conventional therapy, whether due to acquired resistance to previous courses of treatment, 17p deletion or TP53 mutation.[7,171]

1.1.3.3.4. Tyrosine Kinase Inhibitors

Due to the fundamental importance of the microenvironment in CLL pathology, several agents targeting key cell-cell interactions have been proposed for CLL treatment.[17,23,172] However it is a class of tyrosine kinase inhibitors targeting the protein kinases of the BCR signalling cascade that have taken center stage in recent years.[23,35] Agents such as ibrutinib (Fig. 1E), targeting Bruton's tyrosine kinase (BTK), and idelalisib (Fig. 1F), targeting phosphatidylinositide 3-kinases δ (PI3Kδ), benefit from selectivity due to relatively restricted expression of these enzymes in B-lymphocytes.[23] In addition, their target enzymes also play roles in other signalling cascades such as those initiated by integrins and chemokine receptors. As a result, one of the early effects of treatment with these agents is redistribution of CLL cells from the tissue microenvironments to the peripheral blood, which is thought to contribute to treatment efficacy and may make CLL cells more susceptible to other agents.[173–176] Results from clinical trials investigating these agents in relapsed, refractory or high risk CLL cases, have been promising.[177–180] In short, both ibrutinib and idelalisib produce very high response rates and durable remission with continuous treatment, but patients relapse quickly with aggressive disease when treatment is discontinued. Some CLL cases have also progressed during clinical trials with these agents.[181] While the risk of progression is highest in patients with high risk features, including U-CLL, del17p and del11q, this has raised concerns as these patients are difficult to treat and effective options for salvage therapy have not yet been determined.[178,181,182] Additional concerns include off target effects on platelets and cardiac tissue leading to high incidence of bleeding-related adverse events and atrial fibrillation.[183–185] Nevertheless, idelalisib has been

approved for the treatment of relapsed, treatment refractory CLL, and ibrutinib has been approved for the treatment of relapsed, refractory, and 17p deleted CLL by Health Canada.[186,187] Clinical trials are ongoing in other patient groups.[188–196]

1.1.3.3.5. Hematopoietic Stem Cell Transplantation

Allogeneic hematopoietic cell transplantation (alloHCT) represents the only curative treatment available for CLL.[1,6,7] Due to the benefit of graft-versus-leukemia (GVL) activity where, following graft-versus-host disease, residual CLL cells are abolished, persistent absence of detectable disease is achieved in up to 50% of allografted patients;[197] however, its use is limited by the requirement for a related, matched donor and treatment related mortality rates are as high as 15-30%, two years after transplantation.[3,7,197] While autologous hematopoietic stem cell transplantation (ASCT) has also been studied in CLL, it does not benefit from GVL and was not found to be curative. In recent studies ASCT offered no survival advantage in comparison to FCR or when used as consolidation therapy following modern chemotherapeutic regimens.[198–200] In light of a risk as high as 12.4% of treatment related AML or myelodysplasia 5 years after transplantation, ASCT has been discontinued in some centres and alloHCT is offered only to young, clinically fit, relapsed or refractory patients.[3,7,201]

1.1.3.4. Treatment Strategy

As CLL remains incurable, the goal of treatment is to achieve the best possible initial response.[7] To this end, some centres now measure minimal residual disease (MRD, Table 4) by flow cytometric detection of circulating CLL cells following treatment when complete clinical remission has been achieved.[1,7,202] This is predictive of longer PFS and OS.[202,203] At the time of relapse, patients are reassessed and may continue to be treated with the same intent, provided

they remain clinically fit. In unfit patients, however, symptoms are typically treated with palliative intent.[7]

1.1.3.4.1. First-Line Treatment

Given the wide range in patient age and coincident or pre-existing medical conditions, treatment received is dependent on patient fitness.[1,3,6,7] Patients with normal rates of creatinine clearance, good performance status and low numbers of co-morbidities are considered fit and typically receive aggressive chemoimmunotherapy with fludarabine, cyclophosphamide and rituximab (FCR).[1,6,7] While this strategy achieves high response rates and overcomes the poor prognosis associated with del11q, strong myelosuppression and risk of secondary AML and myelodysplasia are limiting factors.[204] Even in this clinically fit group, dose reduction due to treatment toxicity is required for 50%, and early cessation of treatment for 25% of patients.[7] For frail elderly or unfit patients, the high toxicity of these combinations is considered to outweigh their benefits and these patients usually receive milder regimens such as the chlorambucil or bendamustine with or without rituximab or obinutuzumab.[1,6,7] Progression free survival with these regimens is also shortened in del17p and TP53 mutated CLL cases.[1,6] In the absence of more effective treatments, however, FCR still offers improved quality of life.[7]

1.1.3.4.2. Second-Line Treatment

Patients who relapse two years or more after FCR treatment or one year after other regimens are considered drug sensitive and may receive the same treatment.[1,6,7] Those who relapse early or do not respond to initial therapy, are considered treatment refractory and treated with alternate regimens.[1,6,7] Patients who develop resistance to alkylating agents may be treated with FCR, however most patients who remain clinically fit are treated with alemtuzumab-containing

regimens, followed by alloHCT when possible.[1,6,7] Unfit patients may also be treated with alemtuzumab, or with ibrutinib or idelalisib.

1.1.3.5. Emergence of Resistance

CLL cells have a documented propensity to undergo clonal evolution; acquiring new genetic mutations and chromosomal abnormalities throughout the disease course.[3,205,206] While this often entails selection of subpopulations resistant to specific therapeutic agents or classes of agents, as is seen with tyrosine kinase inhibitor treatment,[181] the acquisition of general markers of disease aggressivity, such as 11q and 17p deletion, are also common in both treated and untreated patients, particularly those with U-CLL and ZAP-70 or CD38 positive cases.[3,207,208] As most patients undergo multiple rounds of treatment and relapse, developed multidrug resistance represents a significant challenge for CLL therapy. In many cases, effective treatment options for relapsed refectory patients are not available.[7] There is, therefore, a requirement for new therapeutic approaches to treat these patients.

1.2. NAD Biology

1.2.1. Nicotinamide Phosphoribosyltransferase

The dinucleotide NAD^+ and its phosphorylated and reduced forms (NADH, $NADP^+$ and NADPH) play central roles in multiple metabolic, biosynthetic and signalling pathways. As such, NAD synthesis has recently been recognised as an important regulatory mechanism which coordinates diverse cellular functions including energy metabolism, immune response, proliferation and survival.[70,76] In mammals, NAD can be generated from tryptophan, nicotinic acid, or nicotinamide (Nam); however, as expression of key enzymes involved in NAD synthesis from tryptophan is restricted to liver and kidneys, and nicotinic acid availability is not sufficient

to maintain NAD levels, Nam salvage represents the main source of NAD for most mammalian cells.[76,209] This biosynthetic pathway consists of two steps. First, Nam and phosphoribosyl pyrophosphate (PRPP) are condensed by nicotinamide phosphoribosyltransferase (NAMPT) to form nicotinamide mononucleotide (NMN). NMN is then converted to NAD by NMN adenylyl transferases (NMNATs). The rate limiting enzyme in this process, NAMPT is expressed as an intracellular isoform (iNAMPT), present in the cytosol and nucleus, and an extracellular isoform (eNAMPT), which is thought to result from alternate post-transcriptional modification as it differs by molecular weight but not by sequence.[67,76,209] Both isoforms are catalytically active.[76,77]

As NAD does not passively traverse lipid bilayers, it is maintained in three distinct pools in the cytosol, nucleus and mitochondria. This allows the oxidoreductive state of each of these compartments to be regulated independently. For example, while cytoplasmic NAD/NADH ratio is typically held between 60 and 700 in eukaryotic cells, mitochondrial NAD/NADH ratios are maintained between 7 and 8.[67] Despite the absence of iNAMPT from mitochondria, maintenance of the mitochondrial NAD pool is also attributed to this enzyme as NMN is transported from the cytosol into the mitochondrial matrix to serve as the substrate for NMNAT3.[67] Furthermore, there is debate in the literature as to whether extracellular NAD can be taken up into cytoplasm and mitochondria through unknown transport mechanisms.[210–212] eNAMPT-mediated extracellular NAD synthesis may therefore also play a role in replenishing intracellular NAD pools. Accordingly, the rate of eNAMPT expression has been proposed as a mechanism by which gene regulation may influence the metabolic state of neighboring cells.[211]

eNAMPT was originally described as a secreted protein with a cytokine-like function which increased pre-B-cell colony formation, and named pre-B-cell colony-enhancing factor. It has

since been shown to upregulate IL-6, IL-8 and TNFα secretion in peripheral blood mononuclear cells (PBMCs), and inhibit apoptosis in neutrophils during inflammation and sepsis, and macrophages exhibiting obesity-associated ER-stress.[213–215] Evidence suggests that aberrant eNAMPT expression may play important roles in immune mediated conditions including inflammatory bowel disease, acute lung injury, rheumatoid arthritis and myocardial infarction, and be involved in the pathogenesis of metabolic disorders such as obesity and diabetes.[76] While the importance of eNAMPT's enzymatic activity has not been established in most of these contexts, it is known to be required for pro-inflammatory cytokine induction in rheumatoid arthritis and dispensable for IL-6 induction and cytoprotection in macrophages.[76,214] The enzyme was also once described as a putative insulin mimetic hormone named visfatin, but mounting evidence suggests roles for signalling cross talk or increased extracellular NMN or NAD synthesis in insulin receptor signalling, rather than direct activation of the insulin receptor by eNAMPT.[76,77,216,217] Conversely, eNAMPT is thought to contribute to obesity and diabetes associated vascular inflammation. It has been shown to activate the NF-κB signalling pathway in vascular endothelial cells, leading to increased expression of proteins involved in leukocyte adhesion to endothelium and destabilisation of atherosclerotic plaques.[76,218]

1.2.2. NAD in Reductive and Oxidative Reactions

The earliest recognised function of NAD was its role in cellular metabolism and energy production as a transporter of redox potential (Fig. 2A). In the cytosol, NAD^+ is reduced to NADH by glyceraldehyde-3-phosphate dehydrogenase (GAPDH), the rate-limiting enzyme in the glycolytic pathway.[65–67] In anaerobic cells and in malignant cell exhibiting the Warburg effect, reduction of the NADH produced is coupled to the conversion of the glycolytic product, pyruvate, to lactate by lactate dehydrogenase (LDH, Fig. 2B).[66] In aerobic cells however,

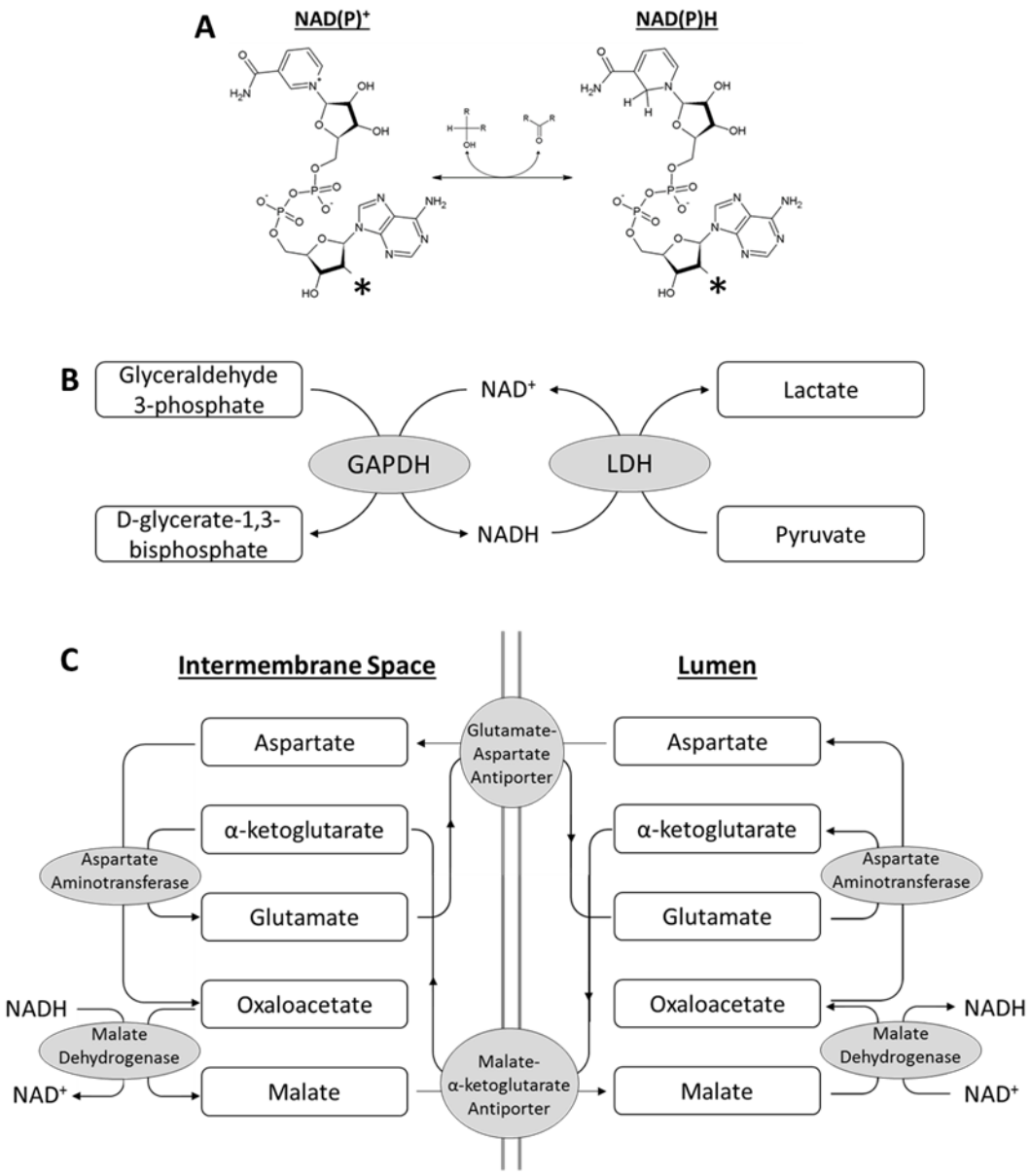

Figure 2: NAD and NADP in redox reactions. Nicotinamide adenine dinucleotide (NAD) and nicotinamide adenine dinucleotide phosphate (NADP) are essential cofactors for multiple cellular redox reactions. (A) The interconversion of their reduced, $NAD(P)^+$ forms and oxidised, NAD(P)H forms is enzymatically coupled to reduction or oxidation of diverse target molecules. * = OH (NAD), PO_4^{2-} (NADP). (B) The rate limiting step in the glycolytic pathway, conversion of glyceraldehyde-3-phosphate to D-glycerate-1,3-bisphosphate is coupled to the oxidation of NAD^+ by glyceraldehyde-3-phosphate dehydrogenase (GAPDH). In anaerobic cells and in malignant cell exhibiting the Warburg effect, reduction of the NADH produced is coupled to the conversion of the glycolytic product, pyruvate, to lactate by lactate dehydrogenase (LDH). (C) In aerobic cells, pyruvate is preferentially oxidised in the mitochondria. In this case, the reduction of cytosolic NADH is couples to the conversion of aspartate and α-ketoglutarate to malate and glutamate. These products are then transferred to the mitochondrial matrix, where the reverse reaction converts mitochondrial NAD+ to NADH.

pyruvate is preferentially oxidised in the mitochondria. In this case, the reduction of cytosolic NADH is coupled to the conversion of aspartate and α-ketoglutarate to malate and glutamate. In a process known as the malate-aspartate shuttle, these products are then transferred to the mitochondrial matrix by specific transporter proteins, where the reverse reaction converts mitochondrial NAD^+ to NADH (Fig. 2C).[66] The reductive potential of cytosolic NADH is therefore transferred to the mitochondria, while maintaining two distinct NAD pools.[67] As CLL cells lack the characteristic lactate production associated with the Warburg effect, this is likely the primary fate of cytosolic NADH in these cells.[64,111,112]

Similarly, in the mitochondrial matrix, NAD^+ is essential for the metabolism of pyruvate, amino acids and FFA. It acts as a cofactor for pyruvate dehydrogenase, tricarboxylic acid (TCA) cycle enzymes; isocitrate dehydrogenase, alpha-ketoglutarate dehydrogenase and malate dehydrogenase, and hydroxyacyl-CoA dehydrogenases in the fatty acid β-oxidation pathway.[66] Here, the NADH produced is the substrate for NADH:ubiquinone oxidoreductase (complex I) which catalyses the initiating event in the electron transport chain (ETC). The ETC couples a series of successive redox reactions to the generation of an electrochemical gradient (Fig. 3) across the mitochondrial inner membrane. As this gradient provides the motor force for the activity of ATP synthase, mitochondrial NAD is essential for the majority of ATP synthesis in the cell.[66]

1.2.3. Nicotinamide Adenine Dinucleotide Phosphate

NAD can also be converted to nicotinamide adenine dinucleotide phosphate (NADP) through the activity of cytosolic NAD kinase. Similarly to NAD, NADP is an essential cofactor for many redox reactions involved in macromolecule synthesis. $NADP^+$ is primarily reduced to NADPH by glucose-6-phosphate dehydrogenase and 6-phosphogluconate dehydrogenase in the

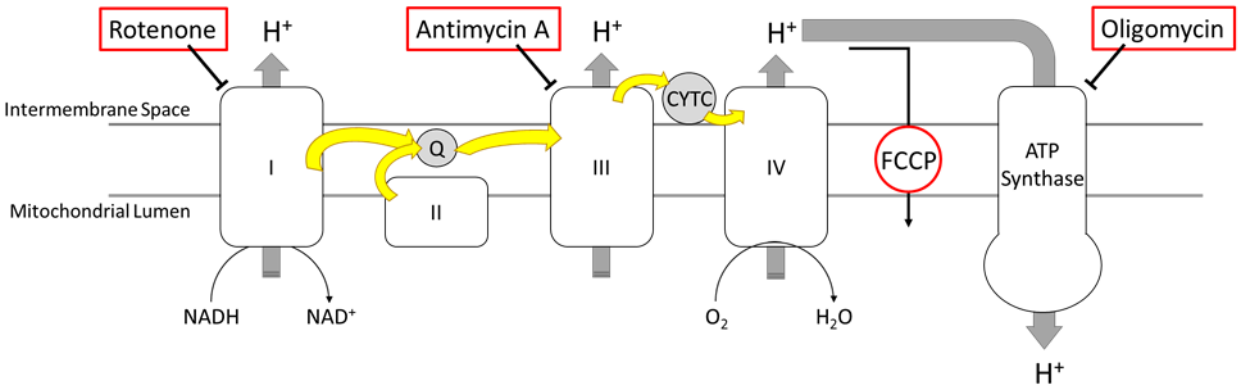

Figure 3: The mitochondrial electron transport chain. The mitochondrial electron transport chain (ETC) couples a series of successive redox reactions to the movement of protons from the mitochondrial matrix to the intermembrane space by complexes I, III and IV, generating an electrochemical gradient across the mitochondrial inner membrane which provides the motor force for the activity of ATP-synthase. Rotenone, antimycin A and oligomycin inhibit complexes I and III, and ATP synthase respectively. Carbonyl cyanide-p-trifluoromethoxyphenylhydrazone (FCCP) is a membrane permeable ionophore and acts as an uncoupling agent by transporting protons across the mitochondrial inner membrane, dissipating the electrochemical gradient.

pentose phosphate pathway, which is also responsible for the generation of ribose-5-phosphate required for nucleotide synthesis.[66] NADPH in turn, provides the reductive potential for reactions involved in lipid, cholesterol and nucleotide synthesis required for cellular proliferation. In addition, a very high cellular NADPH/$NADP^+$ ratio drives these otherwise endergonic reactions. The cellular concentrations of these dinucleotides are therefore tightly regulated, especially in proliferating cells.[66] NADPH can also contribute to energy metabolism as it is required by 2,4-dienoyl-CoA reductase, responsible for reducing problematic double bonds in unsaturated FFA during β-oxydation.[66] Finally, NADPH is an essential coenzyme for glutathione reductase, which maintains the cellular pool of reduced glutathione (GSH).[219]

1.2.4. Glutathione

Glutathione is a tripeptide consisting of glycine, cysteine and glutamate, present in the cytosol, mitochondria and nucleus. It is the primary cellular defense against both electrophilic molecules and ROS, reacting directly and as a substrate for enzymes such as glutathione-S-transferases and glutathione peroxidases to prevent these reactive molecules from interacting with nucleic acids and proteins.[219] Glutathione is therefore important in tumour resistance to both alkylating agents and ROS produced as a by-product of high ETC flux.[220] While reaction with electrophiles results in the formation of glutathione adducts which are exported from most cell types, the antioxidant activity of glutathione results in the oxidation of its reduced form (GSH) to glutathione disulfide (GSSG) and the NADPH-dependant activity of glutathione reductase is required to return it to its GSH form.[219] As discussed in the previous section, the rate limiting enzyme for glutathione synthesis, glutamate-cysteine ligase is highly expressed in CLL and glutathione levels are similarly high.[100,103,104] With the exception of consistently low expression of thioredoxin, no other altered antioxidant pathways have been reported in CLL.[221]

1.2.5. NAD and NADP-dependent Signaling

In addition to their roles in redox reactions, NAD and NADP participate in intra- and intercellular signalling pathways with multiple and diverse functions. Unlike redox reactions, where a single dinucleotide molecule can undergo multiple cycles of oxidation and reduction, NAD and NADP-dependent signalling events, such as ADP ribosylation, NAD-dependent protein deacetylation and the generation of Ca^{2+}-mobilizing second messengers, invariably involve the degradation of the dinucleotide involved and release of nicotinamide (Nam).[70] This results in the continual availability of Nam and a dependence on a constant influx to maintain NAD stores, especially in malignant cells where these signalling pathways are often overactive.[70]

1.2.5.1. ADP-ribosylation

Mono- and poly-ADP-rybosylation are post translational protein modifications in which one or more ADP-rybosyl groups are transferred from NAD to glutamate or lysine residues in target proteins.[71] They are catalysed by ADP-ribosyltransferases (ARTs) and poly-ADP-ribose polymerases (PARPs) respectively, and reversed by ADP-rybosyl hydrolases and glycohydrolases. While the functions of mono-ADP-rybosylation remain largely unknown, two recent discoveries point to roles for these protein modifications in tumour biology.[70] First, deletion of the ARH1 gene encoding ADP-ribosylarginine hydrolase 1 increases the incidence of adeno- and hepatocellular carcinoma, and lymphoma in athymic nude mice.[222] And second, increased activity of membrane bound ARTs, in response to high extracellular NAD concentrations, inhibit the SRC family kinase LCK in cytotoxic $CD8^+$ T-lymphocytes, leading to reduced cell adhesion and TCR signalling.[68,69] As eNAMPT is highly expressed by CLL cells, this may contribute to the absence of cytotoxic T-cells from the CLL tissue microenvironments.[82]

In contrast, poly-ADP-rybosylation, particularly by poly-ADP-ribose polymerase 1 (PARP1) has been a very active area of research in recent years. This enzyme binds to DNA single strand breaks and modifies nearby proteins, leading to chromatin remodelling and the recruitment of proteins involved in DNA single strand break repair and base excision repair.[70,71] When PARP1 is inhibited, single strand breaks persist into mitosis, cause replication fork collapse, and become double strand breaks. PARP1 inhibition has therefore been explored as a treatment for tumours deficient in double strand break repair proteins such as BRCA1 and BRCA2 in breast and ovarian cancers.[70] As poly-ADP-ribose chains can contain up to 200 ADP-ribose units, this process can also rapidly consume cellular NAD reserves, forming a direct link between signalling events and energy metabolism.[209] In cases of extensive DNA damage, the resulting NAD and ATP depletion lead to cell death by apoptosis or caspase independent mechanisms.[71] Though less is known about the functions of other PARPs, evidence suggests roles in Wnt signalling and telomere maintenance which may also have roles in tumour biology.[71]

1.2.5.2. NAD^+-dependent Protein Deacetylation

Unlike other protein deacetylases, enzymes of the sirtuin family do not directly hydrolyse acetyl-protein bonds but transfer acetyl groups from target proteins onto the ADP-ribose moiety of NAD^+, producing Nam and O- acetyl-ADP-ribose (OAADPR).[70] These enzymes are sensitive to the relative concentrations of NAD^+ and NADH, and link the cellular metabolic state to gene expression by deacetylating transcription factors and histones at specific sites.[223] Of note, SIRT1 is highly expressed in CLL cells and negatively regulates P53 activity, reducing its pro-apoptotic effects.[70,72] In the mitochondria, SIRT3 upregulates superoxide dismutase 2 (SOD2) expression and activity, preventing ROS accumulation due to high energy demand, and precludes ROS mediated metabolic shift towards aerobic glycolysis.[70] Additionally, sirtuins are involved in

regulating metabolic enzymes such as acetyl-CoA synthase, carbamoyl phosphate synthase and glutamate dehydrogenase, maintaining genomic integrity, and global gene expression through regulation of RNA-polymerase I.[70] OAADPR also plays an important role in intracellular signalling as it and the product of its degradation, ADP-ribose (ADPR), are both ligands for Ca^{2+} channels which mediate signals for cell survival and proliferation.[224]

1.2.5.3. Intercellular Signalling

NAD can be both secreted and produced in the extracellular space, notably by eNAMPT activity, and is an active signalling molecule. It directly binds to cell surface receptors of the P2 receptor family on a variety of immune cells including lymphocytes, leading to Ca^{2+} influx, cell activation and chemotaxis.[73–75] Additionally, NAD^+ and $NADP^+$ are substrates for CD38, an ectopic NAD glycohydrolase and ADP-ribosyl cyclase expressed on B- and T-lymphocytes, granulocytes and NK cells. High CD38 expression in CLL is predictive of shorter time to treatment and survival.[132,133] It is upregulated in the tissue microenvironments and its persistent expression by CLL cells in the periphery correlates with unmutated IgVH status and predicts a more aggressive disease course.[132,133] This multifunctional enzyme produces ADPR or cyclic ADPR from NAD^+, or nicotinic acid adenine dinucleotide phosphate from $NADP^+$, all of which signal for calcium mobilization.[70,211,225]

1.3. Targeting NAMPT

Most cancer cells are thought to be uniquely dependant on NAMPT activity due to high demand for energy and metabolites for macromolecule synthesis and proliferation, and chronic activation of PARP1 by DNA damage and genetic instability.[226,227] In fact, high NAMPT expression is associated with cell survival, proliferation, and resistance to chemotherapy and oxidative stress in several tumour types.[78–81] While the regulation and potential alteration of

NAD homeostasis in CLL remain largely unexplored, both iNAMPT and eNAMPT are known to be highly expressed by these cells, particularly in response to BCR signalling,[13,82] and high NAMPT expression has been linked to poor overall survival.[228] As discussed above, eNAMPT may also play important roles in maintaining the supportive CLL microenvironments as it has been implicated in the release of pro-inflammatory cytokines, the differentiation of monocytes into nurse-like cells and the suppression of cytotoxic T-cells.[68,69,82] With the recent description of two classes of specific small molecule NAMPT inhibitors, this enzyme has emerged a promising new target for cancer treatment.[227,229]

FK866 (N-[4-(1-benzoylpiperidin-4-yl) butyl]-3-(pyridin-3-yl) acrylamide, also known as APO866/WK175, Fig. 4A) was originally identified as compound which inhibited proliferation and induced delayed cell death in lung and hepatic cancer cell lines.[227] It was described as non-competitive inhibitor of NAMPT due to its lack of influence on the enzymes Michaelis constant (K_M) and its ability to reduce the maximum rate of NAD synthesis (V_{max}) in the presence of high concentrations of Nam and PRPP.[227] Later structural studies revealed that FK866 competitively binds to the Nam binding pocket of NAMPT. Its specificity is attributed to its long linker region which extends along a unique channel at the dimer interface to expose its distal phenyl ring on the surface of the enzyme.[230,231] The conflicting earlier reports have been attributed to a very slow rate of dissociation, leading to an influence on enzyme kinetics approaching that of an irreversible inhibitor.[230] Furthermore, some reports suggest that FK866 may be a substrate for NAMPT, forming a phosphorybosylated derivative with increased affinity for the enzyme.[232]

FK866 has shown promising activity as a single agent in the treatment of both solid tumours and hematological malignancies *in vitro*,[212,227,233–235] It induces delayed cell death in cell lines and primary cells of multiple lymphomas, myelomas and leukemias including CLL, but not in

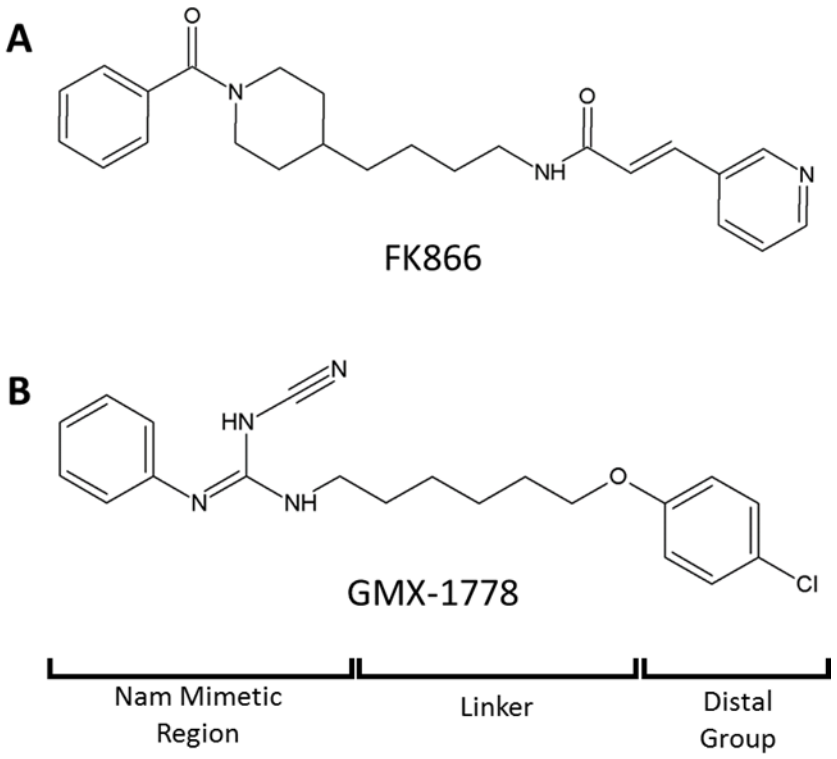

Figure 4: Nicotinamide phosphorybosyltransferase inhibitors. FK866 (A) and GMX-1778 (B) are specific competitive inhibitors of nicotinamide phosphorybosyltransferase (NAMPT). Both agents bind the enzyme's Nicotinamide (Nam) binding pocket by their Nam mimetic regions. Their specificity for NAMPT is attributed to their long linker regions which extend along a channel in the enzyme, unique among phosphorybosyltransferases, to expose their distal phenolic groups on the exterior surface of the enzyme.

healthy peripheral blood mononuclear cells.[235–237] It also prevents tumor growth and prolongs survival in mouse models of human Burkitt lymphoma and acute myeloid leukemia.[235] Phase I clinical trials established steady state blood plasma level of approximately 14 nM and described FK866 as generally well tolerated; however, these trials also revealed dose-limiting toxicities including thrombocytopenia and gastrointestinal symptoms, and very poor response rates were seen at attainable doses.[238]

Similarly, GMX-1778 (N-4-(6-chlorophenoxy)nexyl-N"-cyano-N"-4-pyridylguanidine, formerly CHS-828, Fig. 4B) was originally selected for its anti-proliferative effect in multiple human cancer cell lines.[239] It was later revealed to be a NAMPT-specific, inhibitor which binds the enzyme in a comparable conformation to FK866, with an estimated affinity >1000-fold greater than that of Nam.[229,232] Like FK866, GMX-1778 showed particularly high *in vitro* activity against CLL and other hematological malignancies,[240,241] but has achieved poor clinical results due to dose-limiting bone marrow and gastrointestinal toxicities.[242–244] It is currently under development as the orally bioavailable prodrug GMX-1777.[245]

As demonstrated by clinical trials, the optimal use of NAMPT inhibitors for cancer treatment may require the increased treatment efficacy and reduced toxicity afforded by combination therapy. Moreover, the recent investigation of several drug combinations point to a susceptibility of FK866 and GMX-1778 treated cancer cells to a broad range of current anti-cancer agents including DNA damaging agents, nucleoside analogs and monoclonal antibodies.[80,234,246] Additionally, FK866 exhibits marked synergy with other agents targeting the NAD metabolome, such as the PARP inhibitor olaparib in triple-negative breast cancer cells,[247] and the NAD(P)H:quinone oxidoreductase-1 activator β-lapachone in pancreatic cancer.[248] However, the development of NAMPT inhibition based combination therapies for CLL is

hampered by our pour understanding of CLL specific metabolic alterations and dependencies and of the cellular functions impacted downstream of NAMPT inhibition.

Our laboratory has previously demonstrated the sensitivity of CLL cells to NAMPT inhibition; with a median lethal dose (LD_{50}) of 7.3 nM, compared to 270.7 nM in peripheral blood mononuclear cells from age matched control donors. We also established that sensitivity to FK866 is predicted by negative CD38 status and lymphocyte doubling times greater than 12 months, but otherwise unaffected by common prognostic factors including Rai stage, Zap-70 and IgVH mutational status.[237] In this study, we characterized the downstream effects of NAMPT inhibition on NAD- and NADP-dependent biochemical pathways; glycolysis, mitochondrial respiration and the glutathione antioxidant pathway, in primary CLL cells. We also assessed the efficacy of NAMPT inhibition-based combination therapies for CLL treatment, and identified several synergistic drug combinations, including current chemotherapeutics and targeted agents, and novel targets in CLL.

2. HYPOTHESIS

NAMPT inhibition-induced NAD depletion reduces the capacity of NAD- and NADP-dependent biochemical pathways in CLL cells; including glycolysis, mitochondrial respiration and the glutathione antioxidant pathway. The addition of NAMPT inhibitors will enhance CLL treatment with chemotherapeutics and targeted agents in current clinical use, and synergise with agents targeting these NAD- and NADP-dependent pathways.

3. AIMS

1. Investigate the impact of NAMPT inhibition on NAD- and NADP-dependent biochemical pathways in primary CLL cells.
2. Evaluate the efficacy of FK866 and GMX-1778 for CLL treatment, in combination with current chemotherapeutics and targeted agents, agents targeting glycolysis and mitochondrial respiration, and oxidative stressors.

4. MATERIALS AND METHODS

4.1. Reagents

For flow cytometry, FITC labeled annexin V, propidium iodide (PI) and 7-amino-actinomycin D (7-AAD) were obtained from BD Bioscience. Dihydroethidium (DHE) was obtained from Molecular Probes as a 5 mM solution stabilized with DMSO and stored at -30 °C, protected from light. Tetramethylrhodamine methyl ester (TMRM) was obtained from Molecular Probes, dissolved to a stock concentration of 500 mM in DMSO, stored at 4 °C, protected from light. 2',7'-dichlorodihydrofluorescein diacetate (DCFH-DA) was purchased from Invitrogen, dissolved to a stock concentration in DMSO

Oligomycin, rotenone and antimycin A were obtained from Sigma-Aldrich, dissolved to stock concentrations of 10 mg/ml, 50 mM and 25 mM in DMSO, respectively, and stored at -80 °C. Carbonyl cyanide-p-trifluoromethoxyphenylhydrazone (FCCP) was obtained from Sigma-Aldrich, dissolved to a stock concentration of 50 mM in ethanol, and stored at -80 °C. D-glucose and 2-deoxy-D-glucose (2-DG) were obtained from Sigma-Aldrich, stored at room temperature and freshly dissolved before use. Nitrotetrazolium blue was obtained from ThermoFisher Scientific, stored at room temperature and freshly dissolved before use.

β-NAD^+ sodium salt was obtained from Sigma-Aldrich, stored at -20 °C and freshly dissolved before use. β-NADH disodium salt was purchased from Sigma-Aldrich, dissolved in Tris-HCl buffer (pH 8.5) to a stock concentration of 10 µg/L and stored at -20°C. FK866 and GMX-1778 were purchased from Sigma-Aldrich, dissolved in DMSO to stock concentrations of 10 mmol/L, and stored at -30°C. Fludarabine, chlorambucil, bendamustine, ibrutinib and idelalisib were purchased from Selleck Chemicals, dissolved in DMSO to stock concentrations of 10 mM for fludarabine, chlorambucil and bendamustine, and 100 mM for ibrutinib and idelalisib, and stored at -80 °C for up to 6 months. Phorbol 12-myristate 13-acetate was obtained from Sigma-Aldrich as a 30% aqueous solution and freshly diluted in culture media before use.

4.2. Primary cell isolation and culture

Peripheral blood mononuclear cells (PBMCs) were isolated from the peripheral blood of consenting donors by density gradient centrifugation using Ficoll-Paque PLUS density gradient medium (GE Healthcare Life Sciences). Where CLL patents presented with white blood cell counts $\leq 40 \times 10^3/\mu L$, and for control donors, B-lymphocytes were negatively selected using Rosette Sep B-Cell Enrichment Antibody Cocktail (STEMCELL Technologies). Unless otherwise noted, cells were cultured at a density of 4×10^6 cells/mL in RPMI-1640 medium containing 1% penicillin/streptomycin and 10% fetal bovine serum at 37°C, 5% CO2 in a humidified atmosphere. This study is approved by the human research ethics board of the University of Manitoba (approval number HS15746) and the CancerCare Manitoba Research Resource Impact committee (approval number 81-2012).

4.3. ATP, NAD, NADP, glutathione and caspase 3/7 assays

CellTiter-Glo Luminescent Cell Viability Assay, NAD/NADH Glo Assay, NADP/NADPH-Glo Assay , GSH-Glo Glutathione Assay and Caspase-3/7 Glo Assay kits (Promega Corporation) were used according to the manufacturer instructions to assess total cellular ATP content, NAD content and NADP content, reduced glutathione content, and caspase-3/7 activity, respectively. Luminescence was measured using a SPECTRAmax GEMINI XS luminometer (Molecular Devices).

4.4. Flow cytometry

Cells were collected by centrifugation for 10 minutes at 1200 rpm and washed in PBS. To assess cell viability, cells were then resuspended and incubated for 15 minutes at room temperature, protected from light, in Annexin V Binding Buffer (556454; BD Bioscience) containing annexin V- FITC and PI or 7-AAD, as indicated. Annexin V-negative/PI-negative and annexin V-negative/7-AAD-negative cells were considered viable. To assess mitochondrial membrane potential, cells were incubated for 30 minutes at room temperature in PBS containing 25 nM TMRM. To assess cellular ROS content, cells were incubated for 30 minutes at 37 °C in PBS containing the superoxide specific indicator DHE at a concentration of 2.5 µM or the peroxide and reactive nitrogen species specific indicator DCFH-DA. Fluorescence was assessed using a LSRII flow cytometer and FACSDiva software (BD Biosciences) or using a NovoCyte flow cytometer and NovoExpress software (ACEA Biosciences). All data were normalized to vehicle treated controls.

4.5. Extracellular flux analysis

Extracellular flux analysis was performed using a XF24 Extracellular Flux Analyzer (Seahorse Bioscience). Cells were pelleted by centrifugation for 10 minutes at 1200 rpm at room temperature and resuspended in assay media. Cells were then transferred to XF analyzer 24-well plates coated with 1.13 µg Cell-Tak (354240; Corning) per well, at a density of 900,000 cells per well. Plates were centrifuged at 1200 rpm for 10 min at room temperature, with slow acceleration and deceleration. Finally, cells were incubated at 37 °C, at ambient carbon dioxide concentration for 1 hour prior to assay.

To assess mitochondrial respiration, assay media consisted of unbuffered DMEM media (102353-100; Seahorse Bioscience) supplemented with 2 g/L D-glucose and 1 mmol/L sodium pyruvate, at pH 7.4. Extracellular oxygen consumption rates (OCR) were measured in triplicate at baseline (basal respiration), and following sequential injection of oligomycin (1.25 µM, proton leak), FCCP (2 µmol/L, maximum respiratory capacity), and Rotenone and Antimycin A (1 µmol/L each, non-mitochondrial oxygen consumption). Measurements were normalised to non-mitochondrial oxygen consumption.

To assess glycolysis, assay media consisted of unbuffered DMEM media containing 2 mmol/L L-alanyl-L-glutamine dipeptide (35050-061; Thermo Fisher Scientific), at pH 7.4. Extracellular acidification rates (ECAR) served as a surrogate for production and secretion of lactate, the end product of anaerobic glycolysis. ECAR was measured in triplicate at baseline (non-glycolytic acidification), and following sequential injection of glucose (1.6 g/L, glycolysis), oligomycin (1 mg/L, maximum glycolytic capacity), and 2-deoxy-D-glucose (15 g/L) as negative control. Measurements were normalised to non-glycolytic acidification.

4.6. Blue-Native polyacrylamide gel electrophoresis and in-gel activity assay

Mitochondrial enrichment was performed using the Mitochondria Isolation Kit for Cultured Cells (ab110170; Abcam) following the manufacturer's instructions. Mitochondrial protein was then quantified using Bio-Rad Protein Assay Dye Reagent (#500-0006). For Blue-Native Polyacrylamide Gel Electrophoresis (BN-PAGE), mitochondria were solubilized in NativePAGE Sample Buffer (BN2003; ThermoFisher Scientific) containing 0.2% n-dodecyl β-D-maltoside (BN2005), at a concentration of 1 g/L mitochondrial protein, for 15 minutes on ice. The extract was centrifuged at 20,000xg for 30 minutes at 4°C. 5% v/v G-250 Sample Additive (BN2004) was added to the supernatant. The resulting samples were separated on 3-12% Bis-Tris precast gels (BN1001) at 150 V for 120 minutes using NativePAGE Running Buffer (BN2001), with cathode buffer containing Cathode Buffer Additive (BN2002; Thermo Fisher Scientific). Following electrophoresis, gels were fixed in 40% Methanol, 10% Acetic Acid for 15 minutes at 37°C and de-stained in 8% Acetic Acid at 37°C for a minimum of 2 hours.

For in-gel activity assay of NADH dehydrogenase, BN-PAGE was performed as described above except that cathode buffer was replaced with clear NativePAGE Running Buffer after 30 minutes of electrophoresis. Following de-staining, gel was washed in water and incubated in Tris-HCl Buffer (pH 7.4) containing 2.5 µg/L nitrotetrazolium blue and 100ng/L NADH for 7.5 minutes. Imaging was performed using an Expression 1680 scanner (Epson). Densitometric analysis was performed using Licor Image Studio Lite v.5.2.

4.7. Drug combination analysis

In order to account for both the full range of each drug's effect and a broad range of drug ratios, drug combination experiments were designed following a full factorial approach;

considering all possible combinations of the selected doses of individual drugs. Additionally, data were analysed by two complimentary methods; each chosen to addresses the limitations of the other. Therefore, consideration of both predictions provides a more complete understanding of the dynamics of each drug combination.

4.9.1. Loewe Additivity model

Drug-drug interactions were first assessed according the Loewe additivity model using Combenefit software v2.021 (http://www.cruk.cam.ac.uk/research-groups/jodrell-group/combenefit, University of Cambridge, UK). Briefly, median dose-response (DR) curves were generated for each individual agent (single-agent DR curves) based on normalised cell viability measures and served to predict cell viability for each combination of doses assessed, according to the Loewe model:[249,250]

$$\frac{d_{ai}}{D_{ai}} + \frac{d_{bi}}{D_{bi}} = 1$$

Where D_a and D_b are doses of agents "a" and "b", respectively, required to produce a given reduction in cell viability (i) in single-agent treatments, and d_a and d_b are doses of agents "a" and "b", respectively, required to produce effect i when given in combination.

Cell viability measures below and above predicted values were interpreted as synergy and antagonism, respectively. Significance of deviations from predicted values were evaluated using the one-sample t-test. Of note, the Loewe model does not provide an objective measure of the magnitude of drug synergy or antagonism. The degree of deviation from predicted values were reported to provide a rough estimate only.

4.9.2. Combination Index model

The Combination Index (CI) model is an adaptation of the Loewe model which provides an objective measure of the magnitude of drug-drug interactions in the form of CI values, defined as: [251]

$$\frac{d_{ai}}{D_{ai}} + \frac{d_{bi}}{D_{bi}} = CI$$

Where D_a, D_b, d_a, d_b and i are defined as above. CI<1, =1 and >1 are interpreted as synergy, additivity and antagonism, respectively.

Using GraphPad Prism 6 software, four-parameter sigmoidal single-agent DR curves were generated for normalised cell viability measures from each patient sample assessed. For each dose combination assessed, single-agent DR curves served to calculate doses required to produce the same relative cell viability (D_{ai} and D_{bi}). Individual CI values were then calculated for each patient sample and the mean CI for each dose combination was determined. The significance of CI deviation from 1 was evaluated using the one-sample t-test. The major limitation of the CI model is its requirement that the effect of each dose combination (i) be attainable by both individual drugs in the combinations.[252] Therefore, as is common in studies assessing drug combinations in biological systems, the maximum effect of each individual agent was assumed to be 100% cell death, for the purpose of single-agent DR curve fitting.[251,253]

4.8. Data management and statistics

Data management and analysis were performed using Microsoft Excel 2013, and GraphPad Prism 6. DR surfaces and Loewe additivity matrices were generated using Combenefit v2.021. Other graphs and plots were generated in GraphPad Prism 6. Molecular models were generated

in ACD/ChemSketch 2015 (Advanced Chemistry Development). All other figures and elements were generated in Microsoft PowerPoint 2013. Statistical analysis was performed using GraphPad Prism 6. P values ≥0.05 were considered not significant (ns), *, **, ***, and **** denote P values <0.05, <0.01, <0.001, and <0.0001, respectively. "N" was used to denote biological replicates and "n" was used to denote technical replicates. Error bars on all graphs represent standard error of the mean.

5. RESULTS

5.1. NAMPT inhibition leads to ATP depletion and cell death mediated by NAD depletion

NAMPT catalyses the rate-limiting step in generating NAD, which is essential for ATP synthesis by both glycolysis and mitochondrial respiration. In order to assess the effect of NAMPT inhibition on energy metabolism in CLL, cells were treated with FK866 at concentrations ranging from 1 nM to 100 nM, or DMSO as vehicle control, and total cellular NAD and ATP content (N=6), and cell viability (N=3) were assessed daily for three days. A 5-fold or greater decrease in cellular NAD was observed within one day of treatment with FK866 doses of 10 nM or more. As previously reported in CLL and other cancer types,[227–229,235] cellular ATP was reduced 2-fold or more by day two and cell viability was reduced 0.6-fold or more by day three at these doses (Fig. 5), suggesting that cellular energy metabolism is supressed following NAMPT inhibition and may contribute to CLL cell death. In contrast, 1 nM FK866 did not significantly reduce cellular NAD, and a trend toward increased ATP and cell viability was noted on day two of treatment with this dose. Data were contributed by Dr. Iris Gehrke.

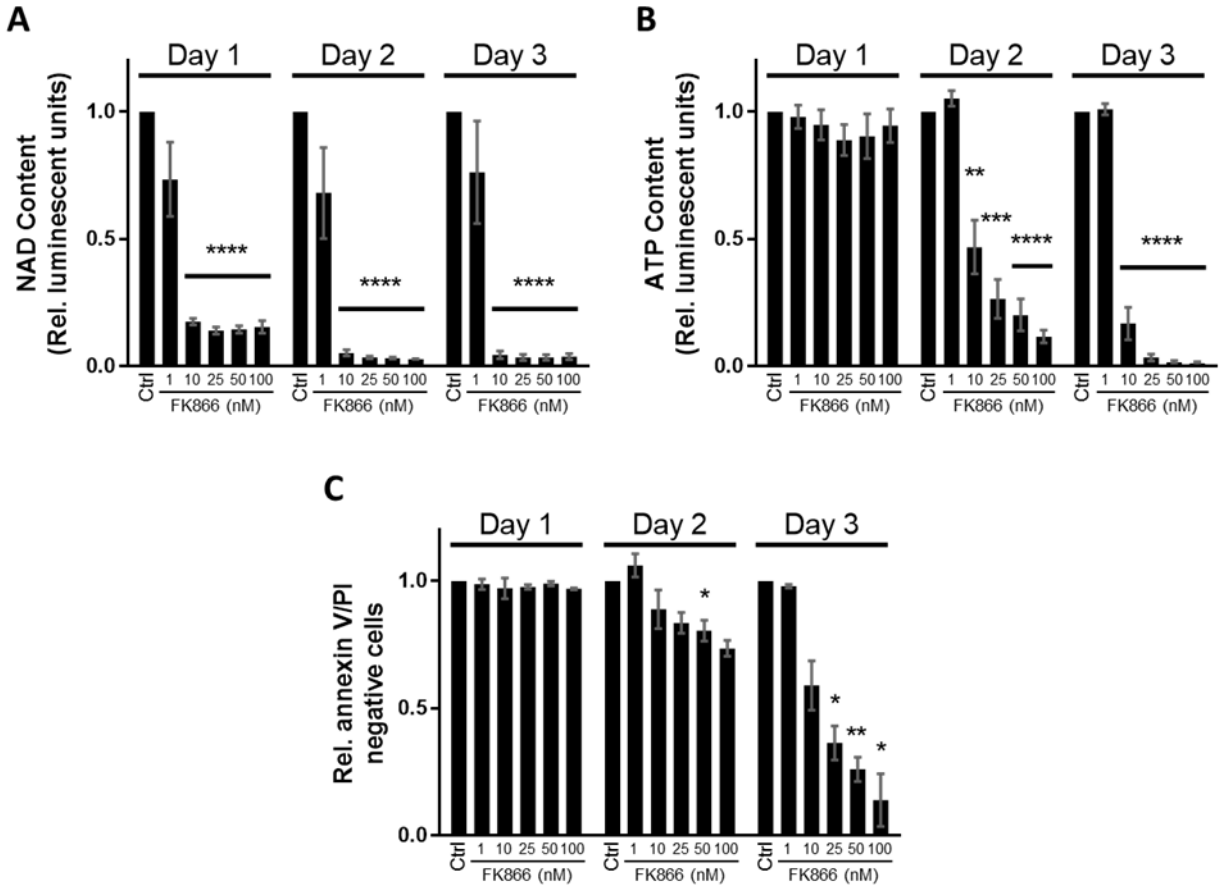

Figure 5: NAMPT inhibition leads to NAD and ATP depletion and loss of CLL cell viability. CLL cells were treated with FK866 at concentrations of 1, 10, 25, 50 and 100 nM, or DMSO as vehicle control (Ctrl). (A) Total cellular NAD and (B) ATP content (N=6, n=3) were assessed daily for three days following treatment by NAD/NADH-Glo and CellTiter-Glo assays, respectively. (C) Cell viability was assessed daily for three days following treatment by flow cytometry with annexin V-FITC and PI staining. Annexin V-FITC negative, PI negative cells were considered viable (N=3). All data were normalized to vehicle controls at each time point. Statistical analysis was performed using the one-sample t-test (* $P \leq 0.05$, ** $P \leq 0.01$, *** $P \leq 0.001$, **** $P \leq 0.0001$). (N= biological replicates, n= technical replicates)

In order to confirm that ATP depletion and loss of cellular viability are on-target effects downstream of NAMPT inhibition, CLL cells were then pre-treated with exogenous NAD (exNAD) for one day. As the majority of cellular NAD degradation is thought to be mediated by PARP1, cells were alternatively pretreated with olaparib, an NAD-mimetic inhibitor of PARP1, PARP2 and PARP3. Cells were then treated with 25 nM FK866 or DMSO as vehicle control. This dose was chosen as it was the lowest concentration evaluated which produced significant cell death within three days of treatment (Fig. 5C). On the third day following FK866 treatment, cellular ATP and viability were significantly rescued by both exNAD and olaparib pre-treatment (Fig. 6), indicating both that ATP depletion and CLL cell death following NAMPT inhibition are downstream effects of NAD depletion and that a large portion of NAD degradation in CLL cells is mediated by PARPs.

5.2. Mitochondrial respiration is supressed by NAMPT inhibition in CLL cells

As the majority of ATP in aerobic cells is synthesised via NADH-dependent mitochondrial respiration, we investigated the impact of NAMPT inhibition on this pathway; however, as NAMPT is not localised to mitochondria, we first confirmed that the mitochondrial NAD pool is depleted following NAMPT inhibition. CLL cells were treated with 10 nM FK866; a concentration above the previously established median lethal dose (LD_{50}) of 7.3 nM and below the published steady state plasma level of 14 nM,[237,238] or DMSO as vehicle control. The NAD content of whole cells (N=6) and isolated mitochondria (N=5) were decreased 5.5- and 3.8-fold respectively by day one and remained low on day two of FK866 treatment (Fig. 7A).

The mitochondrial respiratory profiles of untreated CLL cells and cells treated for one and two days with 10 nM FK866 or DMSO were then assessed by extracellular flux analysis (N=5). While maximum respiratory capacity was slightly increased by DMSO, it was significantly

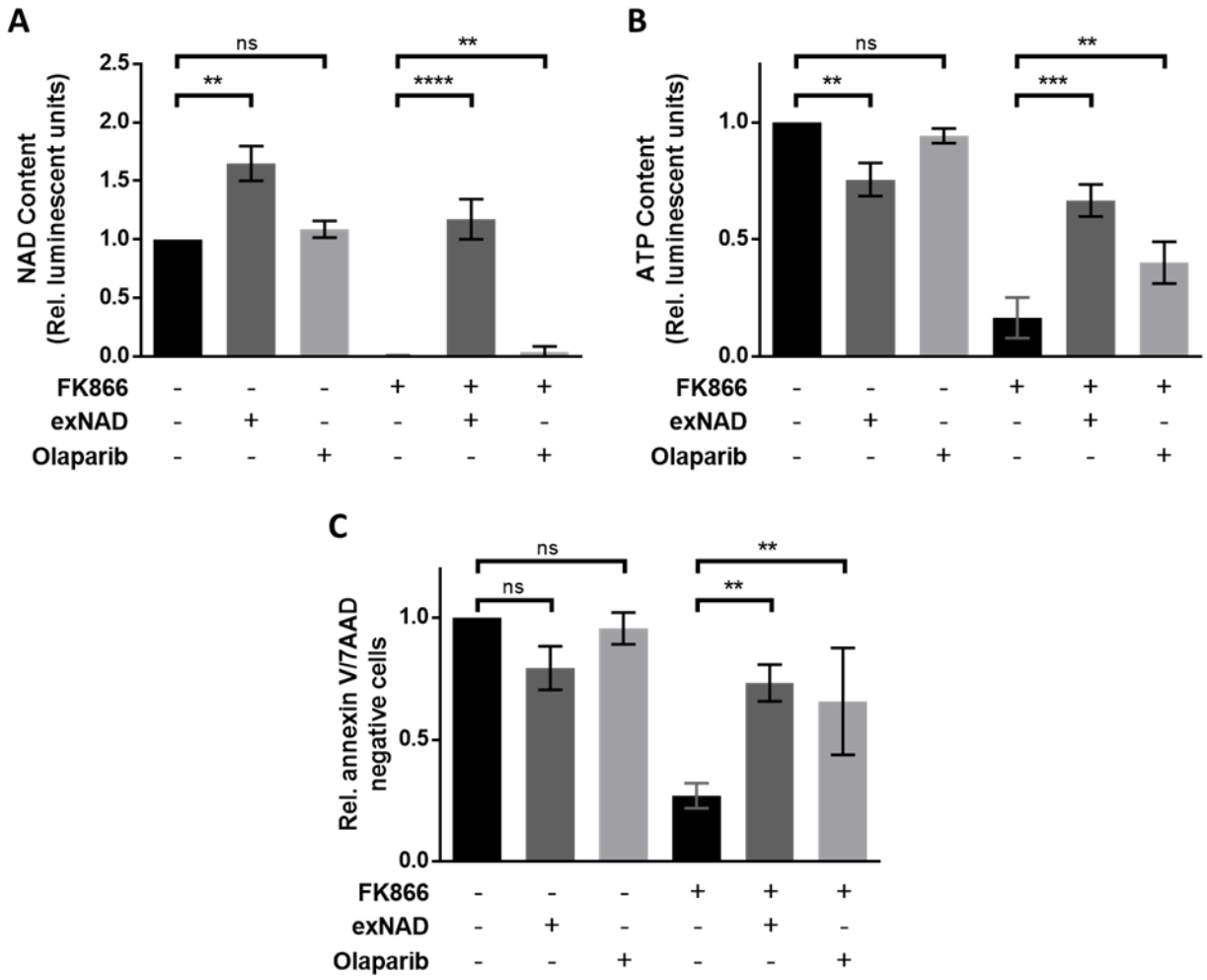

Figure 6: FK866-induced CLL cell death is mediated by NAD depletion. CLL cells were pre-treated with 100 µM exogenous NAD (exNAD) or 1 µM of the PARP inhibitor olaparib, or cultured untreated for one day. Cells were then treated for three days with 25 nM FK866 or DMSO as vehicle control. (A) Cellular NAD and (B) ATP content were assessed by NAD/NADH-Glo and CellTiter-Glo assays, respectively (N=11, n=3). (C) Cell viability was assessed by flow cytometry with annexin V-FITC and 7AAD staining (N=6). Annexin V-FITC negative, 7AAD negative cells were considered viable. All data were normalized to vehicle controls. Statistical analysis was performed using the paired, two-tailed t-test (ns = not significant, ** $P \leq 0.01$, *** $P \leq 0.001$, **** $P \leq 0.0001$). (N= biological replicates, n= technical replicates)

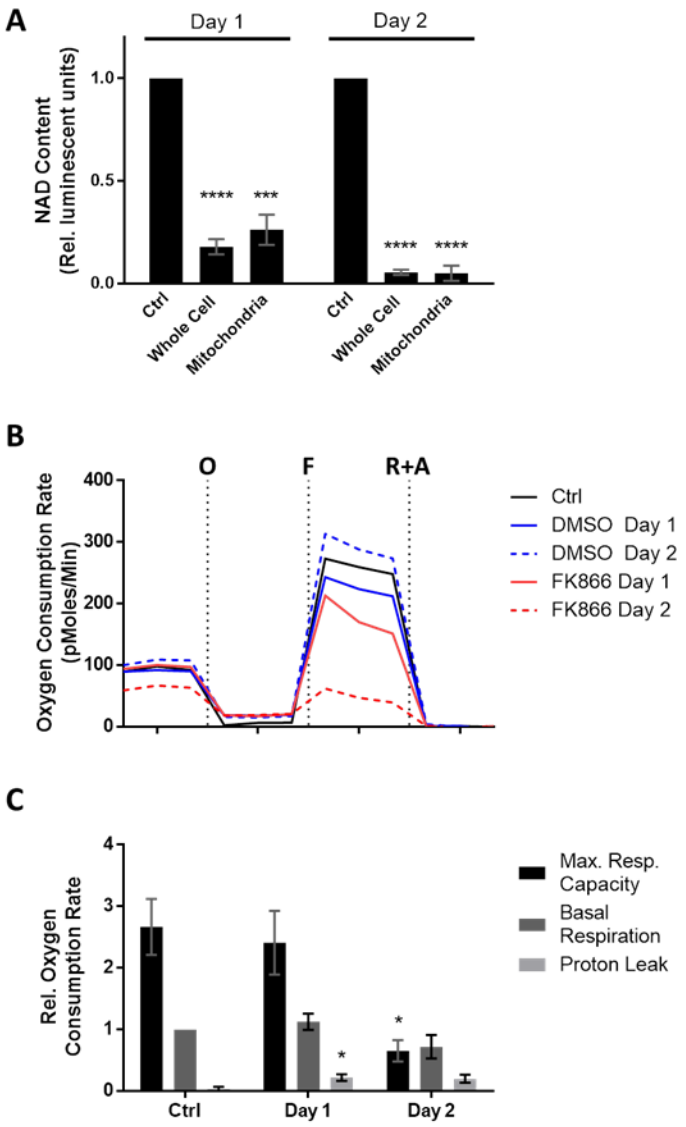

Figure 7: Mitochondrial respiration is supressed by NAMPT inhibition. (A) CLL cells were treated with 10 nM FK866 or DMSO as vehicle control (Ctrl). NAD content of whole cells (N=6, n=3) and isolated mitochondria (N=5, n=3) were assessed daily for two days by NAD/NADH-Glo assay. Data were normalized to vehicle controls. Statistical analysis was performed using the one-sample t-test. (B) CLL cells were cultured for two days untreated (Ctrl), or treated with 10 nM FK866 or DMSO for one and two days (N=5, n=4). Mitochondrial respiratory rates were assessed by extracellular flux analysis at baseline (basal respiration) and following treatment with oligomycin (O, proton leak), FCCP (F, Maximum respiratory capacity), and Rotenone (R) and Antimycin A (A) as negative control. (C) Maximum respiratory capacity, basal respiration and proton leak are summarised. Data were normalized to basal respiration of vehicle controls. Statistical analysis of basal respiration was performed using the one sample t-test. No values were significantly different from 1. Statistical analysis of maximum respiratory capacity and proton leak was performed using the paired, two-tailed t-test (* $P \leq 0.05$, *** $P \leq 0.001$, **** $P \leq 0.0001$). (N= biological replicates, n= technical replicates)

reduced in a time-dependent manner by FK866 treatment. Additionally, both the maximum respiratory capacity and basal respiration rates of CLL cells treated with FK866 for two days trended toward inferiority to the basal respiratory rate of control CLL cells (Fig. 7B, Fig. 7C). Taken together, this suggests that FK866-treated CLL cells are incapable of maintaining their regular rates of ATP synthesis via mitochondrial respiration due to insufficient mitochondrial NADH.

As high basal and maximum respiratory rates were noted in CLL cells from two Zap-70 positive patients, the influence of Zap-70 expression on mitochondrial respiration was further investigated. Untreated CLL cells from Zap-70 positive patients (N=4) exhibited significantly greater basal respiration and respiratory capacity than CLL cells from Zap-70 negative patients (N=7), the latter of which resembled control B-lymphocytes (N=9) in their respiratory profiles (Fig. 8A, Fig. 8B). Nevertheless, a trend toward decreased maximum respiratory capacity and basal respiration rates was seen in cells from Zap-70 negative (N=4) and Zap-70 positive patients (N=2) two days after treatment (Fig. 8C, Fig. 8D), suggesting that CLL cells remain sensitive mitochondrial inhibition mediated by NAD depletion, regardless of Zap-70 status.

As NAD plays many regulatory roles in gene expression and metabolic pathways, it was suggested that altered expression or assembly of electron transport chain (ETC) complexes and supercomplexes may play roles in FK866-induced reduction of mitochondrial respiratory capacity. Contrarily, blue native polyacrylamide gel electrophoresis (BN-PAGE) revealed time-dependent increases in the expression of complexes II and IV, and ATP synthase, and assembly of four supercomplexes with apparent weights between 900 and 1050 KDa, in FK866-treated CLL cells (N=3, Fig. 9A, Fig. 9B, Fig. 9C). These effects are suggestive of upregulation of the ETC pathway in response to NADH insufficiency, decreased mitochondrial membrane potential

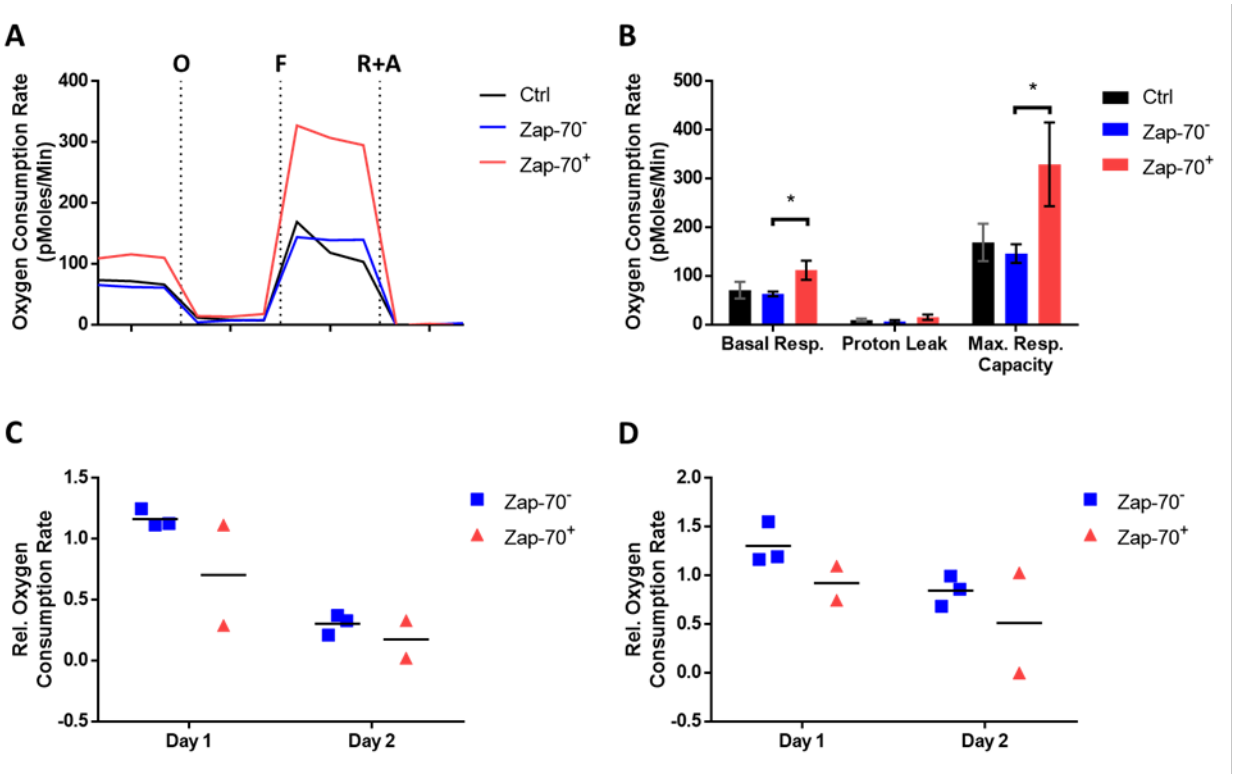

Figure 8: Zap-70 positive CLL cells exhibit increased mitochondrial metabolism but remain sensitive to NAMPT inhibition. (A) Mitochondrial respiratory rates of untreated control B-lymphocytes (N=9, n=4), and CLL cells from Zap-70 negative (Zap-70$^-$, N=7, n=4) and Zap-70 positive (Zap-70$^+$, N=4, n=4) patients were assessed by extracellular flux analysis at baseline (basal respiration) and following treatment with oligomycin (O, proton leak), FCCP (F, Maximum respiratory capacity), and Rotenone (R) and Antimycin A (A) as negative control. (B) Basal respiration, proton leak and maximum respiratory capacity are summarised. Statistical analysis was performed using the paired, two-tailed t-test (* $P \leq 0.05$). (C, D) CLL cells from Zap-70 negative (N=4) and Zap-70 positive (N=2) CLL patients were treated for one and two days with 10nM FK866. (C) Maximum respiratory capacity and (D) basal respiration were assessed by extracellular flux analysis (n=4). Data were normalized to vehicle controls. (N= biological replicates, n= technical replicates)

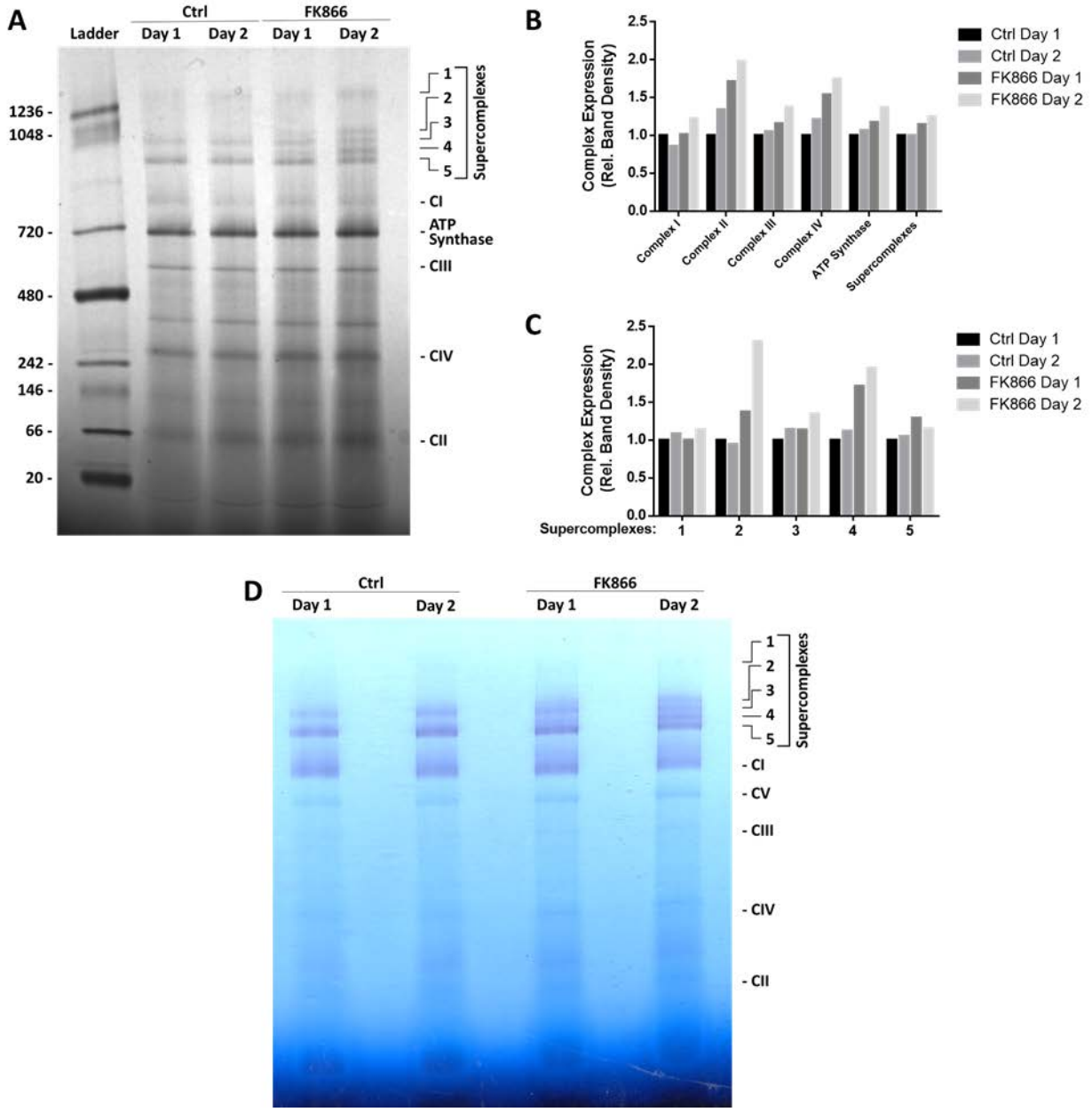

Figure 9: Mitochondrial respiratory complex and supercomplex expression are increased by NAMPT inhibition. CLL cells were treated for one and two days with 10 nM FK866 or DMSO as vehicle control (Ctrl, N=3). (A) Mitochondrial respiratory complex and supercomplex assembly were assessed by BN-PAGE. (B) Densitometric measure of respiratory complexes and (C) supercomplexes were normalised to vehicle control on day one. (D) NADH-reductase activity assay (N=3) confirmed the presence of complex I (indigo bands) as an individual complex and as part of four supercomplexes of distinct apparent molecular weights (labelled 2, 3, 4 and 5). Representative images shown. (N= biological replicates)

or ATP synthesis. Likewise, in-gel activity assay confirmed that these upregulated supercomplexes comprise the NADH-dependent complex I (Fig. 9D). Accordingly, no complexes or supercomplexes were reduced by FK866 treatment.

5.3. Glycolysis is supressed by NAMPT inhibition

The second major source of cellular ATP, glycolysis is capable of maintaining cellular energy stores under conditions of metabolic stress, oxygen insufficiency, and mitochondrial inhibition.[66] As the pathway is also NAD-dependent, the effect of NAMPT inhibition on glycolysis in CLL was also investigated. The glycolysis rates and maximum glycolytic capacities of untreated CLL cells, and CLL cells treated for one and two days with 10 nM FK866 or DMSO were assessed by extracellular flux analysis (N=4, Fig. 10). While maximum glycolytic capacity was slightly increased by DMSO, a trend toward decreased glycolytic capacity was seen in cell treated for one day and it was significantly decreased in cells treated for two days with FK866. Additionally, both the maximum glycolytic capacity and basal glycolysis rates of CLL cells treated with FK866 for two days trended toward inferiority to the basal glycolysis rate of control CLL cells (Fig. 10), suggesting that FK866-treated CLL cells are unable to meet their energetic requirements via glycolysis.

As with mitochondrial respiration, extracellular flux analysis of untreated CLL cells from Zap-70 negative (N=3) and Zap-70 positive (N=2) CLL patients revealed slightly greater glycolysis rates and significantly greater maximum glycolytic capacity in CLL cells from Zap-70 positive patients (Fig. 11A, Fig. 11B). Additionally, while a trend toward time-dependent, lowered maximum glycolytic capacity was seen in FK866-treated CLL cells from both Zap-70 positive (N=2) and Zap-70 negative patients (N=4, Fig. 11C), one of two Zap-70 positive samples tested exhibited a 5.8-fold increase in glycolysis after FK866 treatment for two days

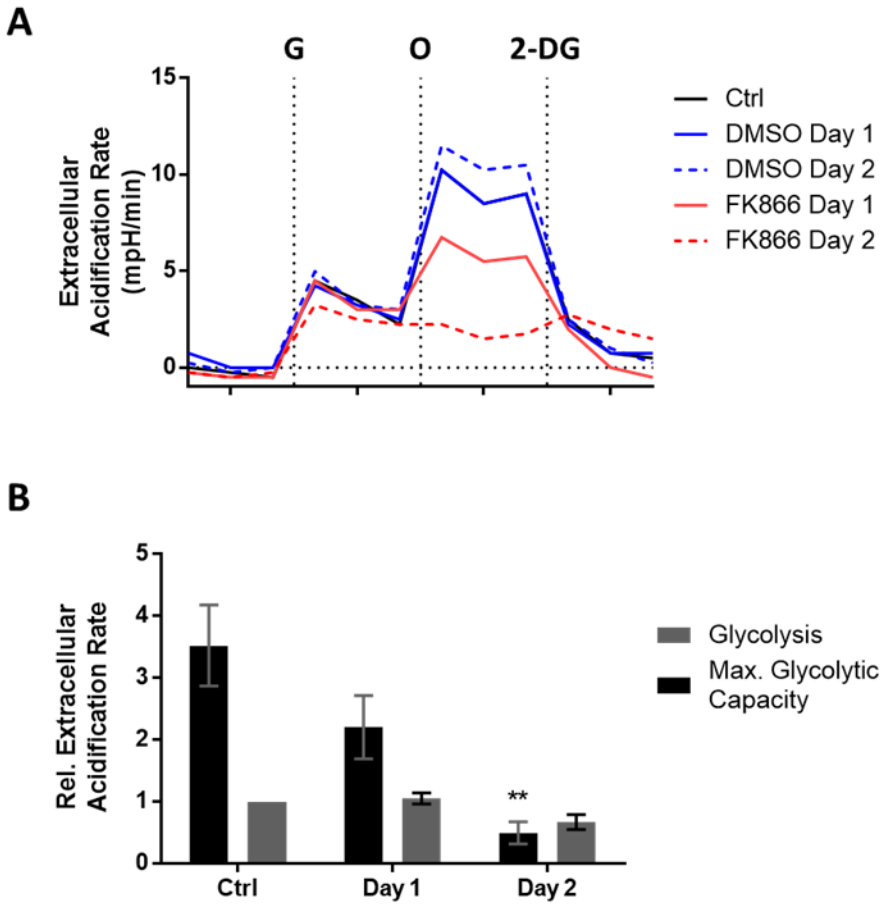

Figure 10: Glycolysis is supressed by NAMPT inhibition. CLL cells were cultured for two days untreated, or treated for one and two days with 10 nM FK866 or DMSO (Ctrl). (A) Glycolysis rates were assessed by extracellular flux analysis at baseline and following treatment with glucose (G, glycolysis), oligomycin (O, maximum glycolytic capacity), and 2-deoxyglucose as negative control (2-DG, N=4, n=4). (B) Glycolysis rates and maximum glycolytic capacity are summarised. Data were normalized to glycolysis rates of vehicle controls. Statistical analysis of glycolysis rates was performed using the one sample t-test. No values were significantly different from 1. Statistical analysis of maximum glycolytic capacity was performed using the paired, two-tailed t-test (** $P \leq 0.01$). (N= biological replicates, n= technical replicates)

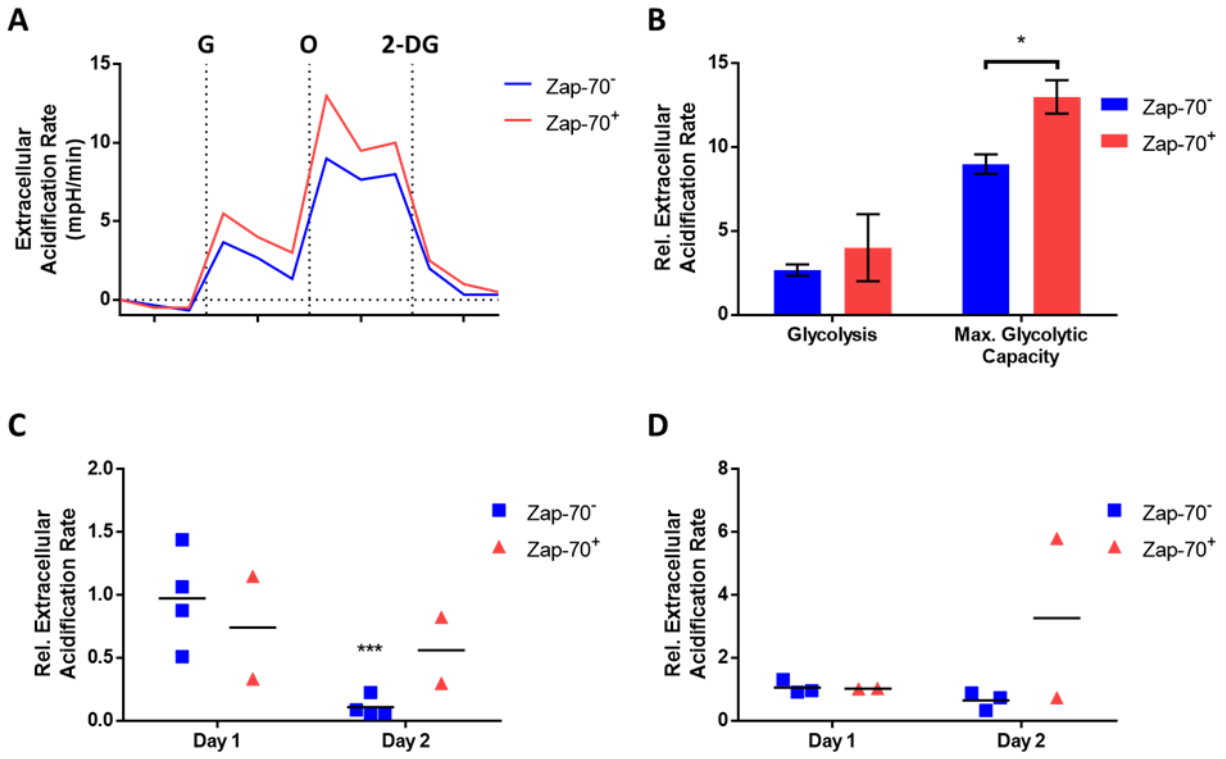

Figure 11: Zap-70+ CLL cells exhibit increased glycolytic capacity and are resistant to FK866-induced inhibition of glycolysis. (A) Glycolysis rates of untreated CLL cells from Zap-70$^-$ (N=3) and Zap-70$^+$ (N=2) patients were assessed by extracellular flux analysis at baseline and following treatment with glucose (G, glycolysis), oligomycin (O, maximum glycolytic capacity), and 2-deoxyglucose as negative control (2-DG, n=4). (B) Glycolysis rates and maximum glycolytic capacity are summarised. Statistical analysis was performed using the paired, two-tailed t-test (* $P \leq 0.05$). (C, D) CLL cells from Zap-70$^-$ (N=4) and Zap-70$^+$ (N=2) patients were treated for one and two days with 10nM FK866. Maximum glycolytic capacity (C) and glycolysis (D) were assessed by extracellular flux analysis (n=4). Data were normalized to vehicle controls. (N= biological replicates, n= technical replicates)

(Fig. 11D). While these results are preliminary, this may indicate a subset of Zap-70 positive CLL cases, which are resistant to glycolytic inhibition downstream of NAMPT inhibition.

5.4. NAMPT inhibition leads to collapse of the glutathione antioxidant pathway

The majority of cellular superoxide anions are typically produced as by-products of electron transport chain (ETC) function. ETC inhibition is therefore generally accompanied by decreased superoxide production and lowered mitochondrial membrane potential (MMP). However, our lab has previously reported increased cellular superoxide content in FK866-treated CLL cells, which was associated with loss of mitochondrial membrane potential (MMP).[237] The role of ROS production in the mechanism of FK866-induced cell death was therefore further investigated. As the previous study found no effect of FK866 on MMP or superoxide within one day for treatment, MMP, superoxide content and cell viability of CLL cells (N=3) and control B-lymphocytes (N=5) were assessed on days two and three following treatment with 10 nM FK866. In agreement with the previous report, a time-dependent trend toward decreased MMP and cell viability was accompanied by significantly increased superoxide content in CLL cells; however, no significant decrease in MMP or viability was observed in control B-lymphocytes, and superoxide content was significantly reduced in these cells by day three of treatment (Fig. 12). Furthermore, superoxide content of CLL cells on days two and three of treatment were poorly correlated to viability on day three ($F(1,1)=0.9120$, $P=0.5149$, $R^2=0.4770$, and $F(1,1)=0.1319$, $P=0.7782$, $R^2=0.1165$, respectively), while the strongest correlation was seen between MMP on day two and cell viability on day three ($F(1, 1)=75.17$, $P=0.0731$, $R^2=0.9869$, Fig. 13). Taken together, these results suggest that superoxide accumulation downstream of NAMPT inhibition is specific to treatment-sensitive cells but may not play a direct role in inducing cell death.

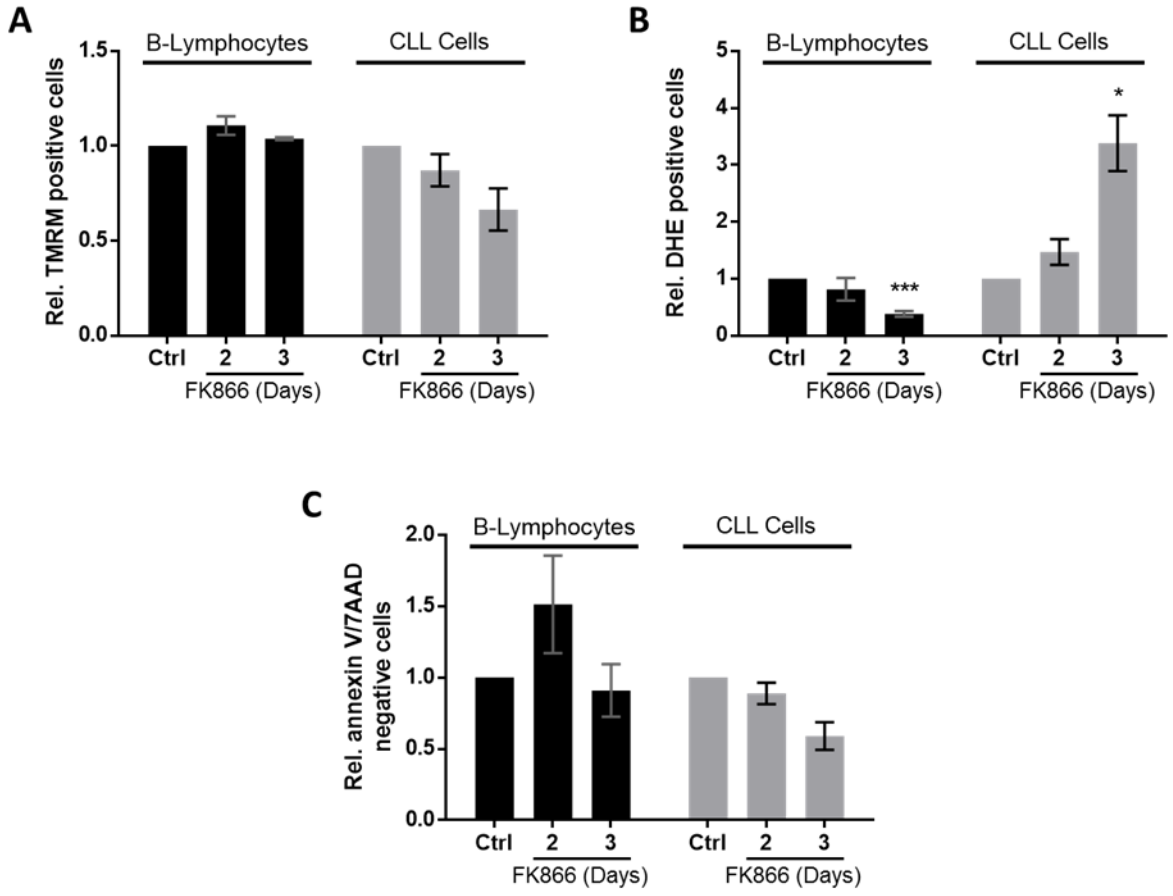

Figure 12: NAMPT inhibition selectively induces loss of mitochondrial membrane potential, superoxide accumulation and loss of viability in CLL cells. Control B-lymphocytes (N=5) and CLL cells (N=3) were treated with 10 nM FK866 or DMSO as vehicle control (Ctrl). (A) Mitochondrial membrane potential, (B) superoxide content and (C) cell viability were assessed on days two and three of treatment, by flow cytometry with TMRM, DHE, and annexin V-FITC and 7AAD staining, respectively. All data were normalized to vehicle controls at each time point. Statistical analysis was performed using one-sample t-tests (* $P \leq 0.05$, *** $P \leq 0.001$). (N= biological replicates)

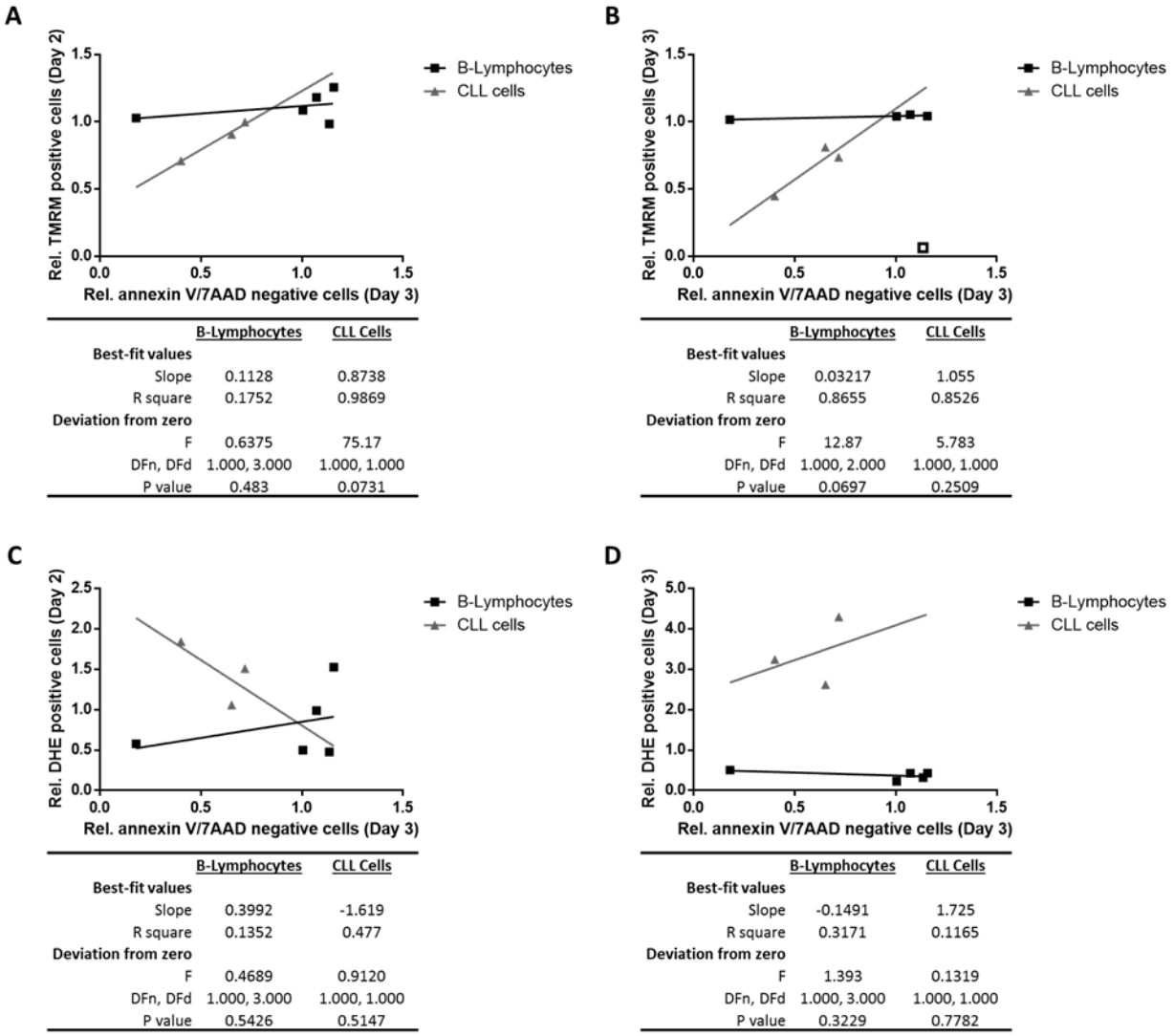

	B-Lymphocytes	CLL Cells
Best-fit values		
Slope	0.1128	0.8738
R square	0.1752	0.9869
Deviation from zero		
F	0.6375	75.17
DFn, DFd	1.000, 3.000	1.000, 1.000
P value	0.483	0.0731

	B-Lymphocytes	CLL Cells
Best-fit values		
Slope	0.03217	1.055
R square	0.8655	0.8526
Deviation from zero		
F	12.87	5.783
DFn, DFd	1.000, 2.000	1.000, 1.000
P value	0.0697	0.2509

	B-Lymphocytes	CLL Cells
Best-fit values		
Slope	0.3992	-1.619
R square	0.1352	0.477
Deviation from zero		
F	0.4689	0.9120
DFn, DFd	1.000, 3.000	1.000, 1.000
P value	0.5426	0.5147

	B-Lymphocytes	CLL Cells
Best-fit values		
Slope	-0.1491	1.725
R square	0.3171	0.1165
Deviation from zero		
F	1.393	0.1319
DFn, DFd	1.000, 3.000	1.000, 1.000
P value	0.3229	0.7782

Figure 13: Early loss of mitochondrial membrane potential predicts FK866 sensitivity in CLL cells. Correlation between FK866 sensitivity and mitochondrial membrane potential on days two (A) and three (B), or cellular superoxide content on days two (C) and three (D) were assessed by linear regression. One outlier was excluded from assessment of control B-lymphocyte MMP on day three (□). Statistical analysis was performed using the f-test (*P*-values indicated).

As the glutathione pathway, responsible for detoxification of cellular ROS, is NADP-dependent, the role of this pathway in ROS accumulation downstream of NAMPT inhibition was also investigated. Cellular NADP was found to be significantly depleted in CLL cells by day one following treatment with FK866 at concentrations from 10 to 50 nM (N=9, Fig. 14A). Similarly, reduced glutathione (GSH) was significantly depleted by day three of FK866-treatment at these concentrations (N=3, Fig. 14B). While cellular superoxide content was increased in a dose-dependent manner by FK866 as previously seen, peroxides were increased to a greater extent by day two, becoming statistically significant on the third day of FK866 treatment (N=4, Fig. 14C, Fig. 14D). Superoxide accumulation is therefore likely a secondary effect of peroxide accumulation due to the insufficiency of NADPH for glutathione recycling, and subsequent GSH depletion.

5.5. NAMPT inhibition sensitises CLL cells to current first-line chemotherapeutics and targeted agents

In order to evaluate the benefit of adding NAMPT inhibitors to current therapeutic regimens, FK866 and GMX-1778 were assessed in combination with current first-line chemotherapeutics and tyrosine kinase inhibitors. First, CLL cells were treated with FK866 at concentrations from 1.25 to 10 nM, alone or in combination with the nucleoside analog fludarabine at concentrations from 1.25 to 10 μM (N=16), and cell viability was assessed on the third day of treatment. A mostly additive drug-drug interaction was observed, with significant synergy identified at the highest doses of both agents only by the Loewe Additivity model (Fig. 15). Combination of FK866 with the alkylating agents chlorambucil (N=15) or bendamustine (N=16) produced more favorable results, with significant synergy identified by both mathematical models employed and

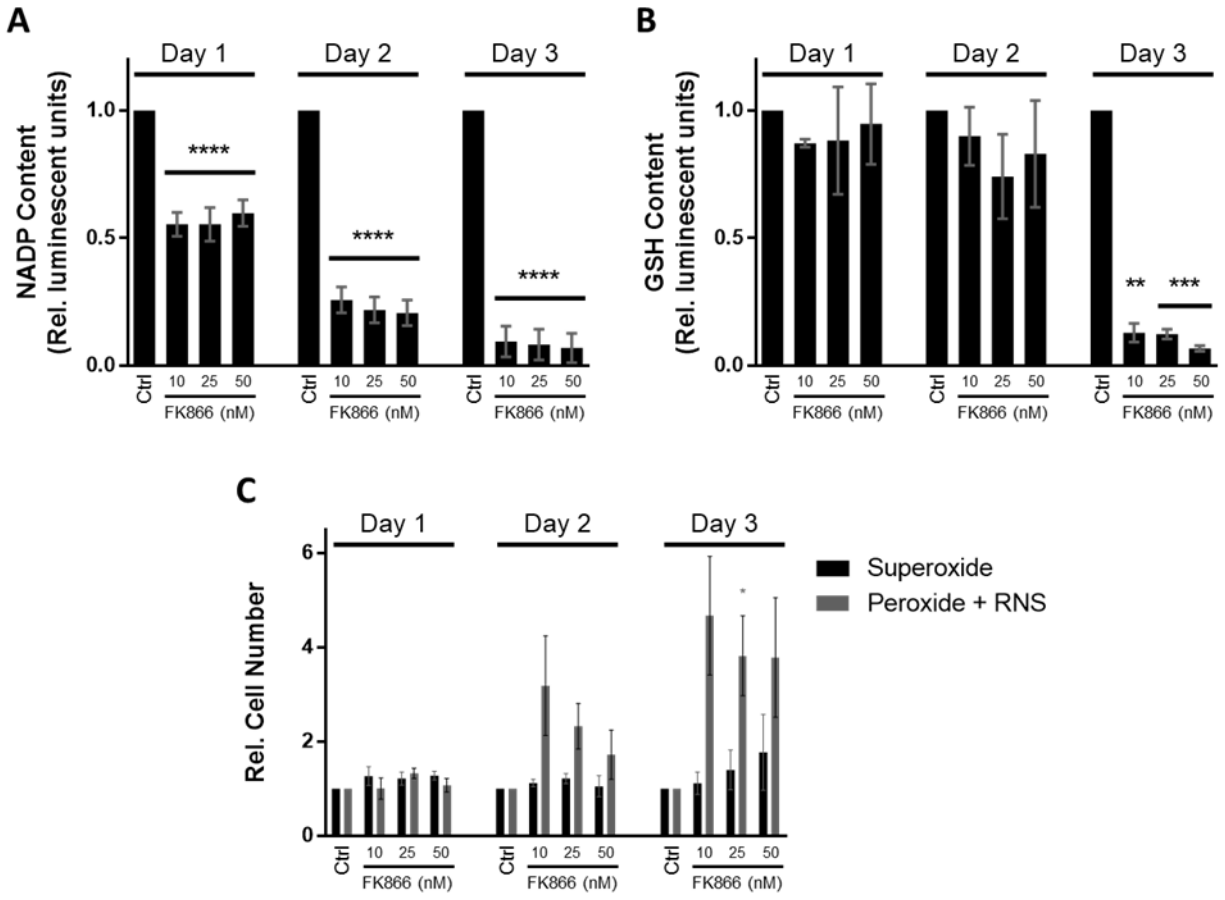

Figure 14: NAMPT inhibition leads to collapse of the glutathione antioxidant pathway. CLL cells were treated with FK866 at concentrations of 10, 25 and 50 nM, or DMSO as vehicle control (Ctrl). (A) Total cellular NADP (N=9, n=3) and (B) GSH (N=3, n=3) were assessed daily for three days by NADP/NADPH-Glo and GSH-Glo assays, respectively. (C) Cellular superoxide, and peroxide and reactive nitrogen species (RNS) content were assessed daily for three days by flow cytometry with DHE and DCFH-DA staining, respectively (N=4). All data were normalized to vehicle controls at each time point. Statistical analysis was performed using the one-sample t-test (* $P \leq 0.05$, ** $P \leq 0.01$, *** $P \leq 0.001$, **** $P \leq 0.0001$). (N= biological replicates, n= technical replicates)

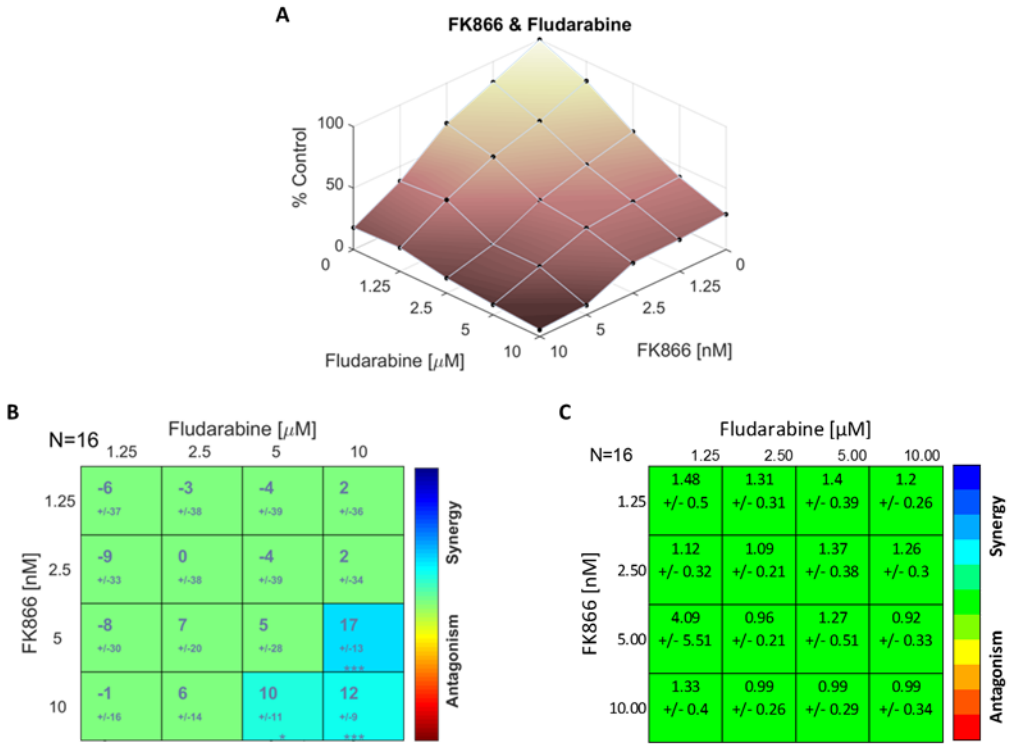

Figure 15: FK866 is additive with fludarabine treatment in CLL cells. CLL cells were treated with FK866, alone or in combination with fludarabine at the concentrations indicated (N=16). Cells were treated with DMSO as vehicle control. (A) Cell viability was assessed on the third day of treatment by flow cytometry with annexin V-FITC and PI staining. Annexin V-FITC negative, PI negative cells were considered viable and normalized to vehicle controls (% Control). (B) Drug-drug interaction was assessed according to the Loewe Additivity model. Deviations from predicted cell viability are given for dose combinations indicated (% dead cells, +/- 95% confidence interval). Values significantly different from zero are coloured (additivity=green, synergy=cyan/blue, antagonism=yellow/red). (C) Drug-drug interaction was assessed according to the Combination Index (CI) model. CIs are given for dose combinations indicated (+/- 95% confidence interval). Statistical analysis was performed using the one-sample t-test (* P≤0.05, *** P≤0.001). Data were contributed by Iris Gehrke.

combination indices (CIs) reaching 0.49 and 0.51 for chlorambucil and bendamustine, respectively (Fig. 16). Data were contributed by Dr. Iris Gehrke.

CLL cells were then treated with FK866 or GMX-1778 in combination with the BTK inhibitor ibrutinib (N=5), or the PI3Kδ inhibitor idelalisib (N=5). Synergy was again observed at the highest doses of ibrutinib (Fig. 17). Additionally, significant synergy was observed at all doses of idelalisib assessed (Fig. 18). Data were contributed by Ryan Saleh.

5.6. NAMPT inhibition is synergistic with inhibition of mitochondrial metabolism, but not glycolysis.

As NAMPT inhibition efficiently inhibited both mitochondrial respiration and glycolysis, FK866- and GMX-1778 were assessed in combination with specific inhibitors of each of these pathways. CLL cells were treated with FK866 (N=4) or GMX-1778 (N=3), in combination with the mitochondrial ATP synthase inhibitor oligomycin at concentrations from 31.25 to 500 ng/ml. While no antagonism was observed between oligomycin and either NAMPT inhibitor, significant synergy was identified with both FK866 and GMX-1778, only by the CI model and at the lowest dose of oligomycin assessed (Fig. 19). However, when CLL cells were treated with FK866 or GMX-1778 in combination with the mitochondrial uncoupler carbonyl cyanide-p-trifluoromethoxyphenylhydrazone (FCCP) at concentrations from 0.25 to 8 μM (N=6), significant synergy was observed between both NAMPT inhibitors and FCCP at broad range of doses and drug ratios. CIs as low as 0.3 and 0.27 were observed for combinations with FK866 and GMX-1778 respectively (Fig. 20). Data were contributed by Ryan Saleh.

To assess NAMPT inhibitors in combination with glycolytic inhibition, CLL cells were treated with FK866 or GMX-1778 in combination with the competitive non-metabolizable

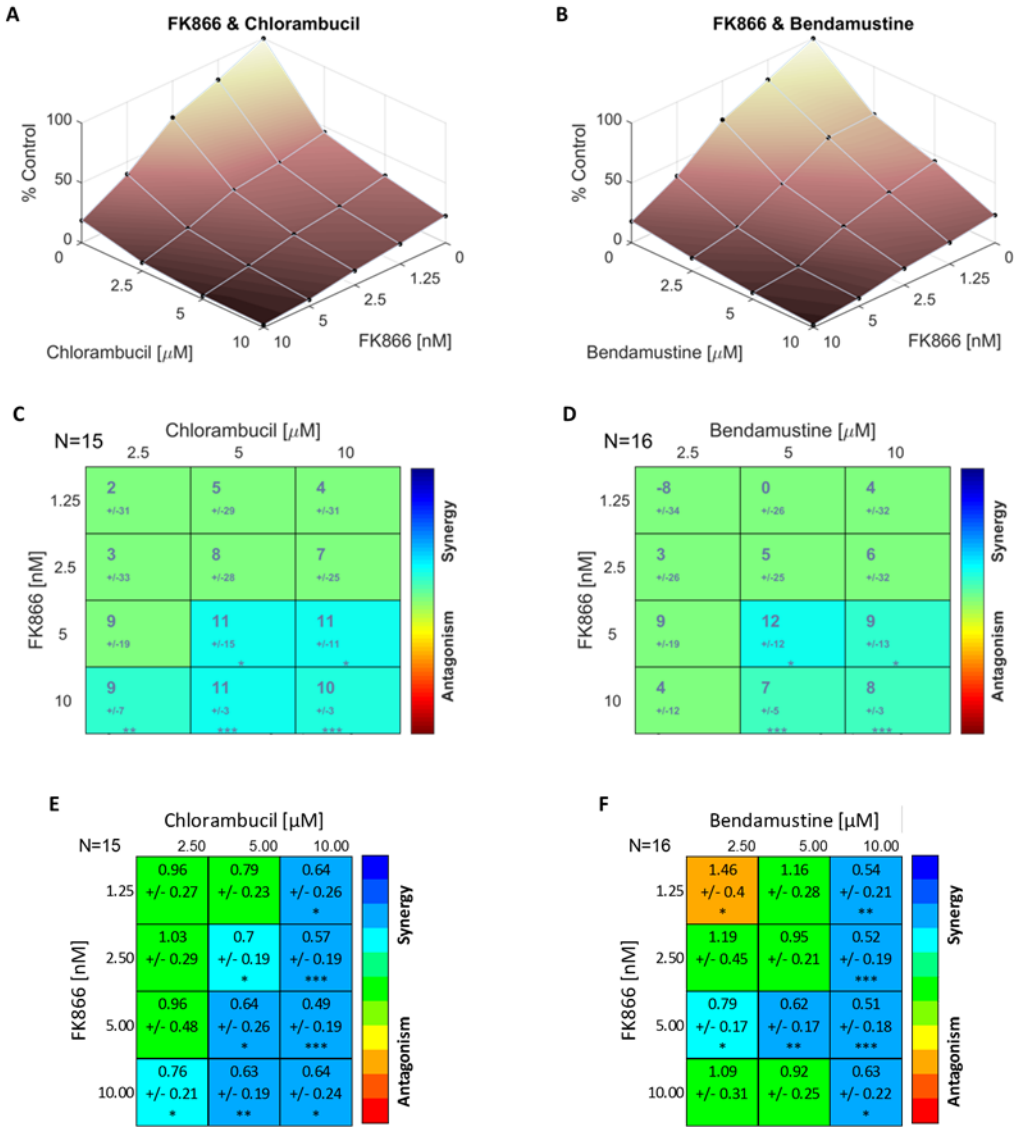

Figure 16: NAMPT inhibition sensitises CLL cells to alkylating agents. CLL cells were treated with FK866, alone or in combination with chlorambucil (N=15) or bendamustine (N=16) at the concentrations indicated. Cells were treated with DMSO as vehicle control. (A, B) Cell viability was assessed on the third day of treatment by flow cytometry with annexin V-FITC and PI staining. Annexin V-FITC negative, PI negative cells were considered viable and normalized to vehicle controls (% Control). (C, D) Drug-drug interactions were assessed according to the Loewe Additivity model. Deviations from predicted cell viability are given for dose combinations indicated (% dead cells, +/- 95% confidence interval). Values significantly different from zero are coloured (additivity=green, synergy=cyan/blue, antagonism=yellow/red). (E, F) Drug-drug interactions were assessed according to the Combination Index (CI) model. CIs are given for dose combinations indicated (+/- 95% confidence interval). Values significantly different from 1 are coloured as above. Statistical analysis was performed using the one-sample t-test (* P≤0.05, ** P≤0.01, *** P≤0.001). Data were contributed by Iris Gehrke.

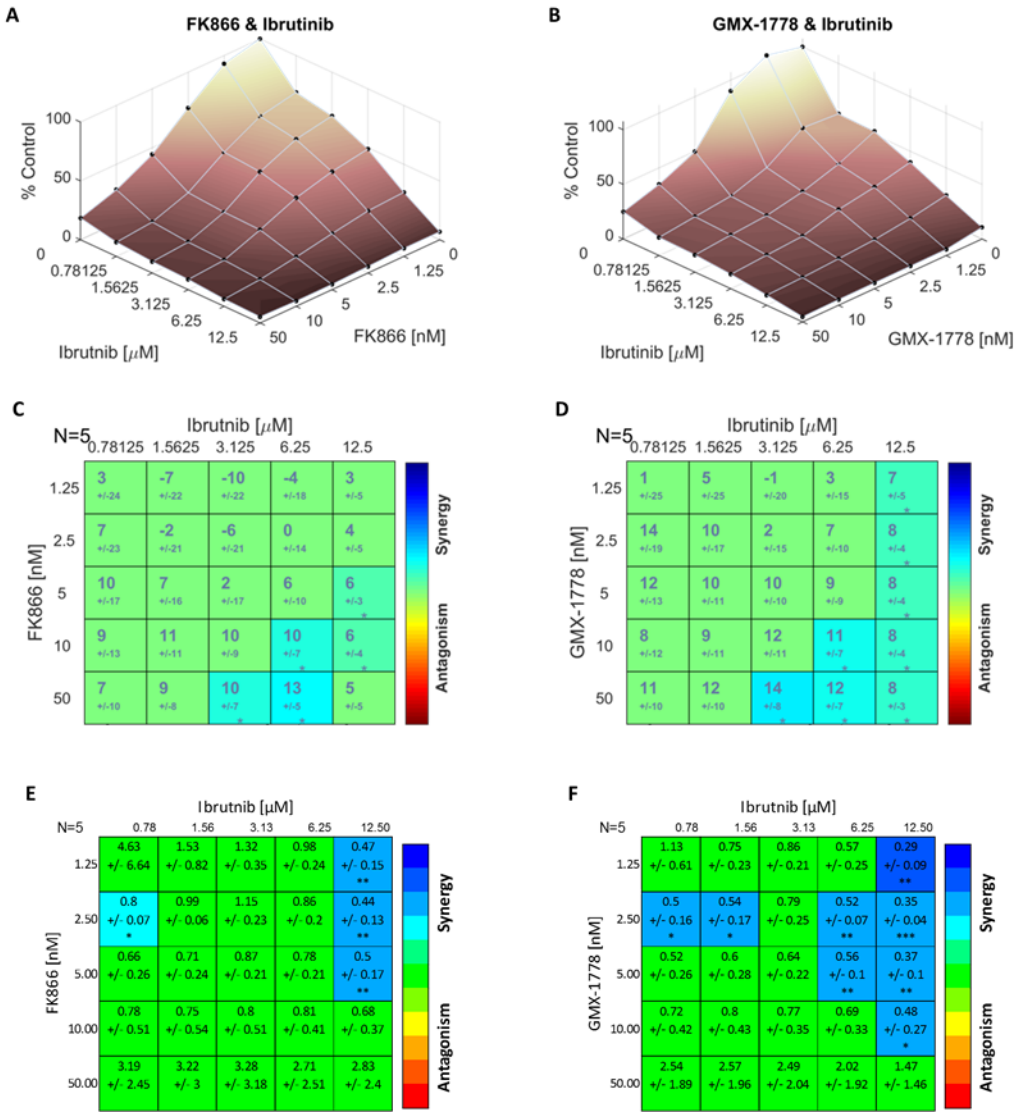

Figure 17: NAMPT inhibition sensitises CLL cells to BTK inhibition. CLL cells were treated with FK866 (left) or GMX-1778 (right), alone or in combination with the BTK inhibitor ibrutinib at the concentrations indicated (N=5). Cells were treated with DMSO as vehicle control. (A, B) Cell viability was assessed on the third day of treatment by flow cytometry with annexin V-FITC and 7AAD staining. Annexin V-FITC negative, 7AAD negative cells were considered viable and normalized to vehicle controls (% Control). (C, D) Drug-drug interactions were assessed according to the Loewe Additivity model. Deviations from predicted cell viability are given for dose combinations indicated (% dead cells, +/- 95% confidence interval). Values significantly different from zero are coloured (additivity=green, synergy=cyan/blue, antagonism=yellow/red). (E, F) Drug-drug interactions were assessed according to the Combination Index (CI) model. CIs are given for dose combinations indicated (+/- 95% confidence interval). Values significantly different from 1 are coloured as above. Statistical analysis was performed using the one-sample t-test (* P≤0.05, ** P≤0.01, *** P≤0.001). Data were contributed by Ryan Saleh.

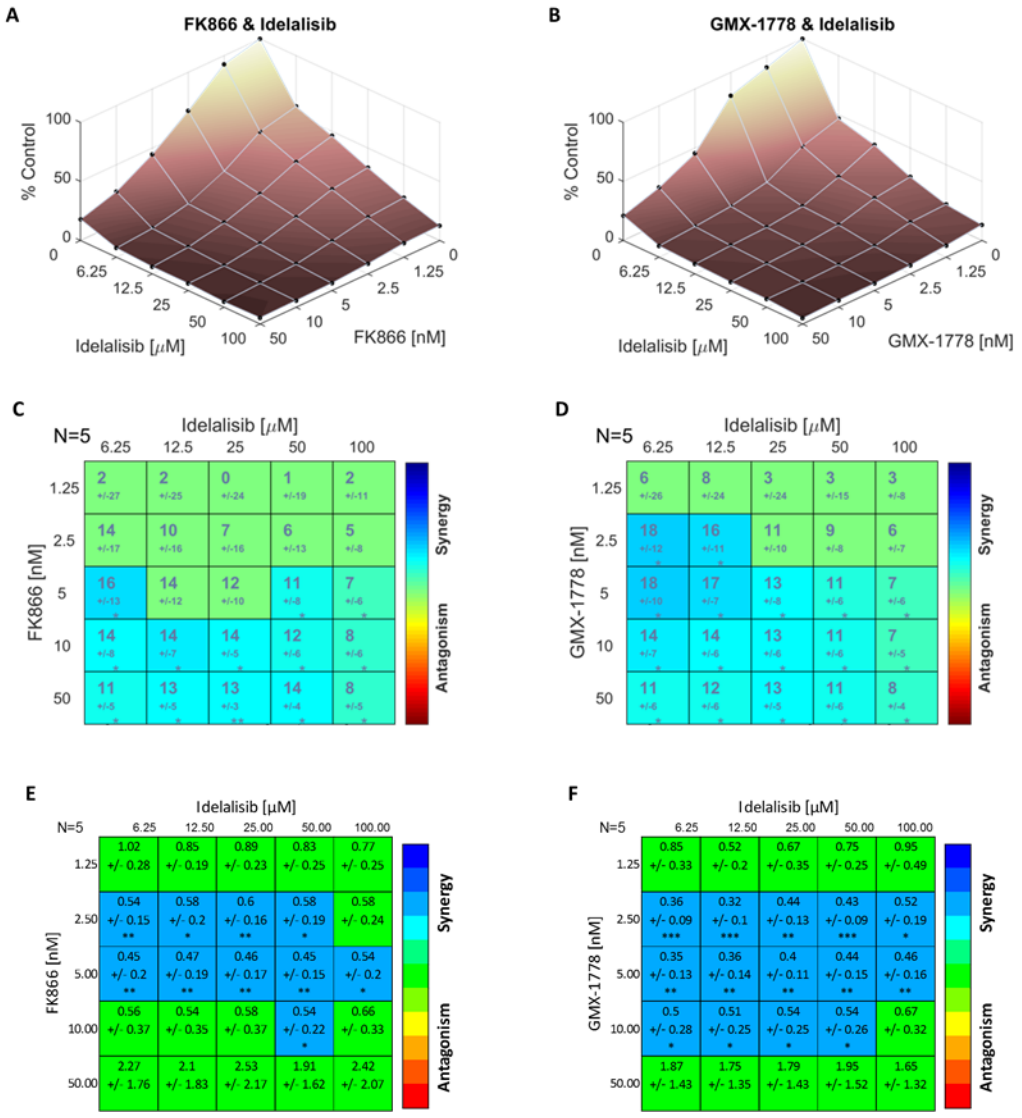

Figure 18: NAMPT inhibition is synergistic with PI3Kδ inhibition. CLL cells were treated with FK866 (left) or GMX-1778 (right), alone or in combination with the PI3Kδ inhibitor idelalisib at the concentrations indicated (N=5). Cells were treated with DMSO as vehicle control. (A, B) Cell viability was assessed on the third day of treatment by flow cytometry with annexin V-FITC and 7AAD staining. Annexin V-FITC negative, 7AAD negative cells were considered viable and normalized to vehicle controls (% Control). (C, D) Drug-drug interactions were assessed according to the Loewe Additivity model. Deviations from predicted cell viability are given for dose combinations indicated (% dead cells, +/- 95% confidence interval). Values significantly different from zero are coloured (additivity=green, synergy=cyan/blue, antagonism=yellow/red). (E, F) Drug-drug interactions were assessed according to the Combination Index (CI) model. CIs are given for dose combinations indicated (+/- 95% confidence interval). Values significantly different from 1 are coloured as above. Statistical analysis was performed using the one-sample t-test (* P≤0.05, ** P≤0.01, *** P≤0.001). Data were contributed by Ryan Saleh.

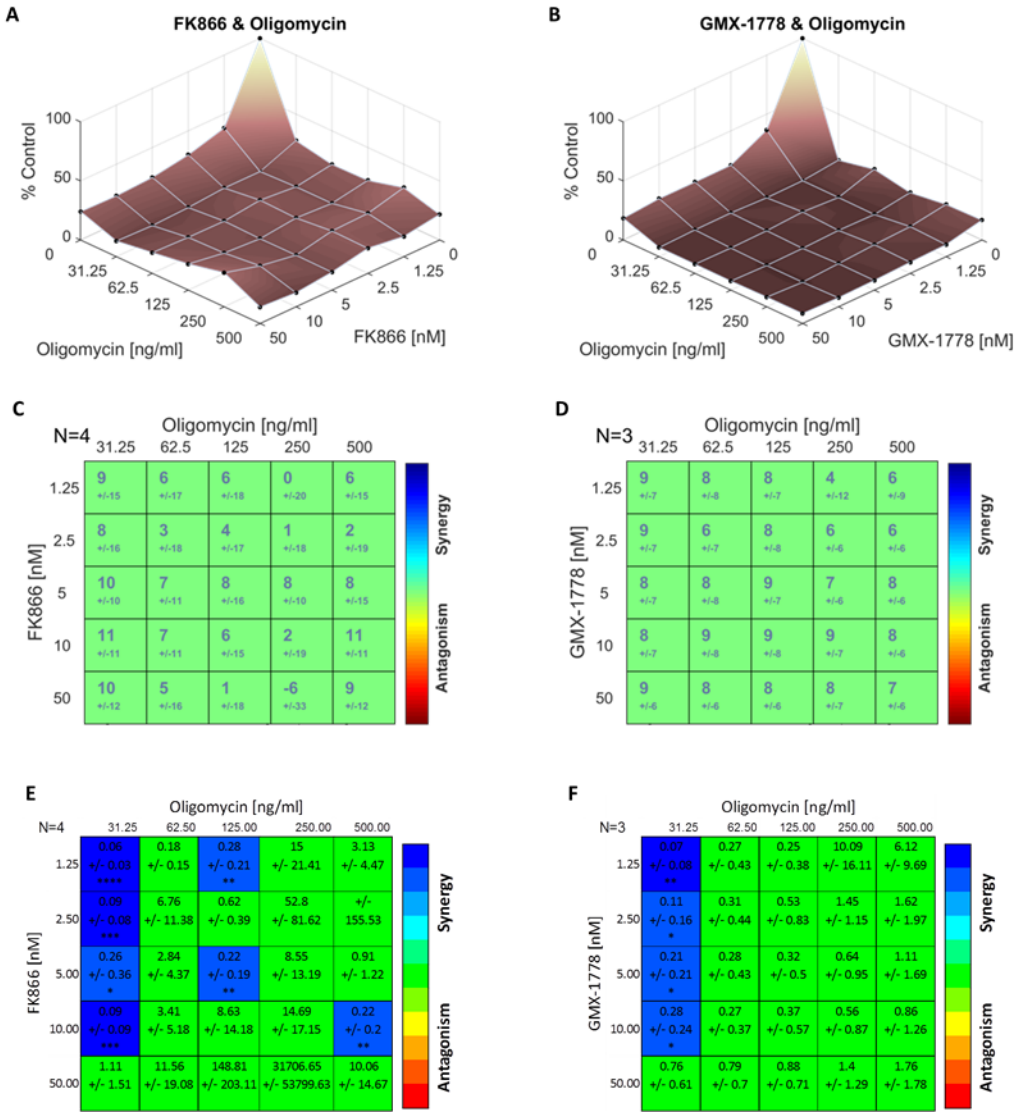

Figure 19: The cytotoxic effect of mitochondrial inhibition is additive with NAMPT inhibition in CLL cells. CLL cells were treated with FK866 (N=4, left) or GMX-1778 (N=3, right), alone or in combination with the ATP synthase inhibitor oligomycin at the concentrations indicated. Cells were treated with DMSO as vehicle control. (A, B) Cell viability was assessed on the third day of treatment by flow cytometry with annexin V-FITC and 7AAD staining. Annexin V-FITC negative, 7AAD negative cells were considered viable and normalized to vehicle controls (% Control). (C, D) Drug-drug interactions were assessed according to the Loewe Additivity model. Deviations from predicted cell viability are given for dose combinations indicated (% dead cells, +/- 95% confidence interval). Values significantly different from zero are coloured (additivity=green, synergy=cyan/blue, antagonism=yellow/red). (E, F) Drug-drug interactions were assessed according to the Combination Index (CI) model. CIs are given for dose combinations indicated (+/- 95% confidence interval). Values significantly different from 1 are coloured as above. Statistical analysis was performed using the one-sample t-test (* P≤0.05, ** P≤0.01, *** P≤0.001, **** P≤0.0001).

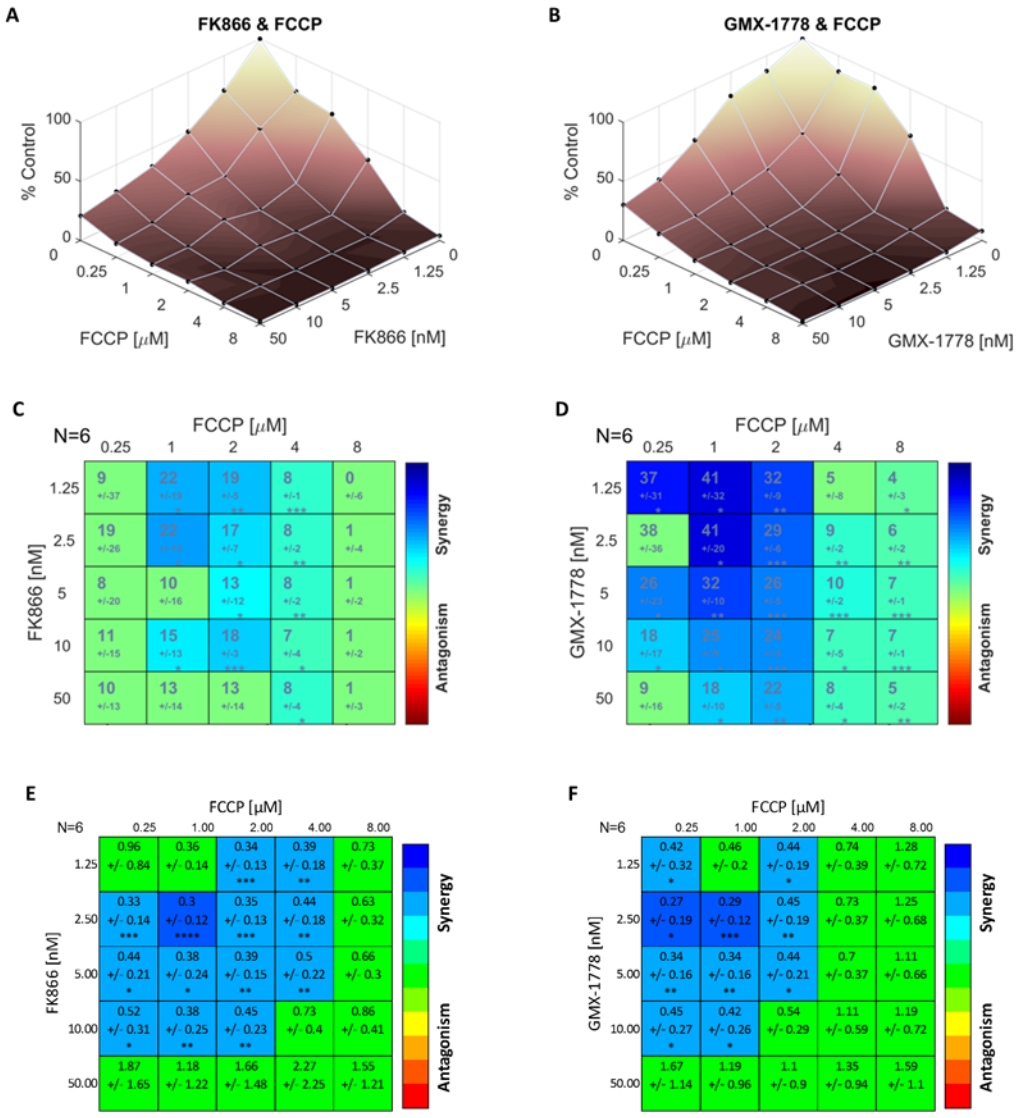

Figure 20: NAMPT inhibition is synergistic with mitochondrial uncoupling in CLL cells. CLL cells were treated with FK866 (left) or GMX-1778 (right), alone or in combination with the mitochondrial uncoupler FCCP at the concentrations indicated (N=6). Cells were treated with DMSO as vehicle control. (A, B) Cell viability was assessed on the third day of treatment by flow cytometry with annexin V-FITC and 7AAD staining. Annexin V-FITC negative, 7AAD negative cells were considered viable and normalized to vehicle controls (% Control). (C, D) Drug-drug interactions were assessed according to the Loewe Additivity model. Deviations from predicted cell viability are given for dose combinations indicated (% dead cells, +/- 95% confidence interval). Values significantly different from zero are coloured (additivity=green, synergy=cyan/blue, antagonism=yellow/red). (E, F) Drug-drug interactions were assessed according to the Combination Index (CI) model. CIs are given for dose combinations indicated (+/- 95% confidence interval). Values significantly different from 1 are coloured as above. Statistical analysis was performed using the one-sample t-test (* P≤0.05, ** P≤0.01, *** P≤0.001, **** P≤0.0001). Data were contributed by Ryan Saleh.

glucose analog 2-deoxi-D-glucose (2-DG) at concentrations from 0.3125 to 5 mM (N=6). While the Loewe Additivity model described mostly additive drug-drug interactions the CI model identified significant synergy at low doses of FK866 and antagonism at high doses of both NAMPT inhibitors (Fig. 21). Data were contributed by Ryan Saleh.

5.7. NAMPT inhibition is additive with ROS production in CLL cells

As NAMPT inhibition was shown to deplete cellular GSH reserves and lead to increases in both cellular peroxides and superoxides, the combined effects of FK866 or GMX-1778 and ROS were evaluated. CLL cells were treated with FK866 or GMX-1778 for two days followed by addition of hydrogen peroxide (H_2O_2) at concentrations from 31.25 to 500 μM, for one day (N=4). Mostly additive interactions were described by both the Loewe Additivity model and the CI model, with mild synergy described only by the Loewe model, and only at high concentrations of H_2O_2 (Fig. 22).

CLL cells were also treated for three days with FK866 or GMX-1778 in combination with the protein kinase C (PKC) activator phorbol 12-myristate 13-acetate (PMA) at concentrations from 3.125 to 50 μM (N=3). PMA-induced cell death is known to be mediated by NADH-dependent mitochondrial superoxide production. Results were highly variable in this small samples set, however significantly synergistic CIs were achieved in a small number of dose combination, at physiologically relevant concentrations of both FK866 and GMX-1778 (Fig. 23).

6. DISCUSSION

Altered cellular metabolism has recently gained popularity as a potential novel target for cancer therapy. In particular, overexpression of the NAD synthesising enzyme NAMPT has been linked to increased cell survival, proliferation, and resistance to chemotherapy and oxidative

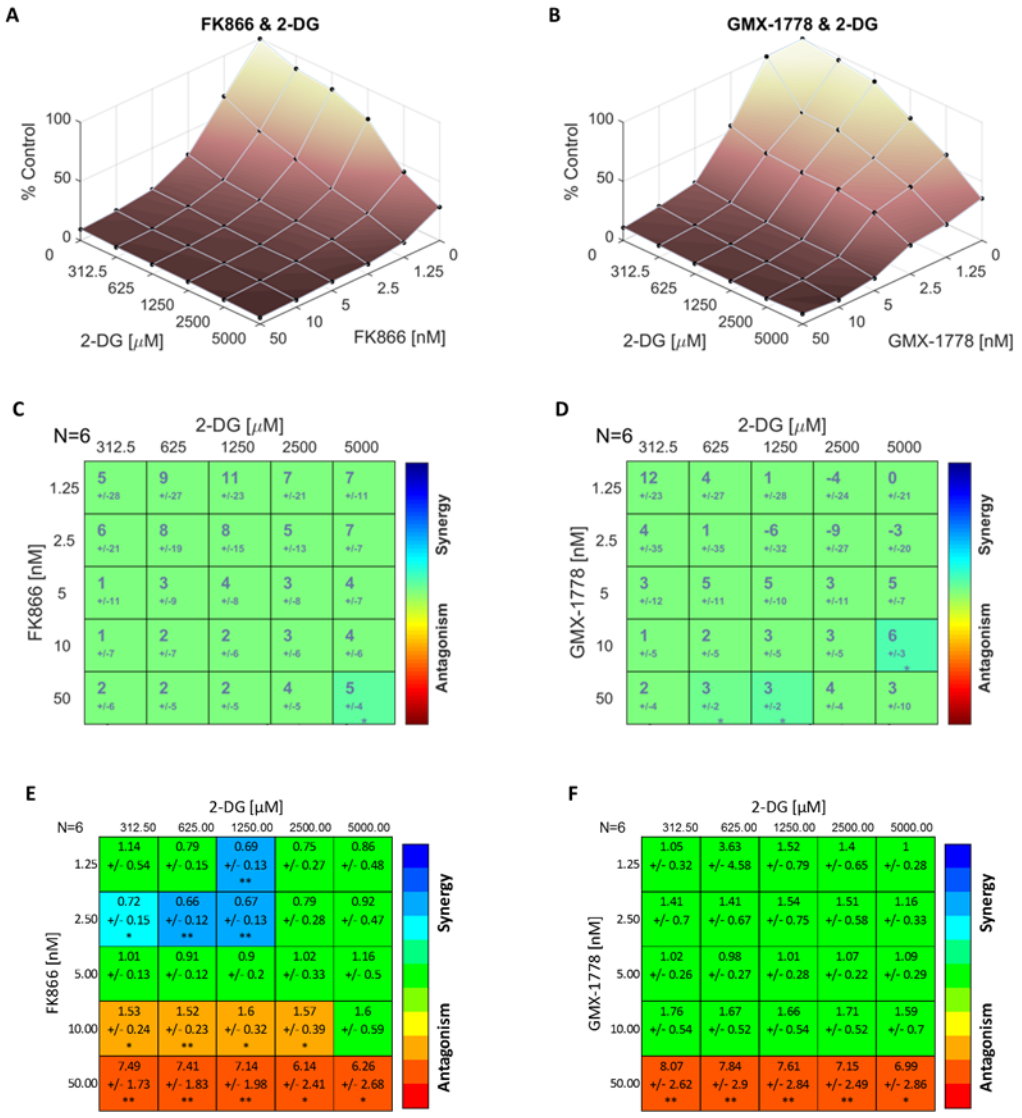

Figure 21: Interaction between NAMPT inhibition and inhibition of glycolysis is dose dependent in CLL cells. CLL cells were treated with FK866 (left) or GMX-1778 (right), alone or in combination with the glucose analogue 2-DG at the concentrations indicated (N=6). Cells were treated with DMSO as vehicle control. (A, B) Cell viability was assessed on the third day of treatment by flow cytometry with annexin V-FITC and 7AAD staining. Annexin V-FITC negative, 7AAD negative cells were considered viable and normalized to vehicle controls (% Control). (C, D) Drug-drug interactions were assessed according to the Loewe Additivity model. Deviations from predicted cell viability are given for dose combinations indicated (% dead cells, +/- 95% confidence interval). Values significantly different from zero are coloured (additivity=green, synergy=cyan/blue, antagonism=yellow/red). (E, F) Drug-drug interactions were assessed according to the Combination Index (CI) model. CIs are given for dose combinations indicated (+/- 95% confidence interval). Values significantly different from 1 are coloured as above. Statistical analysis was performed using the one-sample t-test (* P≤0.05, ** P≤0.01). Data were contributed by Ryan Saleh.

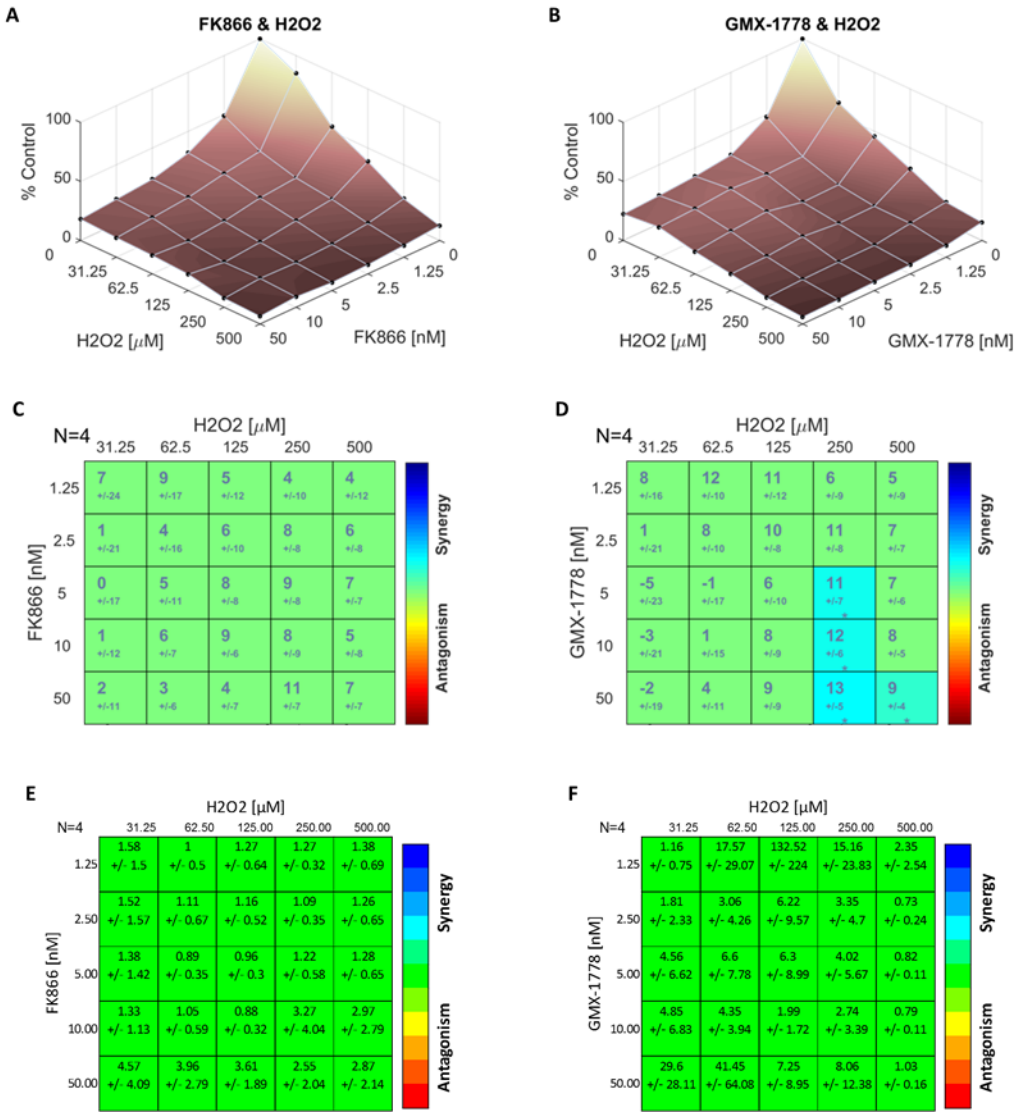

Figure 22: NAMPT inhibition is additive with peroxide in CLL cells. CLL cells were treated with FK866 (left) or GMX-1778 (right), alone or in combination with hydrogen peroxide (H2O2) at the concentrations indicated (N=4). Cells were treated with DMSO as vehicle control. (A, B) Cell viability was assessed on the third day of treatment by flow cytometry with annexin V-FITC and 7AAD staining. Annexin V-FITC negative, 7AAD negative cells were considered viable and normalized to vehicle controls (% Control). (C, D) Drug-drug interactions were assessed according to the Loewe Additivity model. Deviations from predicted cell viability are given for dose combinations indicated (% dead cells, +/- 95% confidence interval). Values significantly different from zero are coloured (additivity=green, synergy=cyan/blue, antagonism=yellow/red). (E, F) Drug-drug interactions were assessed according to the Combination Index (CI) model. CIs are given for dose combinations indicated (+/- 95% confidence interval). Values significantly different from 1 are coloured as above. Statistical analysis was performed using the one-sample t-test (* P≤0.05).

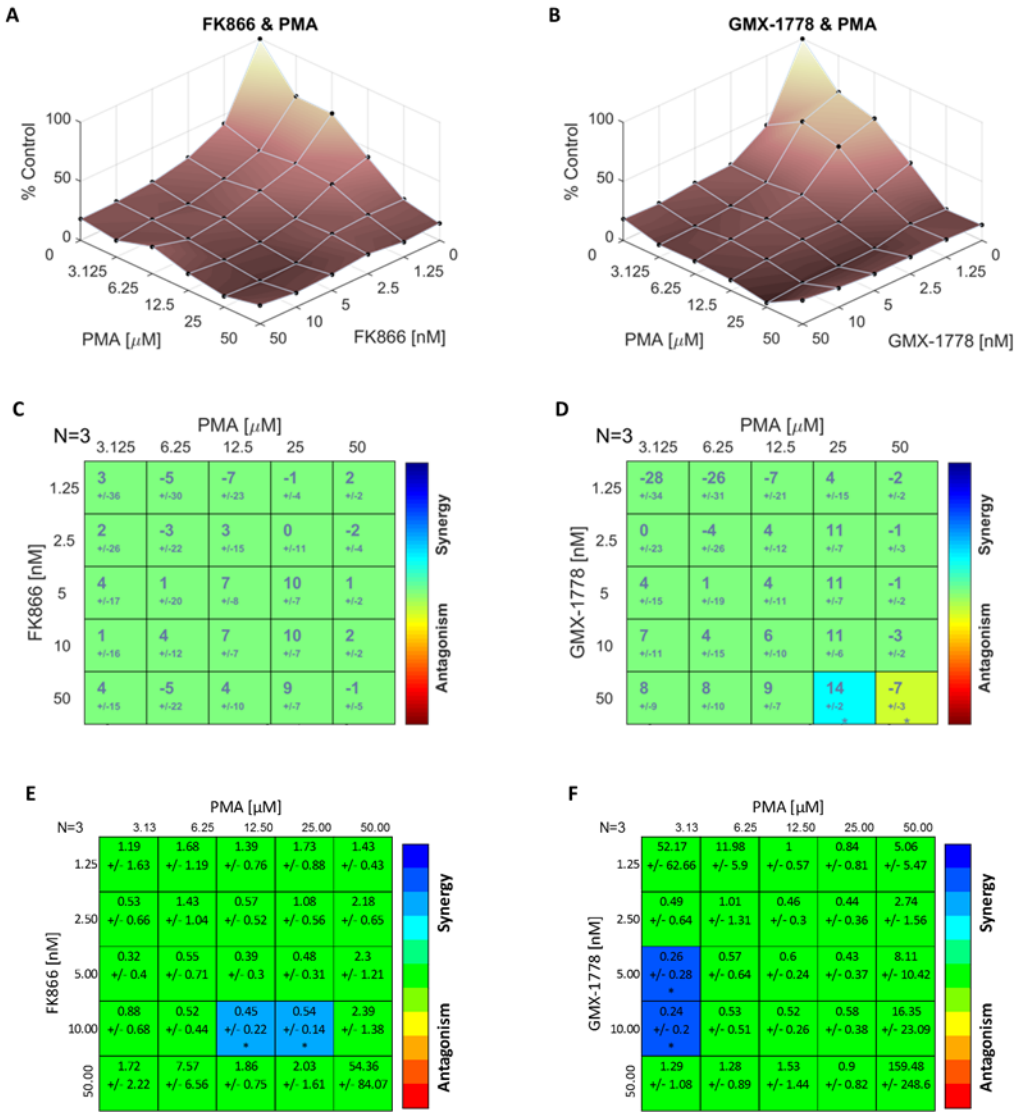

Figure 23: NAMPT inhibition is additive with superoxide production in CLL cells. CLL cells were treated with FK866 (left) or GMX-1778 (right), alone or in combination with the superoxide inducing PKC activator PMA at the concentrations indicated (N=3). Cells were treated with DMSO as vehicle control. (A, B) Cell viability was assessed on the third day of treatment by flow cytometry with annexin V-FITC and 7AAD staining. Annexin V-FITC negative, 7AAD negative cells were considered viable and normalized to vehicle controls (% Control). (C, D) Drug-drug interactions were assessed according to the Loewe Additivity model. Deviations from predicted cell viability are given for dose combinations indicated (% dead cells, +/- 95% confidence interval). Values significantly different from zero are coloured (additivity=green, synergy=cyan/blue, antagonism=yellow/red). (E, F) Drug-drug interactions were assessed according to the Combination Index (CI) model. CIs are given for dose combinations indicated (+/- 95% confidence interval). Values significantly different from 1 are coloured as above. Statistical analysis was performed using the one-sample t-test (* P≤0.05).

stress in multiple tumour types.[78–81] The NAMPT inhibitors FK866 and GMX-1778 are effective in killing cancer cells *in vitro* and decreasing cancer cell survival *in vivo* in multiple tumour models, including models of leukemia, lymphoma and myeloma;[235,240,241,246,254] however, early phase clinical trials have demonstrated a need for the dose reduction and increased treatment efficacy afforded by combination therapies.[238,242–244] In CLL, high NAMPT expression is predictive of poor overall survival,[228] and our group has previously demonstrated a broad therapeutic window for NAMPT inhibition *in vitro*.[237] Nevertheless, the design of combination therapies involving NAMPT inhibition has been hampered by poor understanding of cancer-specific metabolic alterations and dependencies, and of the diverse cellular effects of NAMPT inhibition.

6.1. Effects of NAMPT inhibition on CLL cell metabolism

While the successive depletion of cellular NAD and ATP, and loss of cell viability, following NAMPT inhibition has previously been demonstrated in other disease models,[227,229,235,236] This study demonstrated these effects for the first time in primary CLL cells. Additionally, the timing of these events was in agreement with previous reports. While rescue of the effects of NAMPT inhibition on cellular ATP and viability confirms that these are on-target effects downstream of NAD depletion, similar rescue by the PARP inhibitor olaparib has several implications. First, as NAD degradation by PARPs is thought to be largely mediated by PARP1 in response to DNA damage,[226,227] these results are consistent with a high rate of DNA damage, even in non-proliferative CLL cells *in vitro*. Secondly, as olaparib also inhibits the activity of PARP2 and PARP3, this may indicate an underappreciation of the roles of these enzymes in CLL biology. And finally, olaparib seems to delay but not fully inhibit the effects of NAMPT inhibition, as evidenced by depletion of NAD and partial depletion of ATP in CLL cells treated

with both FK866 and olaparib for three days, suggesting that the activity of other NAD-degrading enzymes is also elevated in CLL (Fig. 6).

Suppression of mitochondrial respiration was documented in the earliest investigations of FK866.[227] Here, we confirmed this effect in CLL, and further, refuted any contribution from ETC dysregulation, supporting the conclusion that mitochondrial dysfunction is a direct result of NAD insufficiency in CLL cells treated with NAMPT inhibitors. However, prior to this study, the impact of NAMPT inhibition on glycolysis remained largely unexplored. We found that glycolytic capacity is reduced in CLL cells as early as one day after FK866 treatment, while respiratory capacity is reduced only after two days of treatment. Additionally, while mitochondrial uncoupling is synergistic with NAMPT inhibition and inhibition of mitochondrial ATP synthase produced synergistic CIs at low doses, glycolytic inhibition with 2-DG, in combination with NAMPT inhibition, produced the only strong antagonism observed in this study, suggesting competition between the two agents. Therefore, cytosolic NAD depletion and subsequent NAD insufficiency for glycolysis likely play a dominant role in mechanism of NAMPT inhibition-induced CLL cell death. This may indicate a dependence on glycolysis for ATP synthesis in CLL, even in aerobic conditions, or a high demand for glycolytic intermediates for amino acid, nucleotide or lipid synthesis in resting CLL cells, and warrants further investigation.

While Zap-70 expression in CLL is associated with increased cell survival and proliferation, the biological function of this kinase in CLL and normal B-lymphocytes is poorly understood. Here, we showed that Zap-70 positive CLL cells exhibit significantly greater basal mitochondrial respiration and capacity for energy metabolism through glycolysis and mitochondrial respiration than Zap-70 negative CLL cells, indicating not only that these cells have increased energy

demands even at rest *in vitro*, but also that they retain or even increase their capacity to upregulate these pathways in response to metabolic or environmental stress. Despite this adaptability, Zap-70 positive CLL samples remain sensitive to mitochondrial inhibition downstream of NAMPT inhibition; however, contrary to all other CLL samples assessed, the rate of glycolysis was increased by FK866 treatment in one of two Zap-70 positive samples. Though this may be incidental, it bears further investigation, as it may indicate a subset of CLL cases in which the activity of NAMPT inhibitors is primarily driven by mitochondrial inhibition.

Another previously unexplored pathway downstream of NAMPT inhibition, the glutathione antioxidant pathway is known to be upregulated in CLL.[100,103,104] This pathway is a major component of the cellular defense against ROS caused by elevated mitochondrial metabolism and chemotherapeutic agents, and directly contributes to clearance and resistance to alkylating agents.[219,220] In this study, we demonstrated NAMPT inhibition-induced depletion of the active, reduced form of glutathione (GSH) and of the NADP required for its regeneration. In opposition to previous reports,[237] this is likely the major cause of increased cellular ROS content following NAMPT inhibition; however, interactions between specific peroxide and superoxide induction, and NAMPT inhibition were variable in the small number of patient samples assessed, and further investigation is required to determine the contribution of ROS accumulation to NAMPT inhibition-induced CLL cell death. Of note, GSH depletion following NAMPT inhibition has since been demonstrated in breast cancer cell lines, where it contributes to cell death induced by metabolic stress.[255]

6.2. Combination Therapy

Several recent studies have demonstrated that NAMPT inhibition sensitises cancer cells of multiple lineages to a broad range of current anti-cancer agents including DNA damaging agents,

nucleoside analogs and monoclonal antibodies, which make up the current first-line therapies for CLL.[80,234,246] In addition, NAMPT inhibition is synergistic with several novel agents which exploit features of the NAD metabolome to produce strong and highly targeted effects in other disease models.[247,248] However, these reports present several limitations common to drug combination studies. First, many of these studies fail to address the dynamics of drug-drug interaction; assessing a single dose of each agent,[234,246,248] or varying the concentration of one agent while keeping the other constant.[80,234] As drug-drug interaction may vary greatly according to dose, drug ratio and intensity of effect, these approaches may underestimate the potential of a drug combination or fail to identify conditions of antagonism which may become relevant *in vivo* due to differing pharmacokinetics.[252,256] Secondly, where mathematical models were used to predict the benefits of drug combination, the methods used do not account for variability of effects or sampling error.[256]

In this study, these issues were addressed by a full factorial assay design and the use of two complimentary data analysis methods chosen to allow evaluation of a broad range drug concentrations and ratios, and statistical analysis of results. Of note, the Loewe model, as applied here, represents the more conservative approach used. Due to its use of median DR curves, this model may overestimate the variability of drug-drug interactions when patient samples are not equally sensitive to the individual drugs combined, and therefore predict fewer cases of significant synergy or antagonism. Conversely, the use of a fixed maximum effect in fitting single-agent DR curves for the CI model may lead to overestimation of the magnitude of drug-drug interactions, as well as their variability, particularly at very low and very high drug concentrations.[253] Despite these limitations, the Loewe and CI models remain among the most

accurate available models for predicting drug synergy without prohibitively large data sets,[256] and were generally in agreement.

As has been reported in other disease models, addition of NAMPT inhibitors was found to benefit a broad range of treatment strategies in CLL. Of agents in current clinical use, combinations with the alkylating agents, chlorambucil and bendamustine were among the most promising for improved treatment efficacy and dose reduction. As nucleophiles such as these agents are targets for detoxification by GSH, inhibition of GSH recycling downstream of NAMPT inhibition, and decreased clearance of these alkylating agents, are the most likely mechanisms for the favorable interaction between these treatment modalities. This bears confirmation by assessing the levels of GSH-alkylating agent adducts secreted into the culture media in the presence and absence of NAMPT inhibitors. Similarly, we demonstrated promising synergy between NAMPT inhibition and PI3Kδ inhibition by idelalisib, which was present at a broader range of doses than synergy seen with the BTK inhibitor ibrutinib. As no direct interaction between NAMPT and PI3Kδ has been described, this likely reflects a combination of increased apoptotic signalling following energy depletion with decreased survival signalling mediated by PI3Kδ. While both PI3Kδ and BTK mediate survival signals, BTK activation also induces NAMPT expression via the NF-κB pathway. BTK inhibition may therefore decrease NAMPT expression, leading to an overlap in the mechanisms of ibrutinib and NAMPT inhibitors which translates as reduced synergy between these agents. Consequently, idelalisib was identified as the more promising agent for NAMPT inhibitor-based combination therapy and is recommended, along with chlorambucil and bendamustine, for animal studies or clinical trials.

Mitochondrial inhibition has recently gained popularity as a promising novel strategy for cancer therapy.[257,258] As a large number mitochondrial inhibitors are in current use as antibiotics,

these agents benefit form demonstrated safety and well documented toxicities, and have the potential to rapidly influence patient care if effective. In this study, mitochondrial inhibition, particularly with uncoupling agents was identified as a promising candidate for NAMPT inhibition-based combination therapies in CLL. As glycolysis is preferentially supressed by NAMPT inhibitors in these cells, we believe that this forms a two-pronged attack on energy metabolism; rapidly depleting CLL cells' ATP stores and leading to enhanced cell killing. New combination therapies exploiting this target are currently being investigated.

7. CONCLUSIONS

In this study, we demonstrated that NAMPT inhibition induces depletion of both the cytoplasmic and mitochondrial NAD pools, in primary CLL cells. This leads to specific suppression of energy metabolism by both mitochondrial respiration and glycolysis, and depletion of cellular ATP. We also established that Zap-70 positive CLL cells exhibit enhanced metabolic capacity in both of these pathways. While these cells remain sensitive to mitochondrial inhibition downstream of NAMPT inhibitions, a subset of Zap-70 positive CLL cases may be resistant to glycolytic inhibition by this mechanism. Additionally, we found that NAMPT inhibition leads to NADP depletion and collapse of the glutathione antioxidant pathway in CLL, accompanied by a significant increase in cellular ROS content.

In drug combinations with current chemotherapeutics and targeted agents, additive or greater effects were produced by both FK866 and GMX-1778 in combination with all current agents assessed, including chemotherapeutics fludarabine, chlorambucil and bendamustine, and tyrosine kinase inhibitors ibrutinib and idelalisib. Synergy was most pronounced with the alkylating agents, chlorambucil and bendamustine and the PI3Kδ inhibitor idelalisib. Similarly,

combination of NAMPT inhibitors with agents targeting mitochondrial metabolism, and ROS production produced additive or greater effects. While combinations with specific ROS-inducing agents offered no objective benefit over combinations with agents in current clinical use, mitochondrial inhibition, particularly with the uncoupling agent FCCP, exhibited strong synergy with NAMPT inhibition over a broad range of low dose combinations. Conversely, interactions between FK866 or GMX-1778, and inhibition of glycolysis were dose dependent and produced strongly antagonistic CIs at high doses of NAMPT inhibitors.

Overall, this study has contributed to our understanding of NAD metabolism in CLL and cancer, and identified glycolysis and anti-oxidation as previously unrecognised targets of NAMPT inhibition. Additionally, several promising drug combinations were identified which may prove to be important advancements in the treatment of this common and incurable disease.

REFERENCES

1. Hallek, M. Chronic lymphocytic leukemia: 2015 Update on diagnosis, risk stratification, and treatment. *Am. J. Hematol.* **90,** 446–460 (2015).

2. Seftel, M. D. *et al.* High incidence of chronic lymphocytic leukemia (CLL) diagnosed by immunophenotyping: a population-based Canadian cohort. *Leuk. Res.* **33,** 1463–8 (2009).

3. Johnston, J. B., Seftel, M. & Gibson, S. B. in *Wintrobe's Hematology, 13th Edition* (eds. Greer, J. P. et al.) 1888–1928 (Lippincott, Williams and Wilkins, 2014).

4. Oppezzo, P. & Dighiero, G. Role of the B-cell receptor and the microenvironment in chronic lymphocytic leukemia. *Blood Cancer J.* **3,** e149 (2013).

5. Dores, G. M. *et al.* Chronic lymphocytic leukaemia and small lymphocytic lymphoma: overview of the descriptive epidemiology. *Br. J. Haematol.* **139,** 809–19 (2007).

6. Eichhorst, B., Dreyling, M., Robak, T., Montserrat, E. & Hallek, M. Chronic lymphocytic leukemia: ESMO Clinical Practice Guidelines for diagnosis, treatment and follow-up. *Ann. Oncol.* **22 Suppl 6,** vi50–4 (2011).

7. CancerCare Manitoba. *Practice Guideline : Disease Management - Consensus Recommendations for the Management of Chronic Lymphocytic Leukemia*. (2015).

8. Dameshek, W. Chronic lymphocytic leukemia--an accumulative disease of immunolgically incompetent lymphocytes. *Blood* **29,** Suppl:566–84 (1967).

9. Bentley, D. P. & Pepper, C. J. The apoptotic pathway: a target for therapy in chronic lymphocytic leukemia. *Hematol. Oncol.* **18,** 87–98 (2000).

10. Kitada, S., Pedersen, I. M., Schimmer, A. D. & Reed, J. C. Dysregulation of apoptosis

genes in hematopoietic malignancies. *Oncogene* **21,** 3459–3474 (2002).

11. Chiorazzi, N. Cell proliferation and death: forgotten features of chronic lymphocytic leukemia B cells. *Best Pract. Res. Clin. Haematol.* **20,** 399–413 (2007).

12. Messmer, B. T. *et al.* In vivo measurements document the dynamic cellular kinetics of chronic lymphocytic leukemia B cells. *J. Clin. Invest.* **115,** 755–64 (2005).

13. Herishanu, Y. *et al.* The lymph node microenvironment promotes B-cell receptor signaling, NF-kappaB activation, and tumor proliferation in chronic lymphocytic leukemia. *Blood* **117,** 563–74 (2011).

14. Dilley, R. L. *et al.* Poly(ADP-ribose) polymerase inhibitor CEP-8983 synergizes with bendamustine in chronic lymphocytic leukemia cells in vitro. *Leuk. Res.* **38,** 411–7 (2014).

15. Burger, J. a, Ghia, P., Rosenwald, A. & Caligaris-cappio, F. The microenvironment in mature B-cell malignancies : a target for new treatment strategies Review article The microenvironment in mature B-cell malignancies : a target for new treatment strategies. *Blood* **114,** 3367–3375 (2009).

16. Audrito, V. *et al.* Targeting the microenvironment in chronic lymphocytic leukemia offers novel therapeutic options. *Cancer Lett.* **328,** 27–35 (2013).

17. Burger, J. a. Nurture versus nature: the microenvironment in chronic lymphocytic leukemia. *Hematology Am. Soc. Hematol. Educ. Program* **2011,** 96–103 (2011).

18. Kurtova, A. V *et al.* Diverse marrow stromal cells protect CLL cells from spontaneous and drug-induced apoptosis: development of a reliable and reproducible system to assess stromal cell adhesion-mediated drug resistance. *Blood* **114,** 4441–50 (2009).

19. LeBien, T. W. & Tedder, T. F. B lymphocytes: how they develop and function. *Blood* **112,** 1570–80 (2008).

20. Osmond, D. G. *et al.* Apoptosis and macrophage-mediated cell deletion in the regulation of B lymphopoiesis in mouse bone marrow. *Immunol Rev* **142,** 209–230 (1994).

21. Radbruch, A. *et al.* Competence and competition: the challenge of becoming a long-lived plasma cell. *Nat. Rev. Immunol.* **6,** 741–750 (2006).

22. Allen, C. D. C. *et al.* Germinal center dark and light zone organization is mediated by CXCR4 and CXCR5. *Nat. Immunol.* **5,** 943–952 (2004).

23. Burger, J. a. & Chiorazzi, N. B cell receptor signaling in chronic lymphocytic leukemia. *Trends Immunol.* **34,** 592–601 (2013).

24. Lam, K. P., Kühn, R. & Rajewsky, K. In vivo ablation of surface immunoglobulin on mature B cells by inducible gene targeting results in rapid cell death. *Cell* **90,** 1073–1083 (1997).

25. Kraus, M., Alimzhanov, M. B., Rajewsky, N. & Rajewsky, K. Survival of resting mature B lymphocytes depends on BCR signaling via the Igalpha/beta heterodimer. *Cell* **117,** 787–800 (2004).

26. Stein, H. *et al.* Immunohistologic analysis of the organization of normal lymphoid tissue and non-Hodgkin's lymphomas. *J. Histochem. Cytochem.* **28,** 746–60 (1980).

27. Burger, J. A. *et al.* Blood-derived nurse-like cells protect chronic lymphocytic leukemia B cells from spontaneous apoptosis through stromal cell – derived factor-1. *Blood* **96,** 2655–2663 (2000).

28. Bürkle, A. & Niedermeier, M. Overexpression of the CXCR5 chemokine receptor, and its ligand, CXCL13 in B-cell chronic lymphocytic leukemia. … **110,** 3316–3325 (2007).

29. Patten, P. E. M. *et al.* CD38 expression in chronic lymphocytic leukemia is regulated by the tumor microenvironment. *Blood* **111,** 5173–5181 (2008).

30. Shaffer, A. L., Young, R. M. & Staudt, L. M. Pathogenesis of human B cell lymphomas. *Annu. Rev. Immunol.* **30,** 565–610 (2012).

31. Davis, R., Ngo, V., Lenz, G. & Tolar, P. Chronic Active B cell receptor signaling in diffuse large B cell lymphoma. *Nature* **463,** 88–92 (2010).

32. Philippen, A. *et al.* SYK carries no activating point mutations in patients with chronic lymphocytic leukaemia (CLL). *Br. J. Haematol.* **150,** 633–6 (2010).

33. Stevenson, F. K. & Caligaris-cappio, F. Chronic lymphocytic leukemia : revelations from the B-cell receptor Review in translational hematology Chronic lymphocytic leukemia : revelations from the B-cell receptor. *In Vitro* **103,** 4389–4395 (2008).

34. Chiorazzi, N. & Efremov, D. G. Chronic lymphocytic leukemia: a tale of one or two signals? *Cell Res.* **23,** 182–5 (2013).

35. Rai, K. R. & Jain, P. Chronic lymphocytic leukemia (CLL) - Then and Now. *Am. J. Hematol.* 1–5 (2015). doi:10.1002/ajh.24282

36. Baliakas, P. *et al.* Not all IGHV3-21 chronic lymphocytic leukemias are equal: prognostic considerations. *Blood* **125,** 856–9 (2015).

37. Gounari, M. *et al.* Excessive antigen reactivity may underlie the clinical aggressiveness of chronic lymphocytic leukemia stereotyped subset #8. *Blood* **125,** 3580–7 (2015).

38. Rossi, D. *et al.* Association between molecular lesions and specific B-cell receptor subsets in chronic lymphocytic leukemia. *Blood* **121,** 4902–4905 (2013).

39. Hamblin, T. J., Davis, Z., Gardiner, A., Oscier, D. G. & Stevenson, F. K. Unmutated Ig V(H) genes are associated with a more aggressive form of chronic lymphocytic leukemia. *Blood* **94,** 1848–54 (1999).

40. Bröker, B. M. *et al.* Chronic lymphocytic leukemic (CLL) cells secrete multispecific autoantibodies. *J. Autoimmun.* **1,** 469–81 (1988).

41. Sthoeger, Z. M. *et al.* Production of autoantibodies by CD5-expressing B lymphocytes from patients with chronic lymphocytic leukemia. *J. Exp. Med.* **169,** 255–68 (1989).

42. Borche, L., Lim, A., Binet, J. L. & Dighiero, G. Evidence that chronic lymphocytic leukemia B lymphocytes are frequently committed to production of natural autoantibodies. *Blood* **76,** 562–9 (1990).

43. Kostareli, E. *et al.* Antigen receptor stereotypy across B-cell lymphoproliferations: the case of IGHV4-59/IGKV3-20 receptors with rheumatoid factor activity. *Leukemia* **26,** 1127–31 (2012).

44. Hoogeboom, R. *et al.* A novel chronic lymphocytic leukemia subset expressing mutated IGHV3-7-encoded rheumatoid factor B-cell receptors that are functionally proficient. *Leukemia* **27,** 738–40 (2013).

45. Hervé, M. *et al.* Unmutated and mutated chronic lymphocytic leukemias derive from self-reactive B cell precursors despite expressing different antibody reactivity. *J. Clin. Invest.* **115,** 1636–43 (2005).

46. Lanemo Myhrinder, A. *et al.* A new perspective: molecular motifs on oxidized LDL, apoptotic cells, and bacteria are targets for chronic lymphocytic leukemia antibodies. *Blood* **111,** 3838–48 (2008).

47. Chu, C. C. *et al.* Chronic lymphocytic leukemia antibodies with a common stereotypic rearrangement recognize nonmuscle myosin heavy chain IIA. *Blood* **112,** 5122–9 (2008).

48. Binder, M. *et al.* Stereotypical chronic lymphocytic leukemia B-cell receptors recognize survival promoting antigens on stromal cells. *PLoS One* **5,** e15992 (2010).

49. Nolz, J. C. *et al.* ZAP-70 is expressed by a subset of normal human B-lymphocytes displaying an activated phenotype. *Leuk. Off. J. Leuk. Soc. Am. Leuk. Res. Fund, U.K* **19,** 1018–1024 (2005).

50. Cutrona, G. *et al.* B lymphocytes in humans express ZAP-70 when activated in vivo. *Eur. J. Immunol.* **36,** 558–69 (2006).

51. Scielzo, C. *et al.* ZAP-70 is expressed by normal and malignant human B-cell subsets of different maturational stage. *Leuk. Off. J. Leuk. Soc. Am. Leuk. Res. Fund, U.K* **20,** 689–695 (2006).

52. Chen, L. *et al.* Expression of ZAP-70 is associated with increased B-cell receptor signaling in chronic lymphocytic leukemia. *Blood* **100,** 4609–4614 (2002).

53. Richardson, S. J. *et al.* ZAP-70 expression is associated with enhanced ability to respond to migratory and survival signals in B-cell chronic lymphocytic leukemia (B-CLL). *Blood* **107,** 3584–3592 (2006).

54. Messmer, D. *et al.* Chronic lymphocytic leukemia cells receive RAF-dependent survival

signals in response to CXCL12 that are sensitive to inhibition by sorafenib. *Blood* **117,** 882–9 (2011).

55. Calpe, E. *et al.* ZAP-70 enhances migration of malignant B lymphocytes toward CCL21 by inducing CCR7 expression via IgM-ERK1/2 activation. *Blood* **118,** 4401–4410 (2011).

56. Lafarge, S. T. *et al.* ZAP70 expression directly promotes chronic lymphocytic leukaemia cell adhesion to bone marrow stromal cells. *Br. J. Haematol.* **168,** 139–142 (2015).

57. Vaisitti, T. *et al.* CD38 increases CXCL12-mediated signals and homing of chronic lymphocytic leukemia cells. *Leukemia* **24,** 958–69 (2010).

58. Contri, A. *et al.* Chronic lymphocytic leukemia B cells contain anomalous Lyn tyrosine kinase, a putative contribution to defective apoptosis. *J. Clin. Invest.* **115,** 369–378 (2005).

59. Gobessi, S. *et al.* Inhibition of constitutive and BCR-induced Syk activation downregulates Mcl-1 and induces apoptosis in chronic lymphocytic leukemia B cells. *Leuk. Off. J. Leuk. Soc. Am. Leuk. Res. Fund, U.K* **23,** 686–697 (2009).

60. Muzio, M. *et al.* Constitutive activation of distinct BCR-signaling pathways in a subset of CLL patients: a molecular signature of anergy. *Blood* **112,** 188–195 (2008).

61. Hewamana, S. *et al.* The NF- B subunit Rel A is associated with in vitro survival and clinical disease progression in chronic lymphocytic leukemia and represents a promising therapeutic target. *Blood* **111,** 4681–4690 (2008).

62. Minden, M. D. *et al.* Chronic lymphocytic leukaemia is driven by antigen-independent cell-autonomous signalling. *Nature* **489,** 309–312 (2012).

63. Binder, M. *et al.* CLL B-cell receptors can recognize themselves: alternative epitopes and

structural clues for autostimulatory mechanisms in CLL. *Blood* **121,** 239–41 (2013).

64. Doughty, C. A. *et al.* Antigen receptor – mediated changes in glucose metabolism in B lymphocytes : role of phosphatidylinositol 3-kinase signaling in the glycolytic control of growth. **107,** 4458–4466 (2016).

65. Shestov, A. A. *et al.* Quantitative determinants of aerobic glycolysis identify flux through the enzyme GAPDH as a limiting step. *Elife* **3,** 1–18 (2014).

66. Voet, D. & Voet, J. G. *Biochimie*. *2e édition* (De Boeck & Larcier s.a., 2005).

67. Stein, L. R. & Imai, S. The dynamic regulation of NAD metabolism in mitochondria. *Trends Endocrinol. Metab.* **23,** 420–8 (2012).

68. Wang, J., Nemoto, E. & Dennert, G. Regulation of CTL by ecto-nictinamide adenine dinucleotide (NAD) involves ADP-ribosylation of a p56lck-associated protein. *J. Immunol.* **156,** 2819–27 (1996).

69. Wang, J., Nemoto, E., Kots, A. Y., Kaslow, H. R. & Dennert, G. Regulation of cytotoxic T cells by ecto-nicotinamide adenine dinucleotide (NAD) correlates with cell surface GPI-anchored/arginine ADP-ribosyltransferase. *J. Immunol.* **153,** 4048–58 (1994).

70. Chiarugi, A., Dölle, C., Felici, R. & Ziegler, M. The NAD metabolome - a key determinant of cancer cell biology. *Nat. Rev. Cancer* **12,** 741–52 (2012).

71. Rouleau, M., Patel, A., Hendzel, M. J., Kaufmann, S. H. & Poirier, G. G. PARP inhibition: PARP1 and beyond. *Nat. Rev. Cancer* **10,** 293–301 (2010).

72. Audrito, V. *et al.* Nicotinamide blocks proliferation and induces apoptosis of chronic lymphocytic leukemia cells through activation of the p53/miR-34a/SIRT1 tumor

suppressor network. *Cancer Res.* **71,** 4473–83 (2011).

73. Moreschi, I. *et al.* Extracellular NAD+ is an agonist of the human P2Y11 purinergic receptor in human granulocytes. *J. Biol. Chem.* **281,** 31419–29 (2006).

74. Klein, C., Grahnert, A., Abdelrahman, A., Müller, C. E. & Hauschildt, S. Extracellular NAD(+) induces a rise in [Ca(2+)](i) in activated human monocytes via engagement of P2Y(1) and P2Y(11) receptors. *Cell Calcium* **46,** 263–72 (2009).

75. Burnstock, G. & Knight, G. E. Cellular distribution and functions of P2 receptor subtypes in different systems. *Int. Rev. Cytol.* **240,** 31–304 (2004).

76. Garten, A., Petzold, S., Körner, A., Imai, S.-I. & Kiess, W. Nampt: linking NAD biology, metabolism and cancer. *Trends Endocrinol. Metab.* **20,** 130–8 (2009).

77. Revollo, J. R. *et al.* Nampt/PBEF/Visfatin regulates insulin secretion in beta cells as a systemic NAD biosynthetic enzyme. *Cell Metab.* **6,** 363–75 (2007).

78. Wang, B. *et al.* NAMPT overexpression in prostate cancer and its contribution to tumor cell survival and stress response. *Oncogene* **30,** 907–21 (2011).

79. Sanokawa-Akakura, R., Ostrakhovitch, E. a, Akakura, S., Goodwin, S. & Tabibzadeh, S. A H2S-Nampt dependent energetic circuit is critical to survival and cytoprotection from damage in cancer cells. *PLoS One* **9,** e108537 (2014).

80. Bi, T.-Q. *et al.* Overexpression of Nampt in gastric cancer and chemopotentiating effects of the Nampt inhibitor FK866 in combination with fluorouracil. *Oncol. Rep.* **26,** 1251–7 (2011).

81. Revollo, J. R., Grimm, A. a & Imai, S. The NAD biosynthesis pathway mediated by

nicotinamide phosphoribosyltransferase regulates Sir2 activity in mammalian cells. *J. Biol. Chem.* **279,** 50754–63 (2004).

82. Audrito, V. *et al.* Extracellular nicotinamide phosphoribosyltransferase (NAMPT) promotes M2 macrophage polarization in chronic lymphocytic leukemia. *Blood* **125,** 111–123 (2015).

83. Chen, Y. & Gibson, S. B. Is mitochondria generation of reactive oxygen species a trigger for autophagy? *Autophagy* **8627,** (2008).

84. Chen, Y., Azad, M. B. & Gibson, S. B. Superoxide is the major reactive oxygen species regulating autophagy. *Cell Death Differ.* **16,** 1040–52 (2009).

85. Simon, H. U., Haj-Yehia, A. & Levi-Schaffer, F. Role of reactive oxygen species (ROS) in apoptosis induction. *Apoptosis* **5,** 415–418 (2000).

86. Adam-Vizi, V. & Chinopoulos, C. Bioenergetics and the formation of mitochondrial reactive oxygen species. *Trends Pharmacol. Sci.* **27,** 639–645 (2006).

87. Acín-Pérez, R., Fernández-Silva, P., Peleato, M. L., Pérez-Martos, A. & Enriquez, J. A. Respiratory active mitochondrial supercomplexes. *Mol. Cell* **32,** 529–39 (2008).

88. Mejia, E., Cole, L. & Hatch, G. Cardiolipin metabolism and the role it plays in heart failure and mitochondrial supercomplex formation. *Cardiovasc Hematol Disord Drug Targets* **14,** 98–106 (2014).

89. Trachootham, D., Alexandre, J. & Huang, P. Targeting cancer cells by ROS-mediated mechanisms: a radical therapeutic approach? *Nat. Rev. Drug Discov.* **8,** 579–591 (2009).

90. Fridman, J. S. & Lowe, S. W. Control of apoptosis by p53. *Oncogene* **22,** 9030–9040

(2003).

91. Galluzzi, L. *et al.* Molecular definitions of cell death subroutines: recommendations of the Nomenclature Committee on Cell Death 2012. *Cell Death Differ.* **19,** 107–20 (2012).

92. Knebel, a, Rahmsdorf, H. J., Ullrich, a & Herrlich, P. Dephosphorylation of receptor tyrosine kinases as target of regulation by radiation, oxidants or alkylating agents. *EMBO J.* **15,** 5314–5325 (1996).

93. Schreck, R., Rieber, P. & Baeuerle, P. A. Reactive oxygen intermediates as apparently widely used messengers in the activation of the NF-kappa B transcription factor and HIV-1. *EMBO J.* **10,** 2247–58 (1991).

94. Hippert, M. M., O'Toole, P. S. & Thorburn, A. Autophagy in cancer: Good, bad, or both? *Cancer Res.* **66,** 9349–9351 (2006).

95. Ishdorj, G., Li, L. & Gibson, S. B. Regulation of autophagy in hematological malignancies: role of reactive oxygen species. *Leuk. Lymphoma* **53,** 26–33 (2012).

96. Edinger, A. L. & Thompson, C. B. Death by design: apoptosis, necrosis and autophagy. *Curr. Opin. Cell Biol.* **16,** 663–9 (2004).

97. Galluzzi, L. *et al.* Essential versus accessory aspects of cell death: recommendations of the NCCD 2015. *Cell Death Differ.* **22,** 58–73 (2015).

98. Wheeler, M. L. & Defranco, A. L. Prolonged production of reactive oxygen species in response to B cell receptor stimulation promotes B cell activation and proliferation. *J. Immunol.* **189,** 4405–16 (2012).

99. Waris, G. & Ahsan, H. Reactive oxygen species: role in the development of cancer and

various chronic conditions. *J. Carcinog.* **5,** 14 (2006).

100. Jitschin, R. *et al.* Mitochondrial metabolism contributes to oxidative stress and reveals therapeutic targets in chronic lymphocytic leukemia. *Blood* **123,** 2663–2672 (2014).

101. Solaini, G., Sgarbi, G. & Baracca, A. Oxidative phosphorylation in cancer cells. *Biochim. Biophys. Acta* **1807,** 534–542 (2011).

102. Collado, R. *et al.* Early ROS-mediated DNA damage and oxidative stress biomarkers in Monoclonal B Lymphocytosis. *Cancer Lett.* **317,** 144–149 (2012).

103. Waris, G. & Ahsan, H. Reactive oxygen species: role in the development of cancer and various chronic conditions. *J. Carcinog.* **5,** 14 (2006).

104. D'Autréaux, B. & Toledano, M. B. ROS as signalling molecules: mechanisms that generate specificity in ROS homeostasis. *Nat. Rev. Mol. Cell Biol.* **8,** 813–24 (2007).

105. Capasso, M. *et al.* HVCN1 modulates BCR signal strength via regulation of BCR-dependent generation of reactive oxygen species. *Nat. Immunol.* **11,** 265–72 (2010).

106. Harlin, H. *et al.* The CD16 □ CD56 bright NK Cell Subset Is Resistant to Reactive and Has Higher Antioxidative Capacity Than the. (2011). doi:10.4049/jimmunol.179.7.4513

107. Rozovski, U., Hazan-Halevy, I., Barzilai, M., Keating, M. J. & Estrov, Z. Metabolism pathways in chronic lymphocytic leukemia. *Leuk. Lymphoma* **8194,** 1–8 (2015).

108. WARBURG, O. On the origin of cancer cells. *Science* **123,** 309–14 (1956).

109. Bhatt, a. P. *et al.* Dysregulation of fatty acid synthesis and glycolysis in non-Hodgkin lymphoma. *Proc. Natl. Acad. Sci.* **109,** 11818–11823 (2012).

110. Kim, T. M. *et al.* Total lesion glycolysis in positron emission tomography is a better predictor of outcome than the International Prognostic Index for patients with diffuse large B cell lymphoma. *Cancer* **119,** 1195–202 (2013).

111. Brody, J. I., Oski, F. A. & Singer, D. E. Impaired pentose phosphate shunt and decreased glycolytic activity in lymphocytes of chronic lymphocytic leukemia. Metabolic pathway. *Blood* **34,** 421–9 (1969).

112. Brody, J. I. & Merlie, K. Metabolic and biosynthetic features of lymphocytes from patients with diabetes mellitus: similarities to lymphocytes in chronic lymphocytic leukaemia. *Br. J. Haematol.* **19,** 193–201 (1970).

113. Karam, M. *et al.* Role of fluorine-18 fluoro-deoxyglucose positron emission tomography scan in the evaluation and follow-up of patients with low-grade lymphomas. *Cancer* **107,** 175–83 (2006).

114. Papajik, T. *et al.* 2-[18F]fluoro-2-deoxy-d-glucose positron emission tomography/computed tomography examination in patients with chronic lymphocytic leukemia may reveal Richter transformation. *Leuk. Lymphoma* **8194,** 1–6 (2013).

115. Falchi, L. *et al.* Correlation between FDG / PET , histology , characteristics , and survival in 332 patients with chronic lymphoid leukemia. **123,** 2783–2791 (2016).

116. Heintel, D. *et al.* High expression of lipoprotein lipase in poor risk B-cell chronic lymphocytic leukemia. *Leukemia* **19,** 1216–23 (2005).

117. Burger, M. *et al.* Small peptide inhibitors of the CXCR4 chemokine receptor (CD184) antagonize the activation, migration, and antiapoptotic responses of CXCL12 in chronic

lymphocytic leukemia B cells. *Blood* **106,** 1824–1830 (2005).

118. Frank, D. A., Mahajan, S. & Ritz, J. B lymphocytes from patients with chronic lymphocytic leukemia contain signal transducer and activator of transcription (STAT) 1 and STAT3 constitutively phosphorylated on serine residues. *J. Clin. Invest.* **100,** 3140–3148 (1997).

119. Hazan-Halevy, I. *et al.* STAT3 is constitutively phosphorylated on serine 727 residues, binds DNA, and activates transcription in CLL cells. *Blood* **115,** 2852–2863 (2010).

120. Rozovski, U. *et al.* Aberrant LPL Expression, Driven by STAT3, Mediates Free Fatty Acid Metabolism in CLL Cells. *Mol. Cancer Res.* **13,** 713–745 (2015).

121. Binet, J. L. *et al.* A clinical staging system for chronic lymphocytic leukemia: prognostic significance. *Cancer* **40,** 855–64 (1977).

122. Rai, K. R. *et al.* Clinical staging of chronic lymphocytic leukemia. *Blood* **46,** 219–34 (1975).

123. Binet, J. L. *et al.* A new prognostic classification of chronic lymphocytic leukemia derived from a multivariate survival analysis. *Cancer* **48,** 198–206 (1981).

124. Shanafelt, T. D. Predicting clinical outcome in CLL : how and why. *Hematol. / Educ. Progr. Am. Soc. Hematol.* 421–429 (2009). doi:10.1182/asheducation-2009.1.421

125. Yoon, J. *et al.* Association of interleukin-6 and interleukin-8 with poor prognosis in elderly patients with chronic lymphocytic leukemia. *Leuk. Lymphoma* **53,** 1735–42 (2012).

126. Baumann, T. *et al.* Chronic lymphocytic leukemia in the elderly: Clinico-biological

features, outcomes, and proposal of a prognostic model. *Haematologica* **99,** 1599–1604 (2014).

127. Molica, S. *et al.* Vitamin D insufficiency predicts time to first treatment (TFT) in early chronic lymphocytic leukemia (CLL). *Leuk. Res.* **36,** 443–447 (2012).

128. Shanafelt, T. D. *et al.* Vitamin D insufficiency and prognosis in chronic lymphocytic leukemia. *Blood* **117,** 1492–8 (2011).

129. Gentile, M. *et al.* Predictive value of beta2-microglobulin (beta2-m) levels in chronic lymphocytic leukemia since Binet A stages. *Haematologica* **94,** 887–8 (2009).

130. Hallek, M. *et al.* Addition of rituximab to fludarabine and cyclophosphamide in patients with chronic lymphocytic leukaemia: a randomised, open-label, phase 3 trial. *Lancet (London, England)* **376,** 1164–74 (2010).

131. Van Bockstaele, F., Verhasselt, B. & Philippé, J. Prognostic markers in chronic lymphocytic leukemia: a comprehensive review. *Blood Rev.* **23,** 25–47 (2009).

132. Rassenti, L. Z. *et al.* Relative value of ZAP-70, CD38, and immunoglobulin mutation status in predicting aggressive disease in chronic lymphocytic leukemia. *Blood* **112,** 1923–1930 (2008).

133. Pepper, C. *et al.* Defining the prognosis of early stage chronic lymphocytic leukaemia patients. *Br. J. Haematol.* **156,** 499–507 (2012).

134. Genentech Inc. Oncology Endpoints in a Changing Landscape. *Manag. Care* 1(suppl):1–12 (2016).

135. Eichhorst, B. F. *et al.* First-line therapy with fludarabine compared with chlorambucil

does not result in a major benefit for elderly patients with advanced chronic lymphocytic leukemia. *Blood* **114,** 3382–91 (2009).

136. Rai, K. R. *et al.* Fludarabine compared with chlorambucil as primary therapy for chronic lymphocytic leukemia. … *Engl. J.* … **343,** 1750–7 (2000).

137. Montserrat, E. & Rozman, C. Chronic lymphocytic leukaemia treatment. *Blood Rev.* **7,** 164–75 (1993).

138. Amrein, L. *et al.* Dual inhibition of the homologous recombinational repair and the nonhomologous end-joining repair pathways in chronic lymphocytic leukemia therapy. *Leuk. Res.* **35,** 1080–6 (2011).

139. Johnston, J. J. B. *et al.* Role of the TRAIL/APO2-L death receptors in chlorambucil- and fludarabine-induced apoptosis in chronic lymphocytic leukemia. *Oncogene* **22,** 8356–69 (2003).

140. Chun, E. H., Gonzales, L., Lewis, F. S., Jones, J. & Rutman, R. J. Differences in the in vivo alkylation and cross-linking of nitrogen mustard-sensitive and -resistant lines of LettrÃ©-Ehrlich asites tumors. *Cancer Res.* **29,** 1184–1194 (1969).

141. Leoni, L. M. *et al.* Bendamustine (Treanda) displays a distinct pattern of cytotoxicity and unique mechanistic features compared with other alkylating agents. *Clin. Cancer Res.* **14,** 309–317 (2008).

142. Oronsky, B. T., Reid, T., Knox, S. J. & Scicinski, J. J. The scarlet letter of alkylation: a mini review of selective alkylating agents. *Transl. Oncol.* **5,** 226–9 (2012).

143. Johnston, J. B. *et al.* P53, MDM-2, BAX and BCL-2 and drug resistance in chronic

lymphocytic leukemia. *Leuk. Lymphoma* **26,** 435–49 (1997).

144. Roué, G. *et al.* Bendamustine is effective in p53-deficient B-cell neoplasms and requires oxidative stress and caspase-independent signaling. *Clin. Cancer Res.* **14,** 6907–6915 (2008).

145. Bröker, L. E., Kruyt, F. A. E. & Giaccone, G. Cell death independent of caspases: a review. *Clin. Cancer Res.* **11,** 3155–62 (2005).

146. Knauf, W. U. *et al.* Bendamustine compared with chlorambucil in previously untreated patients with chronic lymphocytic leukaemia: updated results of a randomized phase III trial. *Br. J. Haematol.* **159,** 67–77 (2012).

147. Carson, D. a *et al.* Oral antilymphocyte activity and induction of apoptosis by 2-chloro-2'-arabino-fluoro-2'-deoxyadenosine. *Proc. Natl. Acad. Sci. U. S. A.* **89,** 2970–4 (1992).

148. Genini, D. *et al.* Deoxyadenosine analogs induce programmed cell death in chronic lymphocytic leukemia cells by damaging the DNA and by directly affecting the mitochondria. *Blood* **96,** 3537–3543 (2000).

149. Genini, D. *et al.* Nucleotide requirements for the in vitro activation of the apoptosis protein-activating factor-1-mediated caspase pathway. *J. Biol. Chem.* **275,** 29–34 (2000).

150. Adkins, J. C., Peters, D. H. & Markham, A. Fludarabine. An update of its pharmacology and use in the treatment of haematological malignancies. *Drugs* **53,** 1005–37 (1997).

151. Yang, S. W., Huang, P., Plunkett, W., Becker, F. F. & Chan, J. Y. Dual mode of inhibition of purified DNA ligase I from human cells by 9-beta-D-arabinofuranosyl-2-fluoroadenine triphosphate. *J. Biol. Chem.* **267,** 2345–9 (1992).

152. Huang, P., Chubb, S. & Plunkett, W. Termination of DNA synthesis by 9-beta-D-arabinofuranosyl-2-fluoroadenine. A mechanism for cytotoxicity. *J. Biol. Chem.* **265,** 16617–25 (1990).

153. Yamauchi, T., Nowak, B. J., Keating, M. J. & Plunkett, W. DNA repair initiated in chronic lymphocytic leukemia lymphocytes by 4-hydroperoxycyclophosphamide is inhibited by fludarabine and clofarabine. *Clin. Cancer Res.* **7,** 3580–9 (2001).

154. El-Mabhouh, A. a. *et al.* Evaluation of bendamustine in combination with fludarabine in primary chronic lymphocytic leukemia cells. *Blood* **123,** 3780–3789 (2014).

155. Flinn, I. W. *et al.* Phase III trial of fludarabine plus cyclophosphamide compared with fludarabine for patients with previously untreated chronic lymphocytic leukemia: US intergroup trial E2997. *J. Clin. Oncol.* **25,** 793–798 (2007).

156. Johnson, S. *et al.* Multicentre prospective randomised trial of fludarabine versus cyclophosphamide, doxorubicin, and prednisone (CAP) for treatment of advanced-stage chronic lymphocytic leukaemia. The French Cooperative Group on CLL. *Lancet (London, England)* **347,** 1432–8 (1996).

157. Leporrier, M. *et al.* Randomized comparison of fludarabine, CAP, and ChOP in 938 previously untreated stage B and C chronic lymphocytic leukemia patients. *Blood* **98,** 2319–25 (2001).

158. Keating, M. J. *et al.* Long-term follow-up of patients with chronic lymphocytic leukemia (CLL) receiving fludarabine regimens as initial therapy. *Blood* **92,** 1165–71 (1998).

159. Tallman, M. S. & Hakimian, D. Purine nucleoside analogs: emerging roles in indolent

lymphoproliferative disorders. *Blood* **86,** 2463–74 (1995).

160. Orchard, J. A., Bolam, S. & Oscier, D. G. Association of myelodysplastic changes with purine analogues. *Br. J. Haematol.* **100,** 677–9 (1998).

161. Nadler, L. M. *et al.* A unique cell surface antigen identifying lymphoid malignancies of B cell origin. *J. Clin. Invest.* **67,** 134–40 (1981).

162. Lim, S. H. *et al.* Anti-CD20 monoclonal antibodies: historical and future perspectives. *Haematologica* **95,** 135–43 (2010).

163. Huhn, D. *et al.* Rituximab therapy of patients with B-cell chronic lymphocytic leukemia. *Blood* **98,** 1326–31 (2001).

164. Winkler, U. *et al.* Cytokine-release syndrome in patients with B-cell chronic lymphocytic leukemia and high lymphocyte counts after treatment with an anti-CD20 monoclonal antibody (rituximab, IDEC-C2B8). *Blood* **94,** 2217–24 (1999).

165. Huh, Y. O. *et al.* Higher levels of surface CD20 expression on circulating lymphocytes compared with bone marrow and lymph nodes in B-cell chronic lymphocytic leukemia. *Am. J. Clin. Pathol.* **116,** 437–43 (2001).

166. Jones, J. D., Hamilton, B. J., Skopelja, S. & Rigby, W. F. C. Induction of interleukin-6 production by rituximab in human B cells. *Arthritis Rheumatol. (Hoboken, N.J.)* **66,** 2938–2946 (2014).

167. Keating, M. J. *et al.* Early results of a chemoimmunotherapy regimen of fludarabine, cyclophosphamide, and rituximab as initial therapy for chronic lymphocytic leukemia. *J. Clin. Oncol.* **23,** 4079–4088 (2005).

168. Alas, S., Emmanouilides, C. & Bonavida, B. Inhibition of interleukin 10 by rituximab results in down-regulation of bcl-2 and sensitization of B-cell non-Hodgkin's lymphoma to apoptosis. *Clin. Cancer Res.* **7,** 709–23 (2001).

169. Alduaij, W. & Illidge, T. M. The future of anti-CD20 monoclonal antibodies: are we making progress? *Blood* **117,** 2993–3001 (2011).

170. Goede, V. *et al.* Obinutuzumab as frontline treatment of chronic lymphocytic leukemia: updated results of the CLL11 study. *Leukemia* **29,** 1602–4 (2015).

171. Osterborg, a *et al.* Management guidelines for the use of alemtuzumab in chronic lymphocytic leukemia. *Leukemia* **23,** 1980–8 (2009).

172. U.S. Food and Drug Administration. FDA Statement: FDA halts clinical trial of drug Revlimid (lenalidomide) for chronic lymphocytic leukemia due to safety concerns. (2013). at <http://www.fda.gov/Drugs/DrugSafety/ucm361444.htm>

173. Ponader, S. *et al.* The Bruton tyrosine kinase inhibitor PCI-32765 thwarts chronic lymphocytic leukemia cell survival and tissue homing in vitro and in vivo. *Blood* **119,** 1182–9 (2012).

174. De Rooij, M. F. M. *et al.* The clinically active BTK inhibitor PCI-32765 targets B-cell receptor- and chemokine-controlled adhesion and migration in chronic lymphocytic leukemia. *Blood* **119,** 2590–2594 (2012).

175. Hoellenriegel, J. *et al.* The phosphoinositide 3'-kinase delta inhibitor, CAL-101, inhibits B-cell receptor signaling and chemokine networks in chronic lymphocytic leukemia. *Blood* **118,** 3603–12 (2011).

176. Friedberg, J. W. *et al.* Inhibition of Syk with fostamatinib disodium has significant clinical activity in non-Hodgkin lymphoma and chronic lymphocytic leukemia. *Blood* **115,** 2578–2585 (2010).

177. Burger, J. A. *et al.* Ibrutinib as Initial Therapy for Patients with Chronic Lymphocytic Leukemia. *N. Engl. J. Med.* **373,** 2425–37 (2015).

178. Byrd, J. C. *et al.* Three-year follow-up of treatment-naïve and previously treated patients with CLL and SLL receiving single-agent ibrutinib. *Blood* **125,** 2497–506 (2015).

179. Furman, R. R. *et al.* Idelalisib and rituximab in relapsed chronic lymphocytic leukemia. *N. Engl. J. Med.* **370,** 997–1007 (2014).

180. O'Brien, S. M. *et al.* A phase 2 study of idelalisib plus rituximab in treatment-naïve older patients with chronic lymphocytic leukemia. *Blood* **126,** 2686–94 (2015).

181. Maddocks, K. J. *et al.* Etiology of Ibrutinib Therapy Discontinuation and Outcomes in Patients With Chronic Lymphocytic Leukemia. *JAMA Oncol.* **1,** 80–7 (2015).

182. Jain, P. *et al.* Outcomes of patients with chronic lymphocytic leukemia after discontinuing ibrutinib. *Blood* **125,** 2062–7 (2015).

183. Lipsky, A. H. *et al.* Incidence and risk factors of bleeding-related adverse events in patients with chronic lymphocytic leukemia treated with ibrutinib. *Haematologica* **100,** 1571–8 (2015).

184. Kamel, S. *et al.* Ibrutinib inhibits collagen-mediated but not ADP-mediated platelet aggregation. *Leukemia* **29,** 783–7 (2015).

185. McMullen, J. R. *et al.* Ibrutinib increases the risk of atrial fibrillation, potentially through

inhibition of cardiac PI3K-Akt signaling. *Blood* **124,** 3829–30 (2014).

186. Health Canada. IMBRUVICA. (2015). at <http://www.hc-sc.gc.ca/dhp-mps/prodpharma/sbd-smd/drug-med/sbd_smd_2015_imbruvica_174029-eng.php>

187. Health Canada. Zydelig. (2015). at <http://www.hc-sc.gc.ca/dhp-mps/prodpharma/sbd-smd/drug-med/sbd_smd_2015_zydelig_172652-eng.php#sbd>

188. The U.S. National Institutes of Health. A Phase II Study Using Ibrutinib and Short-Course Fludarabine in Previously Untreated Patients With Chronic Lymphocytic Leukemia/Small Lymphocytic Lymphoma (CLL/SLL). *ClinicalTrials.gov* (2016). at <https://clinicaltrials.gov/ct2/show/NCT02514083>

189. The U.S. National Institutes of Health. Rituximab and Bendamustine Hydrochloride, Rituximab and Ibrutinib, or Ibrutinib Alone in Treating Older Patients With Previously Untreated Chronic Lymphocytic Leukemia. *ClinicalTrials.gov* (2015). at <https://clinicaltrials.gov/ct2/show/NCT01886872>

190. The U.S. National Institutes of Health. Ibrutinib and Rituximab Compared With Fludarabine Phosphate, Cyclophosphamide, and Rituximab in Treating Patients With Untreated Chronic Lymphocytic Leukemia or Small Lymphocytic Lymphoma. *ClinicalTrials.gov* (2015). at <https://clinicaltrials.gov/ct2/show/NCT02048813>

191. The U.S. National Institutes of Health. A Phase II Study of Ibrutinib Plus FCR in Previously Untreated, Younger Patients With Chronic Lymphocytic Leukemia (iFCR). *ClinicalTrials.gov* (2015). at <https://clinicaltrials.gov/ct2/show/NCT02251548>

192. The U.S. National Institutes of Health. Ibrutinib in Combination With GA101

(Obinutuzumab) in Previously Untreated Chronic Lymphocytic Leukemia (CLL) Patients. *ClinicalTrials.gov* (2015). at <https://clinicaltrials.gov/ct2/show/NCT02315768>

193. The U.S. National Institutes of Health. Efficacy and Safety of Idelalisib in Combination With Rituximab in Patients With Previously Untreated Chronic Lymphocytic Leukemia With 17p Deletion (Havasu). *ClinicalTrials.gov* (2015). at <https://clinicaltrials.gov/ct2/show/NCT02044822>

194. The U.S. National Institutes of Health. A Study of Idelalisib (GS1101, CAL101) + Ofatumumab in Previously Untreated CLL/SLL. *ClinicalTrials.gov* (2015). at <https://clinicaltrials.gov/ct2/show/NCT02135133>

195. The U.S. National Institutes of Health. Efficacy and Safety of Idelalisib in Combination With Bendamustine and Rituximab in Subjects With Previously Untreated Chronic Lymphocytic Leukemia. *ClinicalTrials.gov* (2015). at <https://clinicaltrials.gov/ct2/show/NCT01980888>

196. The U.S. National Institutes of Health. Efficacy and Safety of Idelalisib in Combination With Obinutuzumab Compared to Chlorambucil in Combination With Obinutuzumab for Previously Untreated Chronic Lymphocytic Leukemia. *ClinicalTrials.gov* (2015). at <https://clinicaltrials.gov/ct2/show/NCT01980875>

197. Dreger, P. *et al.* Managing high-risk CLL during transition to a new treatment era: stem cell transplantation or novel agents? *Blood* **124,** 3841–9 (2014).

198. Sutton, L. *et al.* Autologous stem cell transplantation as a first-line treatment strategy for chronic lymphocytic leukemia: a multicenter, randomized, controlled trial from the SFGM-TC and GFLLC. *Blood* **117,** 6109–19 (2011).

199. Michallet, M. *et al.* Autologous hematopoietic stem cell transplantation in chronic lymphocytic leukemia: results of European intergroup randomized trial comparing autografting versus observation. *Blood* **117,** 1516–21 (2011).

200. Dreger, P. *et al.* Early autologous stem cell transplantation for chronic lymphocytic leukemia: long-term follow-up of the German CLL Study Group CLL3 trial. *Blood* **119,** 4851–9 (2012).

201. Milligan, D. W. *et al.* High incidence of myelodysplasia and secondary leukaemia in the UK Medical Research Council Pilot of autografting in chronic lymphocytic leukaemia. *Br. J. Haematol.* **133,** 173–5 (2006).

202. Böttcher, S. *et al.* Minimal residual disease quantification is an independent predictor of progression-free and overall survival in chronic lymphocytic leukemia: A Multivariate analysis from the randomized GCLLSG CLL8 trial. *J. Clin. Oncol.* **30,** 980–988 (2012).

203. Rawstron, a C. *et al.* International standardized approach for flow cytometric residual disease monitoring in chronic lymphocytic leukaemia. *Leukemia* **21,** 956–64 (2007).

204. Zhou, Y. *et al.* Therapy-related myeloid neoplasms following fludarabine, cyclophosphamide, and rituximab (FCR) treatment in patients with chronic lymphocytic leukemia/small lymphocytic lymphoma. *Mod. Pathol.* **25,** 237–45 (2012).

205. Shanafelt, T. D. *et al.* Prospective evaluation of clonal evolution during long-term follow-up of patients with untreated early-stage chronic lymphocytic leukemia. *J. Clin. Oncol.* **24,** 4634–41 (2006).

206. Stilgenbauer, S. *et al.* Clonal evolution in chronic lymphocytic leukemia: Acquisition of

high-risk genomic aberrations associated with unmutated VH, resistance to therapy, and short survival. *Haematologica* **92,** 1242–1245 (2007).

207. Zenz, T., Mertens, D., Küppers, R., Döhner, H. & Stilgenbauer, S. From pathogenesis to treatment of chronic lymphocytic leukaemia. *Nat. Rev. Cancer* **10,** 37–50 (2010).

208. Rosenwald, A. *et al.* Fludarabine treatment of patients with chronic lymphocytic leukemia induces a p53-dependent gene expression response. *Spectrum* **104,** 1428–1434 (2004).

209. Rongvaux, A., Andris, F., Van Gool, F. & Leo, O. Reconstructing eukaryotic NAD metabolism. *Bioessays* **25,** 683–90 (2003).

210. Nikiforov, A., Dölle, C., Niere, M. & Ziegler, M. Pathways and subcellular compartmentation of NAD biosynthesis in human cells: from entry of extracellular precursors to mitochondrial NAD generation. *J. Biol. Chem.* **286,** 21767–78 (2011).

211. Pittelli, M. *et al.* Pharmacological effects of exogenous NAD on mitochondrial bioenergetics, DNA repair, and apoptosis. *Mol. Pharmacol.* **80,** 1136–46 (2011).

212. Billington, R. A., Genazzani, A. A., Travelli, C. & Condorelli, F. NAD depletion by FK866 induces autophagy. *Autophagy* **4,** 385–7 (2008).

213. Jia, S. H. *et al.* Pre-B cell colony-enhancing factor inhibits neutrophil apoptosis in experimental inflammation and clinical sepsis. *J. Clin. Invest.* **113,** 1318–27 (2004).

214. Li, Y. *et al.* Extracellular Nampt promotes macrophage survival via a nonenzymatic interleukin-6/STAT3 signaling mechanism. *J. Biol. Chem.* **283,** 34833–43 (2008).

215. Dahl, T. B. *et al.* Increased expression of visfatin in macrophages of human unstable carotid and coronary atherosclerosis: possible role in inflammation and plaque

destabilization. *Circulation* **115,** 972–80 (2007).

216. Fukuhara, A. *et al.* Visfatin: a protein secreted by visceral fat that mimics the effects of insulin. *Science* **307,** 426–30 (2005).

217. Fukuhara, A. *et al.* Retraction. *Science* **318,** 565 (2007).

218. Adya, R., Tan, B. K., Chen, J. & Randeva, H. S. Nuclear factor-kappaB induction by visfatin in human vascular endothelial cells: its role in MMP-2/9 production and activation. *Diabetes Care* **31,** 758–60 (2008).

219. Pompella, A., Visvikis, A., Paolicchi, A., De Tata, V. & Casini, A. F. The changing faces of glutathione, a cellular protagonist. *Biochem. Pharmacol.* **66,** 1499–503 (2003).

220. Karpusas, M. *et al.* The Interaction of the Chemotherapeutic Drug Chlorambucil with Human Glutathione Transferase A1-1: Kinetic and Structural Analysis. *PLoS One* **8,** (2013).

221. Nilsson, J., Söderberg, O., Nilsson, K., Rosén, A. & So, O. Thioredoxin prolongs survival of B-type chronic lymphocytic leukemia cells. **95,** 1420–1426 (2012).

222. Kato, J. *et al.* ADP-ribosylarginine hydrolase regulates cell proliferation and tumorigenesis. *Cancer Res.* **71,** 5327–35 (2011).

223. Chalkiadaki, A. & Guarente, L. Sirtuins mediate mammalian metabolic responses to nutrient availability. *Nat. Rev. Endocrinol.* **8,** 287–96 (2012).

224. Tong, L. & Denu, J. M. Function and metabolism of sirtuin metabolite O-acetyl-ADP-ribose. *Biochim. Biophys. Acta* **1804,** 1617–25 (2010).

225. Berger, F., Ramirez-Hernandez, M. H. & Ziegler, M. The new life of a centenarian:

signalling functions of NAD(P). *Trends Biochem Sci* **29,** 111–118 (2004).

226. Bi, T. & Che, X. Nampt/PBEF/visfatin and cancer. *Cancer Biol. Ther.* **10,** 119–25 (2010).

227. Hasmann, M. & Schemainda, I. FK866 , a Highly Specific Noncompetitive Inhibitor of Nicotinamide Phosphoribosyltransferase , Represents a Novel Mechanism for Induction of Tumor Cell Apoptosis. *Cancer Res.* **63,** 7436–7442 (2003).

228. Cagnetta, A. *et al.* APO866 Increases Antitumor Activity of Cyclosporin-A by Inducing Mitochondrial and Endoplasmic Reticulum Stress in Leukemia Cells. **21,** 3934–3946 (2015).

229. Watson, M. *et al.* The small molecule GMX1778 is a potent inhibitor of NAD+ biosynthesis: strategy for enhanced therapy in nicotinic acid phosphoribosyltransferase 1-deficient tumors. *Mol. Cell. Biol.* **29,** 5872–88 (2009).

230. Khan, J. a, Tao, X. & Tong, L. Molecular basis for the inhibition of human NMPRTase, a novel target for anticancer agents. *Nat. Struct. Mol. Biol.* **13,** 582–8 (2006).

231. Kang, G. B. *et al.* Crystal structure of Rattus norvegicus Visfatin/PBEF/Nampt in complex with an FK866-based inhibitor. *Mol. Cells* **27,** 667–71 (2009).

232. Wang, W. *et al.* Structural Basis for Resistance to Diverse Classes of NAMPT Inhibitors. *PLoS One* **9,** e109366 (2014).

233. Drevs, J., Löser, R., Rattel, B. & Esser, N. Antiangiogenic potency of FK866/K22.175, a new inhibitor of intracellular NAD biosynthesis, in murine renal cell carcinoma. *Anticancer Res.* **23,** 4853–8 (2003).

234. Travelli, C. *et al.* Reciprocal potentiation of the antitumoral activities of FK866, an

inhibitor of nicotinamide phosphoribosyltransferase, and etoposide or cisplatin in neuroblastoma cells. *J. Pharmacol. Exp. Ther.* **338,** 829–40 (2011).

235. Nahimana, A. *et al.* The NAD biosynthesis inhibitor APO866 has potent antitumor activity against hematologic malignancies. *Blood* **113,** 3276–86 (2009).

236. Wosikowski, K., Mattern, K. & Schemainda, I. WK175 , a Novel Antitumor Agent , Decreases the Intracellular Nicotinamide Adenine Dinucleotide Concentration and Induces the Apoptotic Cascade in Human Leukemia Cells WK175 , a Novel Antitumor Agent , Decreases the Intracellular Nicotinamide in Human Leu. 1057–1062 (2002).

237. Gehrke, I. *et al.* On-Target Effect of FK866, a Nicotinamide Phosphoribosyl Transferase Inhibitor, by Apoptosis-Mediated Death in Chronic Lymphocytic Leukemia Cells. *Clin. Cancer Res.* **20,** 4861–72 (2014).

238. Holen, K., Saltz, L. B., Hollywood, E., Burk, K. & Hanauske, A.-R. The pharmacokinetics, toxicities, and biologic effects of FK866, a nicotinamide adenine dinucleotide biosynthesis inhibitor. *Invest. New Drugs* **26,** 45–51 (2008).

239. Schou, C. *et al.* Novel cyanoguanidines with potent oral antitumour activity. *Bioorg. Med. Chem. Lett.* **7,** 3095–3100 (1997).

240. Aleskog, a *et al.* Activity of CHS 828 in primary cultures of human hematological and solid tumors in vitro. *Anticancer. Drugs* **12,** 821–7 (2001).

241. Hovstadius, P. *et al.* Cytotoxic effect in vivo and in vitro of CHS 828 on human myeloma cell lines. *Anticancer. Drugs* **15,** 63–70 (2004).

242. Hovstadius, P. *et al.* A Phase I study of CHS 828 in patients with solid tumor malignancy.

Clin. Cancer Res. **8,** 2843–50 (2002).

243. Ravaud, A. *et al.* Phase I study and pharmacokinetic of CHS-828, a guanidino-containing compound, administered orally as a single dose every 3 weeks in solid tumours: an ECSG/EORTC study. *Eur. J. Cancer* **41,** 702–7 (2005).

244. von Heideman, A., Berglund, A., Larsson, R. & Nygren, P. Safety and efficacy of NAD depleting cancer drugs: results of a phase I clinical trial of CHS 828 and overview of published data. *Cancer Chemother. Pharmacol.* **65,** 1165–72 (2010).

245. Beauparlant, P. *et al.* Preclinical development of the nicotinamide phosphoribosyl transferase inhibitor prodrug GMX1777. *Anticancer. Drugs* **20,** 346–54 (2009).

246. Nahimana, A. *et al.* The anti-lymphoma activity of APO866, an inhibitor of nicotinamide adenine dinucleotide biosynthesis, is potentialized when used in combination with anti-CD20 antibody. *Leuk. Lymphoma* **55,** 2141–50 (2014).

247. Bajrami, I. *et al.* Synthetic lethality of PARP and NAMPT inhibition in triple-negative breast cancer cells. *EMBO Mol. Med.* **4,** 1087–1096 (2012).

248. Breton, C. S. *et al.* Combinative effects of β-Lapachone and APO866 on pancreatic cancer cell death through reactive oxygen species production and PARP-1 activation. *Biochimie* **116,** 141–153 (2015).

249. LOEWE, S. The problem of synergism and antagonism of combined drugs. *Arzneimittelforschung.* **3,** 285–90 (1953).

250. Berenbaum, M. C. What is synergy? *Pharmacol. Rev.* **41,** 93–141 (1989).

251. Chou, T. C. & Talalay, P. Quantitative analysis of dose-effect relationships: the combined

effects of multiple drugs or enzyme inhibitors. *Adv. Enzyme Regul.* **22,** 27–55 (1984).

252. Chou, T. Drug combination studies and their synergy quantification using the Chou-Talalay method. *Cancer Res.* **70,** 440–6 (2010).

253. Geary, N. Understanding synergy. *Am. J. Physiol. Endocrinol. Metab.* **304,** E237–53 (2013).

254. Cea, M. *et al.* Targeting NAD+ salvage pathway induces autophagy in multiple myeloma cells via mTORC1 and extracellular signal-regulated kinase (ERK1/2) inhibition. *Blood* **120,** 3519–29 (2012).

255. Hong, S. M. *et al.* NAMPT suppresses glucose deprivation-induced oxidative stress by increasing NADPH levels in breast cancer. *Oncogene* 1–11 (2015). doi:10.1038/onc.2015.415

256. Foucquier, J. & Guedj, M. Analysis of drug combinations: current methodological landscape. *Pharmacol. Res. Perspect.* **3,** e00149 (2015).

257. Skrtić, M. *et al.* Inhibition of mitochondrial translation as a therapeutic strategy for human acute myeloid leukemia. *Cancer Cell* **20,** 674–88 (2011).

258. Fiorillo, M. *et al.* Bedaquiline, an FDA-approved antibiotic, inhibits mitochondrial function and potently blocks the proliferative expansion of stem-like cancer cells (CSCs). *Aging (Albany. NY).* **8,** 1–15 (2016).